Addis Ababa University
አዲስ፡አበባ፡ዩኒቨርሲቲ
SEEK WISDOM, ELEVATE YOUR INTELLECT AND SERVE HUMANITY !

COLLEGE OF NATURAL AND COMPUTATIONAL SCIENCES

SCHOOL OF EARTH SCIENCES

Stream: Hydrogeology

Groundwater Resource Potential Assessment in the Upper Guder Catchment, West Shoa, Central Ethiopia

Getu Tarafa Nagawo

ID No: GSR/9897/15

Advisor: Dr. Behailu.B

September, 2024

Addis Ababa Ethiopia

Addis Ababa University

School of Graduate Studies

Department of Earth Sciences

Groundwater Resource Potential Assessment in the upper Guder Catchment, West shoa Zone, Centeral Ethiopia

By

Getu Tarafa Nagawo

September, 2024

Approved by board examiners

Dr. Bayisa Reggasa (Head of the Department)

____

Signature

Dr. Behailu Birhanu (Advisor)_______________________________________

Signature

Dr. Tilahun Azagegn (Examiner) _______________________________________

Signature

Dr. Dessie Nedaw (Examiner)____

Signature

____

Chairman of school or graduate program coordinator

Declaration

I, Getu Tarafa (ID No. GSR/9897/15), declare that I am the author of this MSc Thesis, which is titled "Groundwater Resource Potential Assessment in the Upper Guder Catchment, West Shoa, Centeral Ethiopia," and that it was not submitted to any other academic institution in aspirations of receiving an academic qualification. The thesis's content has not been plagiarized, and any instances in which it has drawn from the work of other scholars have been duly acknowledged.

Candidate's Name	**signature**	**date**
Getu Tarafa	_______________	_______________

ACKNOWLEDGEMENT

I want to thank my Almighty God from the bottom of my heart for giving me grace and peace at the beginning and for giving me the ability and patience to finish this research project from beginning to end.

I have a great deal of gratitude for my supervisor, Dr. Behailu Birhanu, for all of his hard work, dedication, and inspiring mentorship and I appreciate him for his prompt response while we emailed from the beginning. The fact that my supervisor showed genuine concern for my work is something I consider a great blessing.

A special thank you to the administrative staff and staff of the Department of Earth Sciences at AAU for their assistance during my two years at the university.

I would like to express my gratitude to my friends and brothers, especially Mr. Murtessa Teganu, Mr. Urgessa Hirpha, Mr. Lalisa Dessalegn, and others, for their unwavering support, insightful advice, and stimulating conversations during the difficult times I faced while conducting my research.

Furthermore, I would like to extend my sincere gratitude to the West Shoa Shewa Zone Water Resource Development and Energy Office, the Ethiopian Construction Design and Supervision Works Corporation, the National Meteorological Agency, the Engineering Corporation of Oromia, and other private businesses and individuals for their kind provision of the required data.

Finally, I would like to express my deepest appreciation to my wife, Tsion Tesfaye, for her perseverance, inspiration, and selflessness in helping me to accomplish my goals. I hope she lives a long and happy life.

ABSTRACT

The purpose of this research is to assess the upper Guder subbasin's groundwater resource potential using hydrometeorological, hydrogeological, and hydro chemical data analysis. The Guder Catchment, which is the main tributary of the Abay Sub-basin, is located between latitudes 1011758mN and 962477mN and longitudes 321928mE and 405109mE. The watershed spans roughly 2200 km^2. Extremely rough terrain, a dendritic drainage pattern, and a tropical to tropically wet and dry climate are its defining characteristics. The area elevations range from 1700 to 3300 m.a.s.l.

The catchment's annual precipitation is estimated to be 1267.2 mm/year using the long-term mean monthly rainfall data. The estimated PET values, derived from the Penman and Thornthwaite method, are 995.83 mm/year and 738.77 mm/yr. AETs of 774 mm/year and 733.48 mm/year have been determined using the Turc and soil-water balance approaches, respectively.

According to water balance and chloride mass balance methods, the yearly groundwater recharge was estimated to be 148 mm/year and 236.89 mm/year, respectively. The Actual evapotranspiration, surface runoff, and average annual long-term groundwater recharge in the catchment have all been modeled by the wetSpass model. The findings show that the annual results are 558.4 mm/year,340.5mm/year, and 298 mm/year, respectively.

The catchment contains the following lithologic units: Jima lower basalts and Tarmaber formation; Tertiary volcanics (Lower Basalts, Guder-Babicha basalts and Upper basalt, Alaji Rhyolite and plugs); Quaternary sediment (Alluvial and Eluvium); and Mesozoic (Abay beds, sandstone). The most extensive lithology in the study area is found in tertiary volcanic rocks.

The basin is classified as a local aquifer, extensive and moderately productive porous aquifers, extensive and highly productive fissure aquifer, extensive and highly productive porous/fissured aquifer, low productive fissured/porous aquifer, and aquitards based on qualitative and quantitative analysis of aquifer/aquitard characteristics. The primary water-bearing component of the catchment is the weathered and fractured volcanic rocks. Higher discharge, hydraulic conductivity, and transmissivity values are mapped at or near fractured areas and towards the outlet based on the available borehole data.

The regional groundwater flow is typically northward, and water moves from the surrounding highlands to the discharge areas along a low hydraulic gradient.

According to the hydro chemical analysis, the predominant cation is Ca, and the predominant anion is HCO_3. According to graphical plots, the predominant water types in the region are Ca-HCO_3 and Ca-Na/Mg-HCO_3, which have low TDS and EC values in highland areas (recharge zone) and relatively high TDS and EC values relative to the recharge area. The majority of water sample results indicate that the area is suitable for irrigation and residential use.

Key words: - Transmissivity, aquifer, upper Guder Catchment, Groundwater, Evapotranspiration

Table of Contents

List of Figures

List of Tables

CHAPTER ONE

1. Introduction

In order to meet the needs of all life on Earth, groundwater that is stored in the aquifer is continuously used for domestic, industrial, and agricultural purposes after being extracted through wells. This indicates that water is a necessary component of all life on earth (Seifu Kebede, 2023). It is the most important resource for urban, agricultural, and commercial activities. Water utilization is linked to any development, whether directly or indirectly. Nonetheless, it gets increasingly complicated due to industrialization, urbanization, and population growth. One of the most valuable resources that nature has given is groundwater, which is found underground in rock units and makes up more than 98% of the freshwater that is available worldwide (Fetter, 1994).

Safe drinking water is both a fundamental human right and a need for good health. Many regions of the world already have limited supplies of fresh water. It will become even more restrictive in the upcoming century as a result of urbanization, population growth, and climate change (Jackson et al. 2001).

Around 80% of the population in Ethiopia, a developing country, depend on agriculture, which is the foundation of the national economy (Baye,2017; Zerssa et al.,2021). Groundwater is the primary source of domestic water supply. However, in the literature, especially in the last few years, estimates of Ethiopia's potential groundwater resources vary dramatically. Groundwater potential is estimated to be between 2.6 and 1000 billion cubic meters based on existing literature (Berhanu et al., 2014).

Groundwater potential needs to be reliably estimated to use large-scale development. Only a small percentage of water on Earth 22.8% exists as fresh water on land; the majority of water on Earth 97.2% is found in the oceans and seas. The freshwater found on land is distributed as ice caps and glaciers (76.43 %), groundwater and soil moisture (21.96 %), fresh-water lakes (0.32 percent), saline lakes (0.29 percent), and a very small amount as a stream channel (0.04 percent) (Fetter, Applied hydrogeology, 2001) (Kebede, 2013). In Ethiopia, groundwater supplies over 90% of the water used for domestic and industrial use, with surface water accounting for most of the water used for irrigation. The availability of sustainable groundwater resources for future uses is put in jeopardy, and the situation is made considerably worse by inaccurate and inadequate recharge estimation. Over Ethiopia, recharge is wildly inconsistent. The range is almost 0 to 300 mm/yr. Indirect recharge from floods and mountain runoff, as well as rapid recharge from heavy rainfall events, account for nearly 60% of aquifers. According to Kebede (2013), diffuse recharge is only found in the plateau region, which makes up about 30% of the nation.

Groundwater recharge occurs when water becomes available at the water-table surface and enters the saturated zone (Freeze and Cherry, 1979). Since sediments and rocks effectively create a subsurface reservoir or aquifer where groundwater can accumulate and move, groundwater is present in the majority of geological formations. The type of rocks or sediments, fissures and cracks within the rocks, and the depth of burial are some of the factors that affect the hydrogeological properties, porosity, and permeability, of geological layers and their spatial distribution. The hydrogeological setting which can vary greatly even within a single lithology determines groundwater availability. Ethiopia's Upper Blue Nile (UBN) basin is the most significant river basin due to its significant contribution to the nation's irrigation and hydropower potential. This is because groundwater is typically a significant source of surface water. Just a small percentage of the Nile water is used for irrigation in Ethiopia, even though the Ethiopian highlands provide more than 80% of the Nile River's flow (Dile et al., 2017). The Upper Blue Nile Basin, which spans 174,000 km^2 (9.86◦ N, 37.69◦ E basin centroid) and is drained by the mainstream of the Blue Nile River in Ethiopia, is characterized by mountainous terrain with steep hill slopes and relatively flat highlands.

To manage fair water distribution in the study area, the total resource available must be ascertained. Determining the factors causing the depletion of water resources could aid policymakers in handling the situation given the rise in demand. To provide communities with equitable and sustainable water supplies, this research is therefore an essential component of the area's water resource management.

1.2. Statement of the problem

Due to a lack of knowledge and awareness among the populations about the responsible management of groundwater resources, mismanagement of these resources has resulted in a series of cases of groundwater scarcity in the majority of our country. The population in the area expanding, necessitating sufficient supplies of high-quality water in terms of both quantity and quality. Urban expansion is harming the nation's groundwater resources because, at the moment, many rivers inside and near the catchment rivers have confluences because of improper land use practices. Because of its topography, the study area is mostly covered with damp terrain, which makes it unsuitable for urban growth. The study area land use and land cover do not include potential groundwater exploitation areas or well fields; instead, these areas are used for other types of construction. The occurrence, source, flow, and chemical makeup of groundwater are influenced by several factors, including geology/lithology, geomorphology/landforms, drainage density, rainfall, geological structures/lineaments, slope, land use/cover, and soil of the groundwater regime. It's common to run into problems estimating the recharge of groundwater. Problems are more likely to arise from improper site selection and groundwater evaluation. There is no direct method for observing water below the surface since groundwater occurs far below the surface, out of sight. Its existence can only be inferred indirectly.

The Upper Guder sub-basin receives a moderate amount of rainfall each year, but agricultural output has been high, drinking water scarcity has long been a problem, and land degradation has resulted in crop productivity loss. For agricultural development in the study area, however, this groundwater resource remains largely unexploited. With this in mind, it is recommended that this study combine hydrometeorological, hydrogeological, and geological techniques to provide a comprehensive picture of groundwater characteristics and yield results that make sense given the potential of the resource.

1.3. Objectives of the study

1.3.1. General objective of the study

The main objective of the thesis is to assess the groundwater resource potential of the Upper Guder catchment in relation to the deep groundwater resource on the basis of aquifer characterization, recharge mechanism and hydro chemical nature of the groundwater.

1.3.2. Specific objectives of the study

- ✓ To estimate groundwater recharge and major hydrologic components involved in the catchment
- ✓ To differentiate recharge and discharge areas as well as groundwater flow direction.
- ✓ Characterization of the aquifer within the catchment
- ✓ Assessing the quality of water from a domestic and agricultural perspective

1.4. Research Questions

- ✓ How much groundwater recharge occurs in the upper Guder catchment, and how is it distributed geographically and how the hydrologic components involved through the catchment?
- ✓ How the upper Guder Catchment's flow direction and recharge/discharge can be distinguished?
- ✓ What are the parameters to characterize the aquifer within the catchment?

1.5. Significance of the study

Based on hydro metrological and hydrogeological factors (i.e., potential actual evapotranspiration, evapotranspiration, precipitation, and sunshine), the proposed study would produce a groundwater recharge that would divide the study area into distinct portions. In addition to producing a groundwater contour map, the final detailed map of the area can be utilized as one of the inputs for comprehending distributed recharge values. In particular, the relationship between chemical characteristics and water quality in terms of domestic and agricultural uses in the area is a key finding of hydrogeochemical studies conducted in the area. These studies are also crucial for identifying and controlling groundwater interaction processes with aquifer minerals and the chemistry of ground and surface waters.

Moreover, the results of this investigation will function as a foundation of understanding and a point of reference for anybody who wishes to carry out further research on the subject.

1.6. Previous works

The study area does not currently have any comprehensive groundwater potential assessment work to highlight. The area has not been sufficiently studied hydrogeological, except for a few small-scale, regional studies conducted by private companies, town water supplies, and an assessment that was solely based on qualitative and descriptive methods. All other studies do not use both quantitative and qualitative computations of the most relevant hydrogeological factors to show the groundwater potential of the catchment.

The study area has obtained less attention from geologists and hydrogeologists than other regions of the country, like the Rift Zones. Research in the field has so far been limited by a lack of data or too broad (regional in scope). These studies which focus on the volcanic activity of the Ethiopian plateau, especially in the Wenchi area are among the most important ones in the fields of geology and hydrogeology. Others include Smeds (1964), KONDO (1967), Mohr (1971), Herrick et al. (1983), and Adhana (1992) on the Yerer-Tulu WeleJ-Volcano-Tectonic.

The hydrogeological map of Akaki Beseka (NC 37 – 14) Sheet is compiled by (Bereket Fentaw and Mihret Manaye, 2010). The detailed hydrogeologic description is forwarded by this work. The hydrogeological map of Akaki Beseka area is presented by (GSE, 2011) at a 1:250,000 scale.

Hydrogeological, hydrochemical, and engineering geology maps of Addis Ababa (Nc 37-10) The sheet was assembled by (Bereket Fentaw and Tsehay Amare, 2006–2009). This work advances the comprehensive hydrogeologic, hydrochemical, and engineering geological description. (GSE, 2010) presents a 1:250,000 scale hydrogeological map of the Addis Ababa area.

(Tilahun.A, 2008)**.** Using geochemical modeling and isotope hydrology, the hydrogeochemical characterization of the aquifer systems in the upper Awash and adjacent Abay Plateau is studied. The entire Plateau zone, permeable and locally faulted transition zones, and rift zones replenish the aquifer systems, according to the authors' findings. High-yield artesian wells close to the water divides of the Awash and Abay basins are examples of field hydrogeological observations that suggest groundwater transfer between basins.

(Abenezer.K, 2007)**.** With fresh (low TDS) CaHCO3 water and at least two distinct types of water present along the flow path high TDS NaHCO3 and fresh.He described how the hydrogeochemical evolution proceeded westward. Low pH and high electrical conductivity are only found in the water from the Ambo thermal spring emerging sites, Wonchi and Woliso, which are connected by NNW and SSE structures. The low pH is attributed to the Dandi Wonchi-related magma chamber degassing and the high CO2 supply from Mesozoic decarbonation. Deposits of silica sinter and travertine can be found where thermal springs emerge. These deposits are the result of temperature decreases, variations in pressure, and the mingling of thermal spring water with freshwater from ridges at high altitudes.Deep seating structures and the state of the geology generally have a significant impact on the evolution of ions.

(Kasahun.B, 2005)**.** He mentioned that the basin's hydrochemistry is also examined, and the waters are classified as freshwater with the exception of two thermal spring waters that are located along the Ambo-Butajira fault line and have deep geothermal contact. The majority of water bodies have Ca-Mg-CO3 type water with rapid shallow ground water circulation from meteoric sources, which is a characteristic of recharge area water that has undergone low geochemical evolution, with the exception of the two thermal springs and some waters in the lowland areas. However, the two thermal spring waters exhibit high geochemical evolution processes and deep regional circulation.

(Tiketa Adula, 2022). Upper Blue Nile basin, Western Oromia area, with a case study of the Guder sub-basin. Available data were used to prepare maps of the following: geomorphology, lithology/geology, land use/cover, slope, lineament density, drainage density, soil properties (soil texture, soil type), rainfall, and elevation. assigned individual weights along with their subclass divisions based on decision-making based on literature, satellite images, and conventional data. A third of the studied region, or 33.6%, has "good" and "very good" groundwater potentiality, according to the study assessment. Conversely, the percentages that fall into the categories of "good," "moderate," and "poor" are 22.9%, 20.2%, and 23.3%, respectively. There was generally a lack of specificity and in-depth information because published studies and scientific exercises could not be found in the catchment.

(Lemessa.M, 2001). As the main groundwater discharging area is formed by a gentle slope of land stretching east-west between the northern and southern elevated areas, the author points out that the Wanchi and Dandi highlands are recharge areas for both thermal and cold groundwater due to their favorable geological, structural, and geographical conditions.

(Urgessa Hirpha, 2023)**.** WetSpass provided estimates for evapotranspiration, surface runoff, and groundwater recharge by utilizing meteorological data and grids of groundwater depth, topography, slope, land use, and soil texture. He pointed out the Gur catchment's annual recharge. Based on the output of the WetSpass Model, the estimated annual runoff, AET, and groundwater recharge of the catchment area, respectively, 426 mm (39% of the precipitation), 561 mm (51% of the precipitation), and 106 mm (10% of the precipitation).

1.7. Method and materials

Various approaches and methodologies were used to assess the catchment's groundwater potential. They are as follows:

1.7.1. Pre-field work

This phase will involve a variety of tasks, such as: -A comprehensive literature review of all previous research in the field of study, whether published or unpublished, to identify any gaps and gather useful data for the investigation. On the ground, primary geological and hydrogeological data were gathered following the collection of secondary data. Hydrological data collection, including water point identification, water sample collection, and well discharge measurement, were the main objectives of the hydrogeological field investigation. Another goal was to identify the rock units that are significant for groundwater.

Shuttle Rader Topography Mission derived DEM (12.5m)from (https://search.asf.alaska.edu/) free land map, land uses land cover from Sentinel-2 (10×10 m) and automatic watershed delineation (https://mghydro.com/watersheds/) are used to delineate the watershed.

For the analysis of the hydrometeorology of the study area, meteorological and well compilation report data were gathered from the National Meteorological Service Agency and the Ambo water and Energy office, respectively.

The main objective of this data is to calculate evapotranspiration. This is used to determine the water balance of the catchment, which helps with the development and management of its water resources by figuring out recharge.

1.7.2. During fieldwork

hydrogeological aspects, including land cover, land use, geology, topography, and the locations of recharge and discharge zones, are assessed both quantitatively and qualitatively. Water samples were collected from boreholes and springs. Temperature, TDS, EC, and pH were measured in the field in real time using an Ec meter and a pH meter. Primary data will be collected from the study area. This entails gathering field measurements, taking pictures for documentation and interpretation, and taking static readings of the water level, elevation, and borehole location as needed.

1.7.3. After fieldwork

The published and unpublished literature on fieldwork, hydrogeological and geological studies, and data interpretation based on field observations and a review of the literature were finally combined. Aquifer classification and productivity identification based on lithological, structural, topographic setting, and recharge conditions of the study area have been characterized based on comprehensive field observations, yield measurements of water points, chemical analysis of water samples, and secondary data.

Software for image processing and final analysis, such as ArcMap 10.8, Global Mapper 12, Google Earth, Surfer 10, and Microsoft Office Excel 2010, was used to interpret the data. Additionally, the spatially distributed water balance model WetSpass-M 1.3 (2016, release date) was utilized to estimate the catchment's recharge amount. GPS is used to georeferenced the locations of water during fieldwork, along with systematic field methodologies. applying a variety of recharge estimation techniques, including chloride mass balance, soil water balance, and Wetspass model.

1.8. Instruments and Tools

Throughout the research process, a range of pertinent software and materials were utilized both in the field and in the laboratory, including instrumentation for analysis. Fieldwork equipment included topographic maps of the region, a pH, temperature, and electrical conductivity (EC) meter, a Global Positioning System (GPS) and compass, and bottles for gathering water samples for testing in the lab.

CHAPTER TWO

2. Description of study area

2.1. Location

Upper Guder Watershed, part of the Upper Blue Nile basin has a drainage area of 2200 km^2 is situated in the Northwest of Ethiopia; in the South-eastern part of the Blue Nile Basin. it is bounded between coordinates 1011758mN to 962477mN latitude and 321928mE to 405109mE longitude, using the UTM coordinate system with the Adindan datum and Z-37 zone, and the elevation within the area ranges from 1700 to 3300 l(m.a.s.l.), the area is located 12 km west of Ambo. Guder is well-known for its Guder River Falls and year-round fruit production utilizing an abundance of local water resources. The Guder River, which is reachable via the Addis Ababa, Ambo, and Guder asphalt road, is the river's outlet as it flows northward from the south.

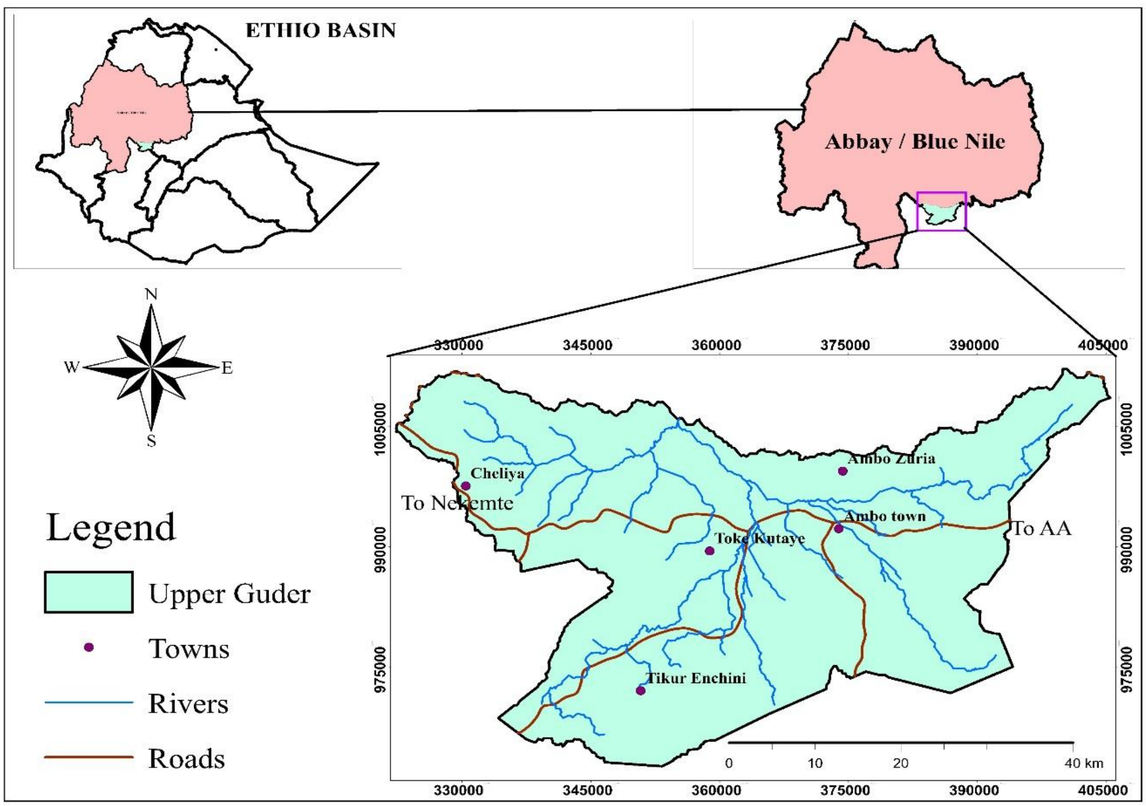

Figure 2. 1 Location map of the study area

2.2. Climate

The study area's climate is categorized as having unimodal characteristics, meaning there is only one wet and one dry season. The dry season runs from November to April, and the rainy season is from May to October. Rainfall is most concentrated in July and August. In the upper Guder Catchment, the main rainy season runs from June to September, exhibiting a monomial rainfall pattern. In addition, there's a shorter wet season from March to May. Because of this shorter rainy season, farmers in the area usually start farming in March.

The climate of the basin fluctuates greatly within a small range of elevations, ranging from cool (in the highlands) to moderately hot (in the relative lowland areas), all because of the topographic variations. The average annual temperature varies from approximately 13°C in the mountainous regions south of Ambo and Guder towns to approximately 28°C in the moderately lowland areas and study area contributes to its relatively mild climate even though it is close equator.

2.3. Physiography

Based on the structural evolution of geological formations, an area's geomorphology provides information about the genesis and description of its landforms (J. The Kattimani, A. Murthy as well as Kumar (2018). The region illustrates both its depositional and erosional landforms in a different sense, using geomorphologic terminology. Many different geomorphological features, including rising hills, rolling plateaus, undulating plains with gently sloping foot slopes, escapements, basins, and colluvial margins, are present in the study area.

The Guder sub-basin is located 1700-3300 m.a.s.l The districts of Toke Kutaye, Dendi, and Chalia are mostly made up of low plateaus and rolling plains. Rolling plateaus with rolling hills at the middle periphery dominate the northwest and northeast of the subbasin, including Chalia Ridge, Roge Mountain, and Dendi Mountain. In contrast, decreasing plateaus predominate in the southern part of Ambo District and Guder Plain.

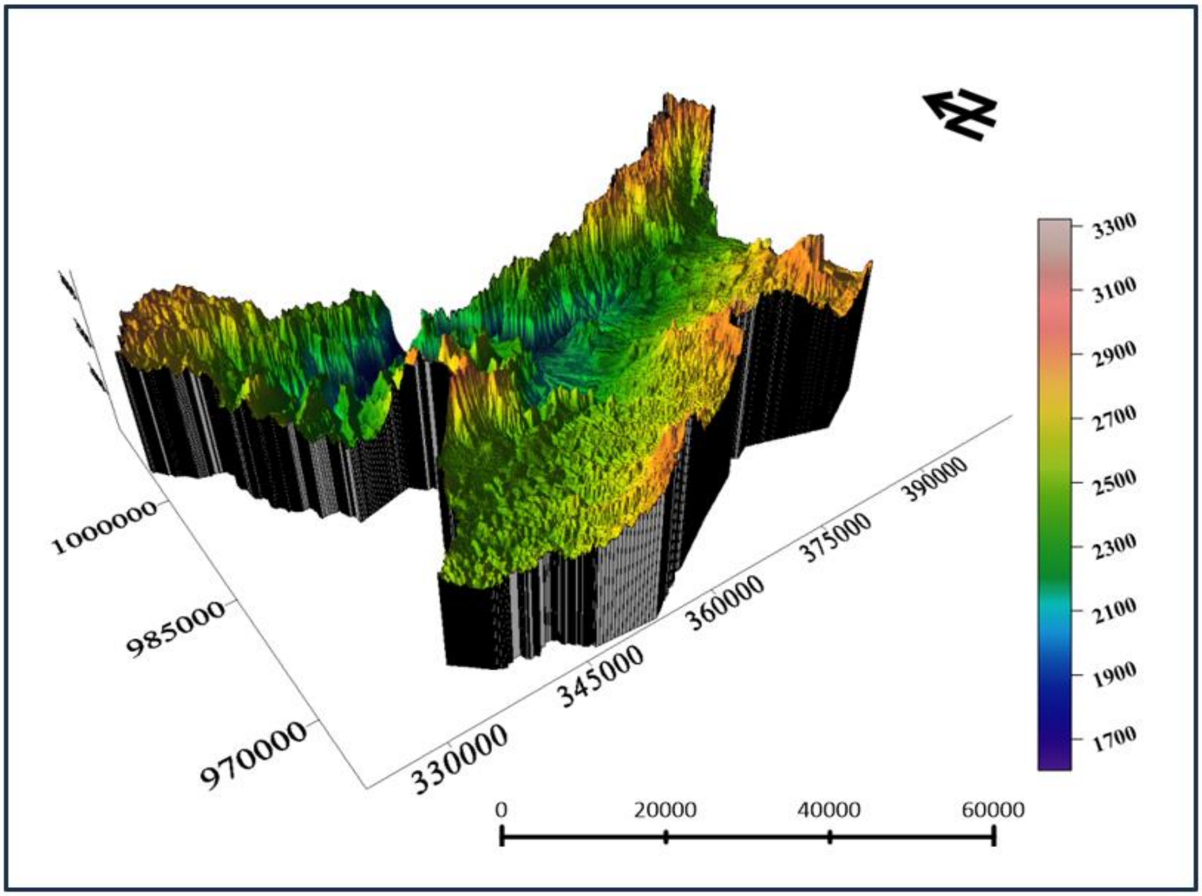

Figure 2. 2 3D physiographic map

The study area typically consists of a flat plain with varying slopes and rugged terrain with deeply cut and dissected morphology and undulating topography. The study area varies in elevation from about 1,700 m.a.s.l to over 3,300 m.a.s.l.

In general, the following land forms make up the study area: A rough-surfaced, mountainous volcanic plateau, Flat top ridge and low plateau with hills in moderate to high relief and Plains with varying landforms and recent deposits.

2.4. Soil

Texture is the primary determinant of soil water-holding capacity, infiltration, and runoff characteristics. Variations in geology, topography, slope gradient, climate, land use/cover, and agricultural practices all affect the distribution and characteristics of different types of soil. The texture of soils derived from fine-grained rocks is fine, while the texture of soils derived from coarse-grained rocks is coarse. This shows that soils reflect their original environment.

The soil's moisture content, infiltration rate, hydraulic conductivity, soil permeability, grain size, and unique composition are all influenced by the texture of the soil, and these factors in turn have a significant impact on recharge potentiality. Clay has a lower capacity for infiltration than loam and sandy loam.

Rainwater is held in reserve in the soil's pores until it seeps down deeper and replenishes the aquifer system. The water that was kept in thin soils evaporated right away, replenishing the aquifer. Thick layers of soil water are either absorbed by plant roots and transpired into the atmosphere, or they join the saturated zone. The three factors of soil texture, soil structure, and soil moisture content determine how much water the soil can hold and move. As a result, the amount of transpiration that occurs depends on the type of soil. Compared to thinner soil, deeper soil can hold more soil moisture, which allows for more water to evaporate. Thus, the hydrogeology of the region is largely determined by the soil.

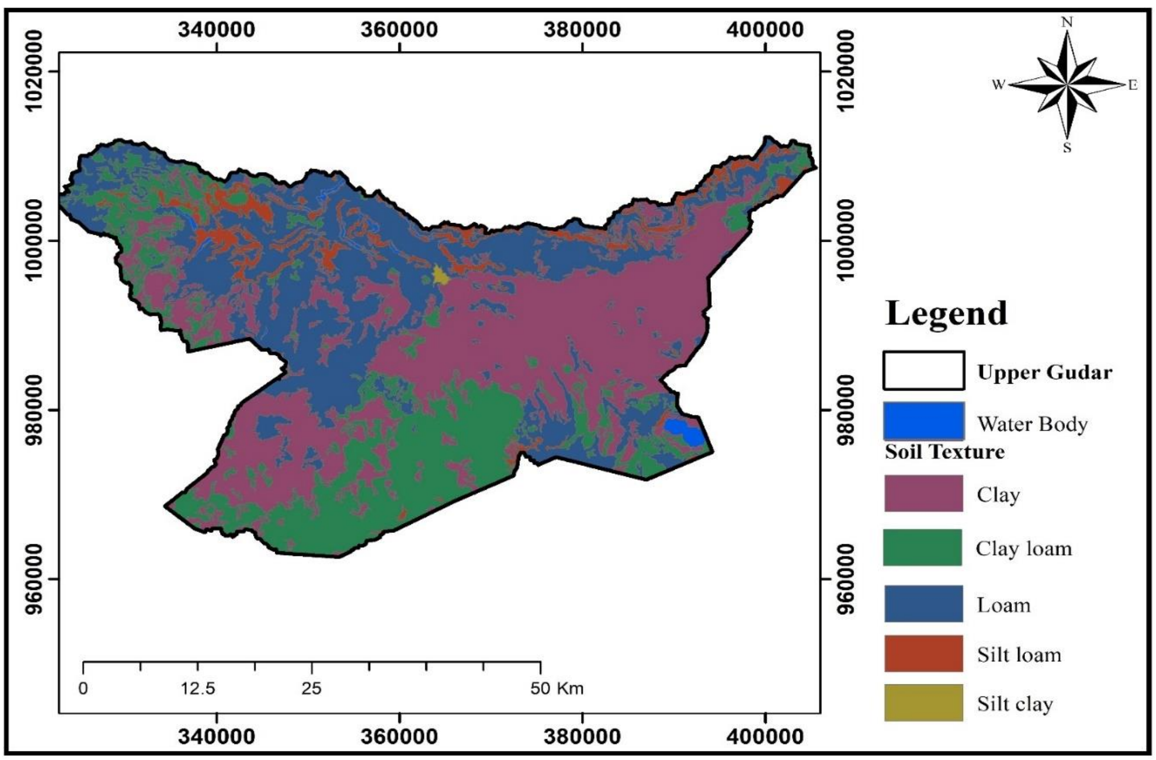

Figure 2. 3. Soil map

Table 2. 1. Texture of the soil in the catchment

Texture class	**Area(km^2)**	**Area (%)**
Clay	836.2	38.01
Clay Loam	500.5	22.75
Loam soil	707.4	32.15
Waterbody	20.6	0.94
silt Loam	2.7	0.12
Silt Clay	132.7	6.03
Total	2200.0	100.00

The statistics (Table 2.1) indicate that five textural categories have dominated the soils in the study area. Clay dominated the upper Guder Basin's soil texture, covering an aerial area of 836.2 km^2 (38.01%). The areas covered by loam and clay loam were 707.4km^2 (32.15%) and 500.5km^2 (22.75%), respectively; the area covered by silt loam was 2.7km^2 (0.12%); the area covered by a water body was 2.6km^2 (0.94%); and the area covered by silt clay was 132.7km^2 (6.03%).

2.5. Drainage

Slope, relief, geology, geomorphology, and structures are all reflected in drainage. It is the configuration of streams in space. A region's drainage patterns are influenced by several factors, including slope, the makeup of the bedrock beneath it, and the locations of faults, fractures, joints, and folds in the geology. A drainage network's pattern and texture can be used to characterize it. Regardless of whether they are used by a perennial or permanent stream, the overall layout of an area's drainage channels forms the drainage pattern.

The upper side of the watershed collects surface runoff from Huluka, Bello, Fetto, Melke, and Indies; the middle part of the watershed collects surface runoff from Dabis; and in the downstream part, Guder xiqqaa (the smaller Guder) and Guder Guddaa (the bigger Guder) that contribute to the main Guder River are some of the major tributaries of the Guder catchment (Nadew et al., 2018).

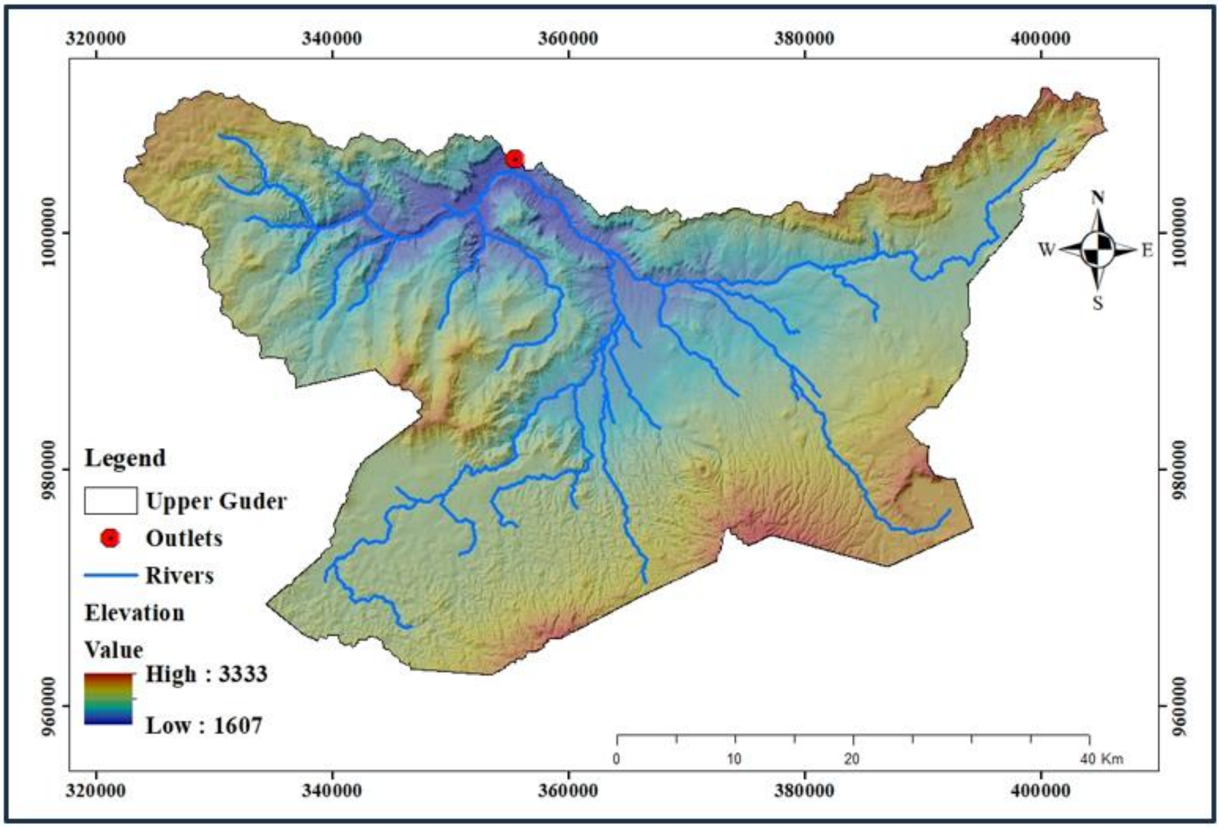

Figure 2. 4. Drainage Map

2.6. Land use and landcover

Any watershed ability to collect runoff, allow infiltration, and replenish groundwater is greatly influenced by the land use and land cover (Ahmad, et.al 2022), in addition to offering soil data on surface water and groundwater levels, soil moisture content, and a prospectus indicator for groundwater.

Land usage has altered the land cover. Vegetation shields the soil's surface from the effects of precipitation. Due to the increased presence of various impermeable surfaces (such as rooftops, asphalt, and concrete), urban areas and urbanization often reduce infiltration rates and increase surface runoff. Vegetation root systems have been shown to increase soil porosity and permeability (Kresic, 2007). Urban settings not only allow for percolation but also enhance water runoff. Most of the basin has been planted with annual crops.

One parameter to consider during a hydrological assessment is vegetation because it has an impact on the infiltration process. The purpose of an area's vegetation cover is to increase water infiltration into the soil and groundwater table, intercept rainfall, and reduce water loss or degradation from surface runoff or flooding. Location-specific variations in altitude, climatic conditions, and population density influence the distribution of vegetation in the study area. With the greatest rainfall, the study area's northern region is largely covered in green forests, while its eastern region, which receives less rainfall, is primarily made up of vast farmlands and sporadic trees (Tsegaye, 2021).

The groundwater potential of the study area was also assessed using the land use and cover of the area. Classifications of land use and land cover were produced by applying ArcGIS 10.8 software to image classification of Sentinel-2A satellite imagery of the study area. The imagery was obtained using Sentinel-2A satellites with various band ranges and 10 m spatial resolution. The following land covers are present in the study area. The study area's land cover and use are depicted on the map (Fig. 2.5).

To allow for maturation and harvesting during the dry season (October-January), crops are shown during or right after the rainy season (June-September). Rainfed crops grown in the subbasin include teff, wheat, barley, maize, sorghum, fava beans, field peas, linseed, oats, potatoes, head cabbage, onion, tomato, shallot, red/green pepper, garlic, beetroot, carrot, taro, sweet potato, sugarcane, and other major vegetable crops.

After December's crop harvest, which is dependent on residual moisture, soil preparation is the first step in irrigation during the dry season. You can stagger the planting dates from January to March, depending on the crop. Maize and vegetables (tomato, potato, onion, shallot, garlic, head cabbage, and beetroot) are planted with irrigation water during the growing season. According to OWWDSE (2018).

The watershed's farming method dates back hundreds of years and involves raising cattle and producing cereal crops using oxen plows. Because of this, the main land use types in the watershed are plantations, grazed, extremely sparse, shrub/bushes, and various other lands and forest areas (Timketa.et.al, (2020)).

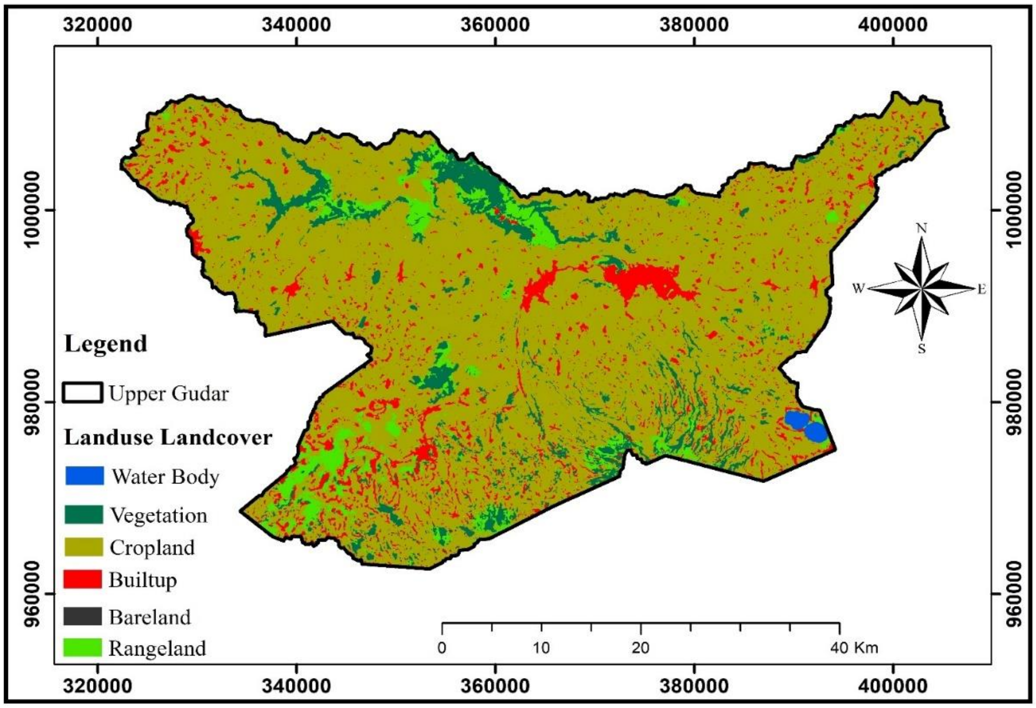

Figure 2. 5. Land-use and land-cover map

Guder xiqqaa (smaller Guder) and Guder Guddaa (larger Guder) are the two main river routes that are dominated by trees and vegetation. The area used to be extensively vegetated, but due to population growth, it is now only sparsely vegetated. Population growth and deforestation are occurring at the same time due to the high demand for wood, charcoal, and building materials.

Table 2. 2. The percentage of land utilized within the total area covered

Land use class	Area(km^2)	Area (%)
Waterbody	7.8	0.4
Trees	161.7	7.3
Crops	1741.9	79.2
Built up	176.1	8.0
Others	1.4	0.1
Rangeland	111.2	5.1
Total	**2200**	**100.0**

The statistics indicate that six land-use categories have dominated the land use/cover of the study area (Table 2.2). Crops dominated the upper Guder Basin's land cover, covering an aerial area of 1741.9 km^2 (79.2%). The next largest land areas were 167.7km^2 (7.3%) and 111.2 km^2 (5.1%) for tree land and grassland, respectively; the built-up area was 176.1 km^2 (8%); the water body was 7.8 km^2 (0.4%); and the other land was 1.4 km^2 (0.1%).

CHAPTER THREE

3. Regional Geology

There are four main physiographic regions in Ethiopia: The Main Ethiopian Rift (MER), the Afar Depression (AD), the Western Plateau, and the Southeast Plateau. The Precambrian rocks of the Afro-Arabian Shield are located beneath the Ethiopian plateau. The majority of the Permian to Paleogene glacial and marine sediments, as well as Tertiary volcanic rocks and associated sediments, cover the Precambrian basement. Precambrian basement exposures can be found in the following locations: Tibet in the north, Sidamo and Bale in the south, Gojam, Wollega, Illubabor, and Kefa in the west along the Sudan border, and Harerghe in the east. Ethiopia's Precambrian rocks include high-grade gneiss, sedimentary rocks from metamorphosed volcanoes, and related ultramafic and mafic intrusive that ranging from mafic to granitic composition.

Precambrian rock, the oldest in the region, is found in the basement. Mesozoic sedimentary succession and/or Cenozoic volcanic rocks lie beneath this basement rock. This generalization does not apply in some situations, such as those where the basement rocks are exposed to the atmosphere or have sediments from the Quaternary or Paleozoic era covering them.

Precambrian rocks are exposed throughout the region, particularly in the northern (Tigray region), southern, and western areas. They are composed of numerous intrusive bodies as well as a variety of high-, medium-, and low-grade metamorphic rocks, including gneisses, schists, and other meta-volcano sedimentary rocks. Sea transgression-regression, which includes both marine and continental depositions and is similar to the Abay basin, formed the entire stratigraphic successions of Mesozoic sedimentary rocks, including lower and upper sandstone, limestone, shales, mudstones, and marls (Antalo) (Kazmin, 1975).

The majority of the country's eastern region and several steep valley gorges are now covered in sedimentary rocks that were deposited by early Mesozoic marine intrusion from the SE and NW. The only indication of deposition in the central and western parts of Ethiopia during the Mesozoic era comes from a thin unit of presumably continental sediments (Mohr, 1971). These regions of Ethiopia were still continental land areas. The country's remaining sedimentary rocks originated in the late Paleozoic era. Sedimentary rocks have since evolved. Sedimentary rocks from the late

Paleozoic and Mesozoic periods and Quaternary deposits account for 25% and 20%, respectively, of the region total outcrop.

Sea transgression and regression brought on by epeirogenic sinking and rising (uplifting) of Africa's coastline resulted in the deposition of Mesozoic sedimentary rocks. For sea transgression, the axis was SE-NW, and for regression, the opposite was true. The age range varies within each unit along the SE-NW axis of transgression and regression, and the lower and upper sandstones were deposited during sea transgression and regression, respectively. The Antalo group formed in the intermediate between the two episodes, according to Mohr (1971), who divided Mesozoic rocks into the following three groupings based on lithology rather than age.

The lower sandstone is generally recognized as quartz sandstone because of its massive, thickly bedded texture with occasional cross-bedding, quartz over feldspar predominance, fine to medium grain size, and conglomerates that are rich in iron, particularly near the base. Less thick sandstone is generally uniform within a given region, though it varies from place to place. According to Mohr, (1971) estimated that the average thickness of the Abay Basin was 500 m.

Kazmin (1975) states that the Antalo group includes the Agula Shale (which correlates to Mugher Mudstone), the Abay bed, and the Antalo limestone. In contrast to certain areas in southeast Ethiopia, the basement in both northern and central Ethiopia is not directly covered by the Antalo limestone (Mohr, 1971). The most westerly exposure of Upper sandstone in the Abay basin can be found in Mugher Gorge. Both the Antalo limestone and Upper sandstone are absent from the Guder valley near the confluence with Abay.

A significant portion of the land (roughly 32 %) is covered in volcanic rocks of various ages. Age (tertiary and Quaternary volcanic) and rift formation (pre-rift and post-rift volcanic) are two categories that can be used to categorize these volcanic rocks. The terms Trap series and Aden volcanic series, which are interchangeable with post-rift (middle Miocene to Quaternary) volcanic, are also frequently used to characterize the nation's volcanic rocks. Though it is younger, the Aden volcanic series is the oldest in the nation.

The major elevation that was followed by the breaking of the horn of Africa created the Trap series. Particularly in the upper section, it is primarily flood basalt with some trachyte and rhyolites. The

NW and SE plateaus are the result of this trap series, which reaches a maximum thickness of 3 km in central Ethiopia, (Mengesha, T.et.al, (1996) its whole stratigraphy can be seen in deep gorges.

The western Precambrian basement is covered by sandstone from the Paleozoic and Mesozoic eras or tertiary volcanic products. The Abbay sedimentary sequence in central Ethiopia is assumed to extend southward into sandstone (Geological Survey of Ethiopia, 2000). Most of the Ethiopian plateaus are composed of trap series, which are tertiary volcanic that span western Ethiopia. The west and southeast of Ethiopia's volcanic plateau are distinct regions.

The regional and large E-W-oriented rift transversal structure known as the Addis Ababa Nekemte tectonic line (Tasisa,et.al, (2015)) or the Yerer-Tulu Wollel Volcano Tectonic Lineament (YTVL) (Tsegaye Abebe, et al., 1998) has divided the western plateau volcanic into Northwestern and Southwestern Plateau. The southwestern plateau, which includes the study area, is distinguished by heavier volcanic rock.

According to Mohr (1971), quaternary volcanism was not confined to the Rift but also happened on the plateaus. (Mengesha, T. et.al,1996) states that the majority of the Quaternary alkaline basalts found in the western Shewa Zone on the NW Plateau are Quaternary volcanic. (Mengesha, T.et.al, (1996), On the plateaus to the northwest and southeast, these Quaternary alkaline basalts and tachytes erupted along pre-existing structures. Their recent age is indicated by their well-preserved structures and/or unaltered geomorphologic features, such as small collapsing craters and cinder cones.

Several faults cross the Rift system in the northwest Ethiopian plateau, despite the country's main geological structures generally running parallel to it. A line segment that runs east-west from the Cassam River in the east through Addis Ababa to Ambo in the west is an example of this. Commencing at the western escarpment of the rift and extending even farther to Wollega, this lineament is known as the Ambo fault belt (Mengesha, T.et.al, (1996).

3.1. Local Geology

The study area is a portion of the central plateau of Ethiopia and is made up of Mesozoic sedimentary rocks, specifically sandstone, pyroclastic deposits like unwelded tuff, and volcanic rocks of various kinds, mostly basaltic and trachytic lava flows. The area was mapped under Quaternary plateau basalt which included trachyte and alkaline basalt. However, the Ethiopian trap series, which dates from the Oligocene to the Miocene, includes the northern portion of the study area, which forms an east-west-oriented basaltic escarpment. It falls under the transitional alkaline basalt Termaber-Magazaz formation on the 1996 revised geological map of Ethiopia. The Addis-Ambo-Guder fault escarpment divides this older basaltic lava flow from the younger Quaternary volcanic of the Ambo area.

Plate 3.1. Outcrop of Teramber-Magazaz formation

The study area is part of the Quaternary volcanic region that covers the southern side of the fault escarpment; the northern side of the escarpment is Tertiary in age. The term "Addis-Guder fault escarpment" is used by some researchers, including (Tsegaye Abebe, 1993).

The central type volcanoes, Wenchi and Dandi, which are situated in the southern portion of the study area, are assumed to be the source of the Quaternary volcanics in the region (Tsegaye Abebe, 1993). The Yerer-Tullu Welle Volcano-Tectonic Lineament, which is a representation of the east-west oriented volcano-tectonic lineament, includes the central type volcanoes of Wenchi and Dandi on the Ethiopian plateau (Tsegaye Abebe, et al., 1998).

There are two main steps on the escarpment to the northern side of the Dabis River: the first is the Mesozoic sandstone cliff next to the Dabis River. When it reaches the other side of the Awaro area, this cliff pinches out. Beyond the sandstone lies the next extreme cliff, which is made up primarily of basalt volcanic rocks. This second phase continues even further eastward throughout the study area. In the study area, the general stratigraphy is as follows, arranged from youngest to oldest: Quaternary volcanic (basalt, trachyte, and pyroclastic deposits), Tertiary volcanic (basaltic lava flow), and Mesozoic Sandstone.

3.1.1. Paleozoic Sandstone (Plst)

In the study area's northwest and western gorges of the Abay and Guder rivers, sandstone (Abay sandstone) is exposed. The sandstone that covers the foliated granite and biotite gneiss is non-conformably layered on top of the Mesozoic sandstone unit (Ilfious.W, 2008). Its lithology is typified by varying concentrations of mudstone, sandstone, siltstone, shale, and some paleosoil. Shale predominates at the bottom, while sandstone dominates at the top. Siltstone often occupies the middle section, and mudstone occurs as intercalation inside each unit. A 2-3 m thick layer of paleosoil has formed between the Paleozoic and Mesozoic sandstones. The sandstone unit in some outcrops can have a thickness of 200 m.

The color of sandstone can be light gray, reddish brown, or yellowish-grey. The sandstone has a medium to coarse-grained texture, some conglomeratic texture, and a strong to moderate brown color. When it's new, it's light gray, but as it ages, it turns reddish brown. Sandstone has some jointing and is highly compacted. There are also siltstone, large and compacted mudstone, and severely fractured shale intercalations.

3.1.2. Mesozoic Sandstone (Msst)

Parts of the region that are located in the north, west, southwest, and center contain this sandstone unit, also known as Lower Sandstone. The Abay and Guder River gorges' cliffs are the result of it; they are formed above Paleozoic sandstone and basement rocks and below volcanic rocks, mainly below Mesozoic limestone. Thicker than 1,131 m is possible (Ilfious, 2008). Paleosoil, mudstone, and siltstone are thinly intercalated throughout the sandstone-dominated succession. Reddish brown to light gray, the uppermost layer is conglomeratic, fine to medium-grained. It forms lamination and cross-bedding structures most of the time. A significant amount of weathering and fracture is present in the upper half.

3.1.3. Tertiary Volcanic Rocks

Most of the Ethiopian plateau is made up of tertiary volcanic rocks. From highly viscous acidic rhyolite that represents a fissured and central type of volcanism to liquid basalt rocks, they are found in a wide range of environments. There have been varying lengths of time when rivers, lakes, and soils within volcanic sequences have developed after volcanic episodes and lava flows.

3.1.4. Olivine – Plagioclase Porphyric Basalt (Tv2)

In the center and south of the map, this basalt (Tarmaber-Megzeze basalt) is visible. Because of fissure eruption, it typically takes the shape of a plateau with a moderate slope. Certain locations also feature extensive ridges and mountains, like the Chilmo and Cheleka Mountains. Concerning the upper sandstone and the lower ignimbrite, the basalt rests non-conformably and conformably. Different compositions and structures are found in its tiered layers. Aphanitic to porphyritic, with occasionally very coarse-grained porphyritic basalt and vesicular basalt, make up the layers. Spheroidal weathering, intense fracture, and columnar jointing are all typical features. (Meten et al., 2015) Distinguish this unit by differences in composition and structure into porphyritic aphanitic and very coarse-grained porphyritic basalt. Strong weathering and fractures are visible in the rock.

3.1.5. Adigrat Sandstone (Ms)

This unit is exposed in the northwest and southern regions of the study area, at the base of the Kella horst, and in the Serkole River close to Ambo town. In fresh samples, brown grey to dark gray, and in aged samples, pinkish yellow to reddish brown, are the most common fine- to medium-grained, light gray outcrops. Its maximum thickness of 150 meters is reached at the Kella horse formation cliffs. Because of the thick and uneven bed, it is enormous. Efrem Beshawered (2010) states that although the beds are generally horizontal, there are some places where they are mild to severely slanted to the west. The biotite gneiss in the Kella horst indicates that this unit is nonconformable. There is a slight difference in the sandstone exposed to the northwest of the study area near Ambo town. It is available in red, yellow, or light grey. This unit is composed of colored mudstone and intercalated siltstone from the Ambo quarry. The mudstone has a thickness ranging from 0.5 to 1 m. As stated by (Beshawered.et.al, 2010), its grain size is typically fine- to medium-grained, somewhat sorted, and arranged texturally in a mesukurtic to lipturitic type. Ripple marks, cross-stratification, and lamination are the most common sedimentary structures to form.

Plate 3.2. Adigrat sandstone at Ambo Quary site

3.1.6. Babich-Guder basalt (Npb)

This unit has exposed topography that is rocky and undulating in the northeastern corner of the map. It is a fine-grained, opaque, black rock primarily composed of plagioclase pyroxene (Beshawered.et.al, 2010). It is usually compact, with either no secondary material present or filled vesicular cavities. This granite has been extensively weathered, as evidenced by the exposure of the rock on the Guder to Babich road. In certain outcrops, the rock is sliced by quartz veins and dykes.

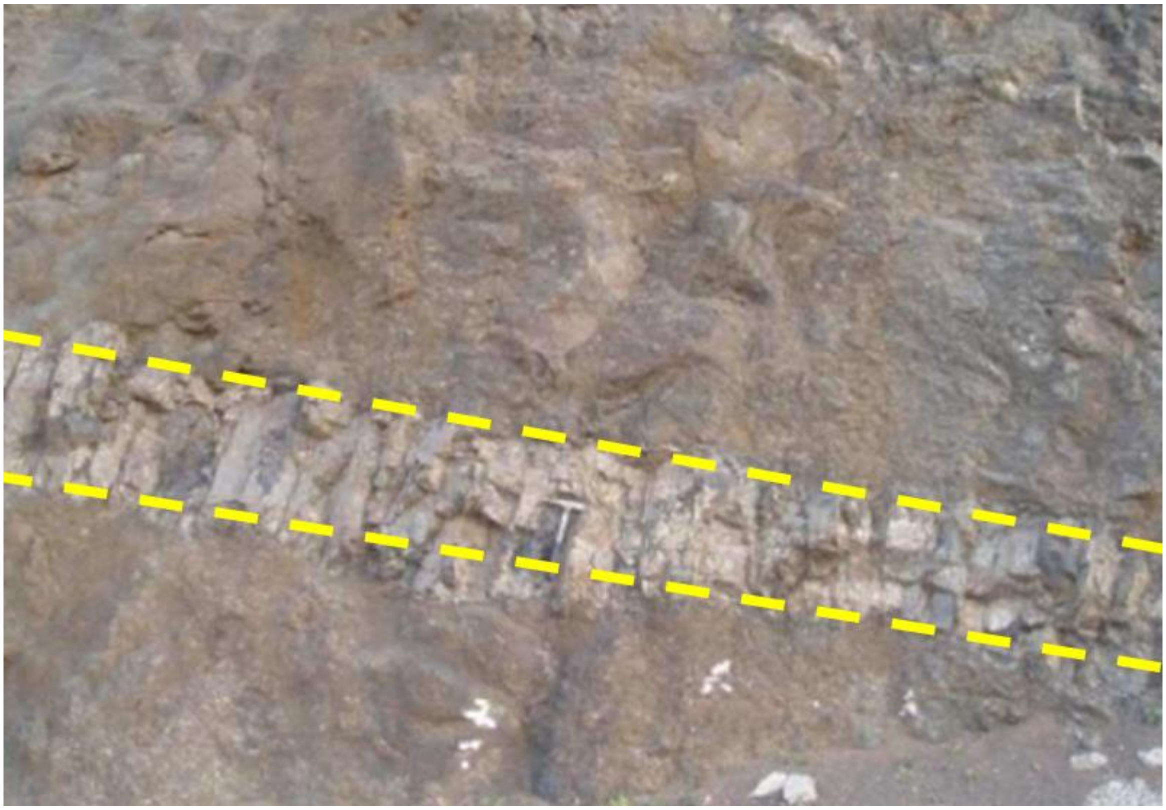

Plate 3.3. Exposure of Babicha-Guder Basalt cut by a diorite dyke on the way Guder to Gedyo

3.1.7. Woliso Ambo Basalts

The northern and western boundaries of the mapped area expose the Woliso Ambo basalt rock unit. It is made up of minimal Tuff, basalt breccias, and porphyritic basalt with much larger-sized crystals of pyroxene, olivine, and plagioclase (Tsegaye Abebe et al., 1999). This unit, which spans from the Pliocene to the present, is described as a link between basalt lava flows and volcanic centers (QVCB) in the Woliso region.

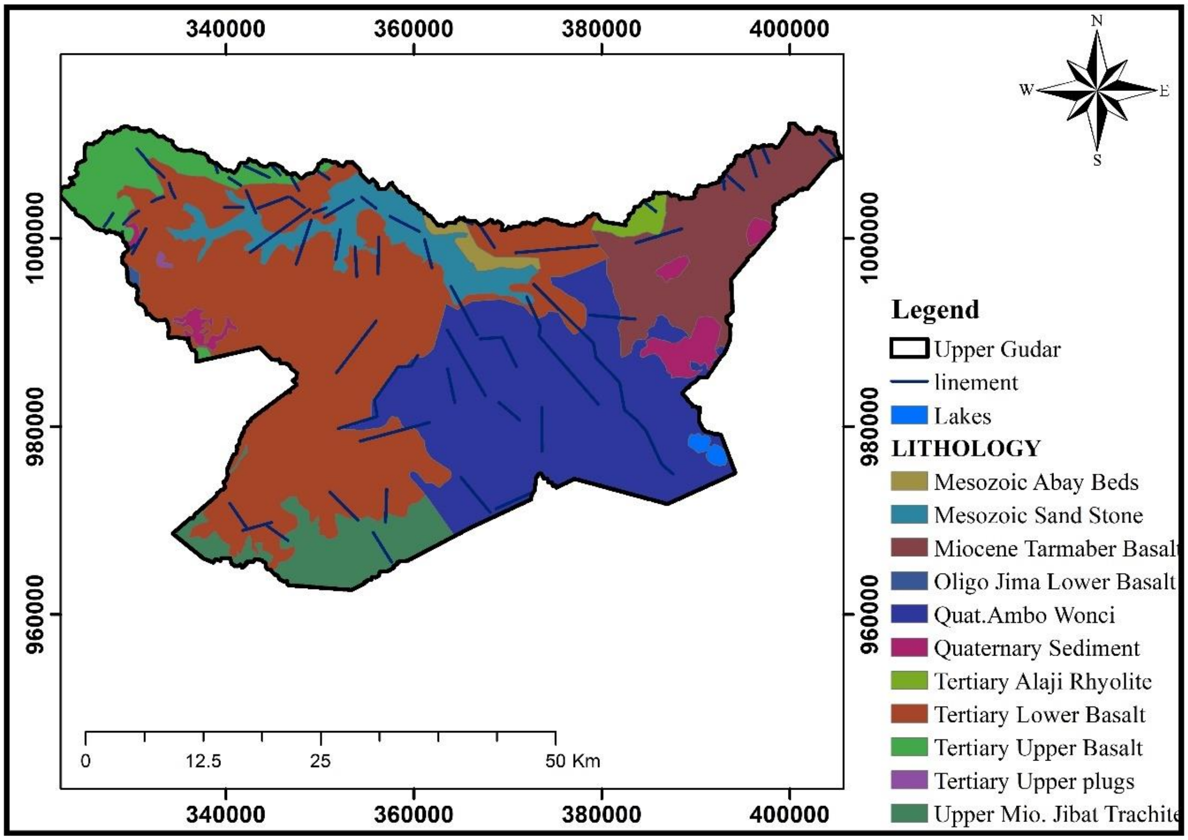

Figure 3. 1. Geological map

The study area included a variety of lithological units, including: - Biotite and Hornblende gneisses; granulite and migmatite with minor metasedimentary gneiss; Basalt flows; scatter cones and hyaloclastites; and the Gabredarre Formation (Kimmeridgian-Tithonian; (Jg2) Upper unit) and (Jg1) Lower unit (limestone with shaly and gypsiferous units).

3.2. Geological structures

Normal faults, bedding and joints, block faulting, fissuring, and tilting of the rocks are some of the geological structures that affect the area's different rock units. The process of interpreting satellite imagery identifies two sets of fault features. Additionally noted is the extensive brittle deformation characterized by fractures and dislocations, according to WWDSE (2008):

1. All of the western escarpment's rock types are impacted by the oldest fault system, the NW fault system, which has a long history. Their age may extend to the early Paleozoic, but they were reactivated later with the main tectonic event in the region. Their crustal scale

served as a conduit for the extensive volcanic formation in the area. This NW fault system can be connected to the Bede Gebaba - Wecheca volcanic belt's trend.

2. The Ethiopian Rift margin's upper boundary, the EW fault system, runs roughly E-W north of the Addis Ababa Ambo Road. These are significant faults that heavily impact the Tarmaber basalt in the region on the western plateau.

The area is located within the Yerer-Tullu-Wellel volcano-tectonic lineament zone. Afar Rift (Western margin), the Red Sea, the southern edge of the Gulf of Aden, and the MER are the four main azimuthal strands identified in the region based on the Yerer-Tullu-Wellel volcano-tectonic lineament analysis (Tsegaye Abebe,1998). These volcanoes are located at the intersections of the North West and North East trends. The alignment of the volcanics along the YTVL is intrinsically linked to the formation of the east-west trend. The geothermal hot springs are oriented along the much younger Ambo-Butajira line, which trends from northwest to southeast and descends southeast. On the north edge of the basin, this structure cuts across every lithostratigraphic secession.

CHAPTER FOUR

4.1. Hydrometeorological Description

A science that unites meteorology and hydrology is called hydrometeorology. It examines the hydrological cycle, which includes processes at the surface of the earth and in the atmosphere (Shaw.E.M, 1994). The hydrometeorological elements of precipitation, wind speed, evapotranspiration, sunlight hours, humidity, and air temperature are the most useful. Determining evapotranspiration is the primary goal of studying hydrometeorological data. This figure is then used to compute the catchment's water balance, which aids in the development and management of the water resource by figuring out recharge.

4.1.1. Sunshine

The process of groundwater recharge depends heavily on sunshine. Water from lakes, oceans, and other bodies of water evaporates when sunlight strikes the surface of the Earth. When this water evaporates, it condenses into clouds and eventually returns as precipitation, recharging groundwater supplies.

Sunshine has a major effect on groundwater levels in arid regions. (Smith, A., Johnson, B., & Lee, C, 2023) According to the study, exposure to more sunlight raised evaporation rates, which in turn affected groundwater recharge. For sustainable management of water resources, particularly in regions where water scarcity is a concern, an understanding of this relationship is imperative.

The factors that cause incoming solar radiation to be absorbed, scattered, and reflected vary in height, cloud cover, vegetation, and seasonal variations. These factors also affect the length and intensity of Sunshine Hour. Evapotranspiration is directly correlated with sunshine hour. Three stations with available sunshine hour records are located in the study area. Seasonal variation in weather conditions is shown by the data. The calculated value rises from July's minimum (3) to October's maximum (11.1). Rainfall causes clouds and fog to obscure the atmosphere during the rainy season, reducing the amount of time that sunlight can reach the surface. Thus, during the dry season, when the sky is clear, the study area experiences high sunshine hours, which decrease during the intensely rainy (Kiremt) months.

Table 4. 1. Long term means monthly sunshine hours of the study area.

Months	Jan	Feb	Mar	Apr	May	Jun	Jul	Aug	Sep	Oct	Nov	Dec	Annual
Mean	9.7	10.2	8.6	8.4	8.6	7.0	3.7	3.7	7.5	10.0	10.2	10.0	8.13

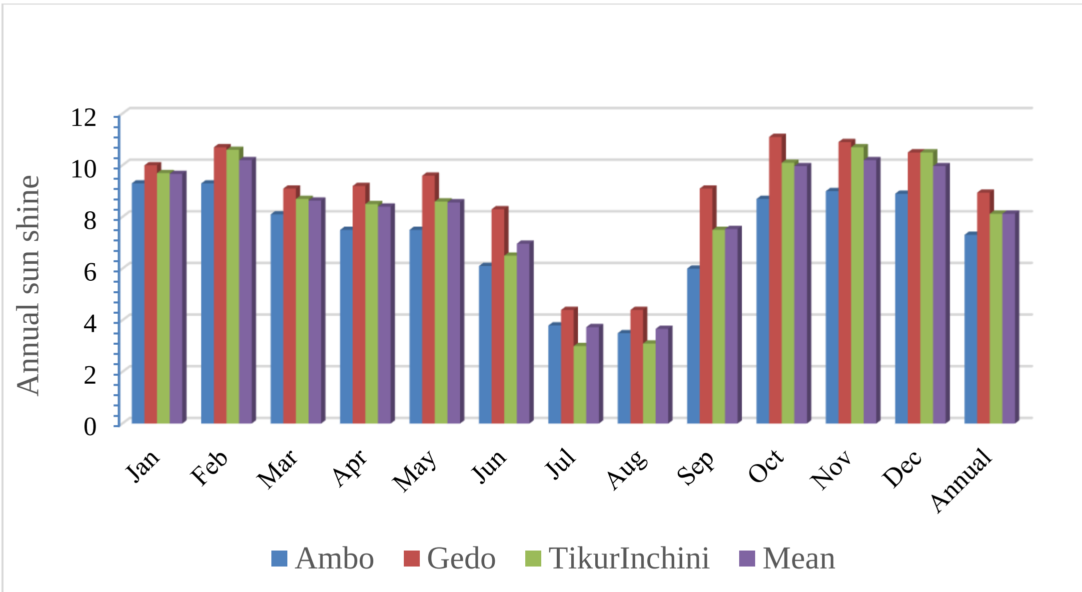

Figure 4. 1 . Mean monthly sunshine hour for available stations in the study area

4.1.2. Wind speed

The quickness and slowness of pressure-controlled air movements is known as wind speed. Turbulence and wind speed affect moisture transfer and air movement. Since the saturated vapor above the surface cannot be instantly removed, the rate of evaporation decreases as the wind speed decreases.

In groundwater studies, windspeed can also be very important, especially when it comes to the transpiration and evaporation of groundwater. Elevated wind speeds have the potential to accelerate the evaporation of surface water bodies, thereby causing fluctuations in groundwater levels. Winds can also modify the movement of water vapor in the atmosphere, which can have an impact on precipitation patterns and, in turn, groundwater recharge.

The effect of wind speed on groundwater dynamics in a coastal aquifer system was investigated by (Garcia, M., Martinez, J., & Lopez, A., 2022). The study showed that changes in wind speed had a direct impact on the rate of evapotranspiration, which in turn had an impact on groundwater levels. Accurate modeling and long-term groundwater resource management depend on an understanding of the connection between wind speed and groundwater processes.

The wind speed data measured at height of 2 m above the ground level was obtained from five stations (Ambo, Gedo, Tikur inchini, Dendi, and Hamus Gaba) showing spatial variation. Higher wind speed is recorded in Dendi and Tikur Inchini while Ambo shows low wind speed record relative to them. Because Dendi and Tikur Inichini are extremely elevated areas of the catchment and have higher average wind speeds than the other stations, this variation is directly related to the topographic altitude of the stations. At the start of the spring rainy season, the catchment's wind speeds increase.

This is a common occurrence in the country's west during the early rainy season. During this period, winds that carry moisture from various directions most frequently, the westerly trade wind blows strongly toward the study area, bringing with it the spring rainfall. The catchment experiences its highest wind speed during these months. However, it gradually declines as spring ends and summer rain approaches. The average monthly wind speed in the area is 1.55 m/s, with variations from 1.1 m/s in September to 2.0 m/s in February.

Table 4. 2. Long term means monthly wind speed (m/s) at 2 m above ground of the study area.

Months	Jan	Feb	Mar	Apr	May	Jun	Jul	Aug	Sep	Oct	Nov	Dec	Annual
Ambo	1.9	2.1	1.9	1.7	1.3	1	0.9	0.8	0.9	1.4	1.8	1.9	1.47
Gedo	1.6	1.7	1.7	1.9	1.7	1.3	1.2	1.1	1.1	1.6	1.6	1.6	1.51
T/Inchini	1.8	2	1.9	1.9	1.6	1.4	1.4	1.2	1.3	1.8	1.9	1.8	1.67
Mean	1.77	1.93	1.83	1.83	1.53	1.23	1.17	1.03	1.10	1.60	1.77	1.77	1.55

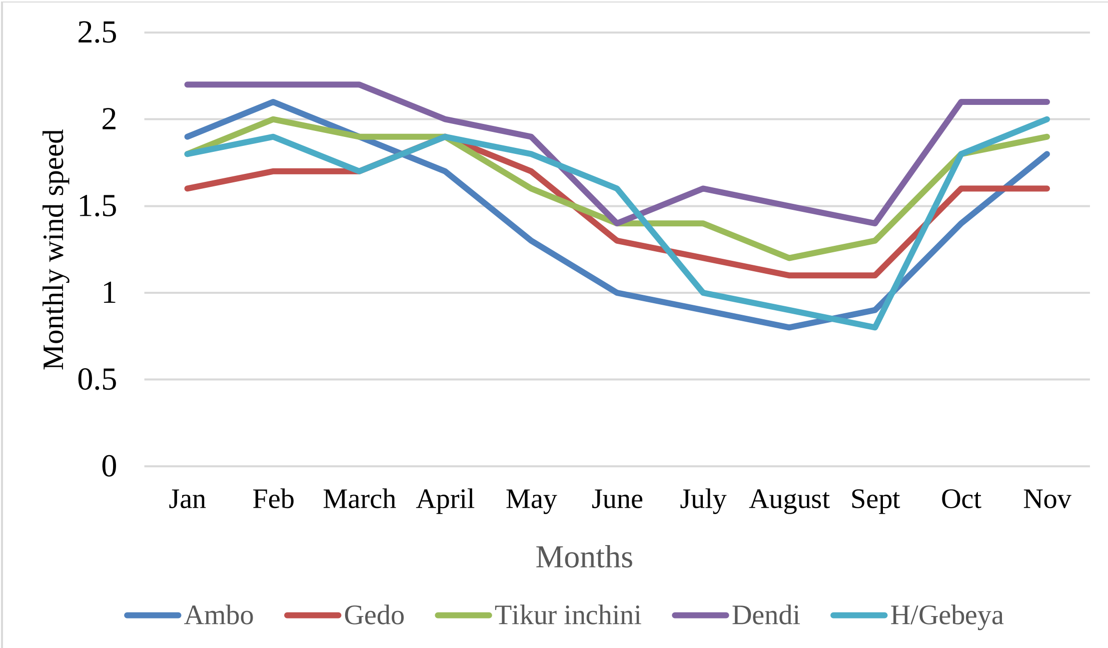

Figure 4. 2 . Mean monthly wind speed.

4.1.3. Temperature

The rate at which water molecules evaporate and become water vapor in the air above is determined by temperature. It's one of the hydrometeorological factors that actively influences water availability. Because water evaporates quickly before percolating in hotter climates, there is less water available for recharge in those areas than in cooler ones.

(Smerdon, J. E., et al., 2020) In groundwater studies, temperature is important because it can reveal important details about the geothermal gradient, groundwater flow patterns, and possible contamination sources. Hydrogeologists can learn more about subsurface processes and manage water resources by keeping an eye on temperature fluctuations in wells and boreholes.

(Li, X., et al., 2021)The importance of ongoing monitoring in identifying environmental trends is highlighted by the possibility that variations in groundwater temperature may be a sign of the effects of climate change on aquifer systems. Furthermore, a deeper comprehension of groundwater dynamics is now possible thanks to improvements in temperature logging technologies that have made measurements more accurate.

Six meteorological stations, both inside and outside the study areas, provided temperature data over a range of periods. The monthly average and minimum temperatures gathered from the stations at Tikur Inchini, Ambo, Gedo, Hamus Gaba, Toke Kutaye, and Guder computed mean Temperature shown in the corresponding Diagram.

The range of average temperature is 6.1ºC to 26.2ºC. Ambo station records the highest mean temperature, while Toke Kutaye station records the lowest. The months of December, January, February, and March are the hottest. August and July have comparatively low temperatures.

Table 4. 3. Long term means monthly Temperature of the study area.

Stations		Jan	Feb	Mar	Apr	May	Jun	Jul	Aug	Sep	Oct	Nov	Dec
Guder	Tmax	22.8	23.8	23.8	23.6	23.1	21.5	19.4	19.3	20.3	21.5	21.8	22.1
	Tmin	8.9	9.9	10.7	11.0	10.9	10.7	10.4	10.2	9.9	9.1	8.9	8.3
	Taverega	15.9	16.8	17.2	17.3	17.0	16.1	14.9	14.8	15.1	15.3	15.4	15.2
Toke kutaye	Tmax	22.8	23.8	23.8	23.6	23.1	21.5	19.4	19.3	20.3	21.5	21.8	22.1
	Tmin	6.6	7.7	8.4	8.8	8.8	8.6	8.3	8.3	7.9	7.0	6.6	6.1
	Taverega	14.7	15.7	16.1	16.2	16.0	15.0	13.9	13.8	14.1	14.2	14.2	14.1
Tikur Enchini	Tmax	25.2	25.9	25.8	25.6	24.8	22.5	20.8	21.0	22.0	23.5	24.2	24.7
	Tmin	8.3	9.3	9.9	10.3	10.4	10.2	9.8	9.8	9.6	9.0	8.5	8.1
	Taverega	16.7	17.6	17.8	17.9	17.6	16.3	15.3	15.4	15.8	16.2	16.4	16.4
Gedo	Tmax	23.1	23.7	23.6	23.5	22.5	20.2	18.3	18.4	19.5	21.1	21.7	22.3
	Tmin	7.9	8.6	8.9	9.2	9.3	8.9	8.3	8.2	8.3	8.3	8.3	7.8
	Taverega	15.5	16.2	16.2	16.4	15.9	14.5	13.3	13.3	13.9	14.7	15.0	15.0
Dendi	Tmax	24.3	25.4	25.5	25.1	25.0	23.8	21.7	21.4	22.4	23.5	23.9	23.9
	Tmin	8.2	9.4	10.5	10.9	10.8	10.8	10.8	10.6	10.0	8.7	8.0	7.7
	Taverega	16.3	17.4	18.0	18.0	17.9	17.3	16.3	16.0	16.2	16.1	15.9	15.8

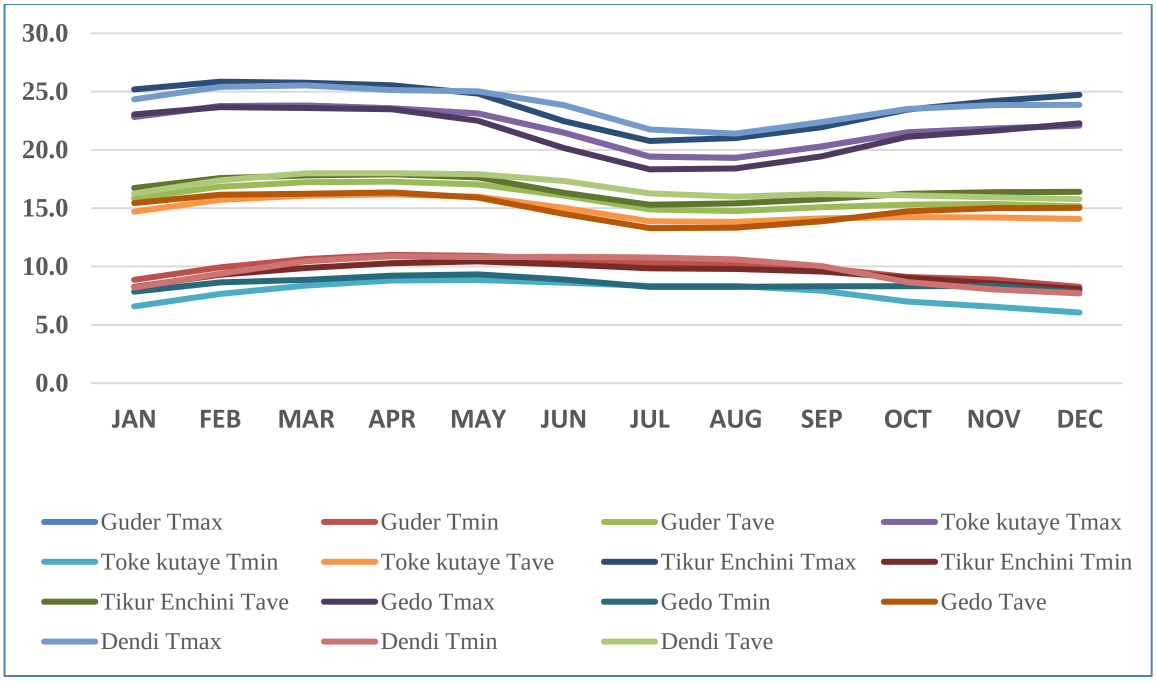

Figure 4. 3 .Mean monthly Temperature.

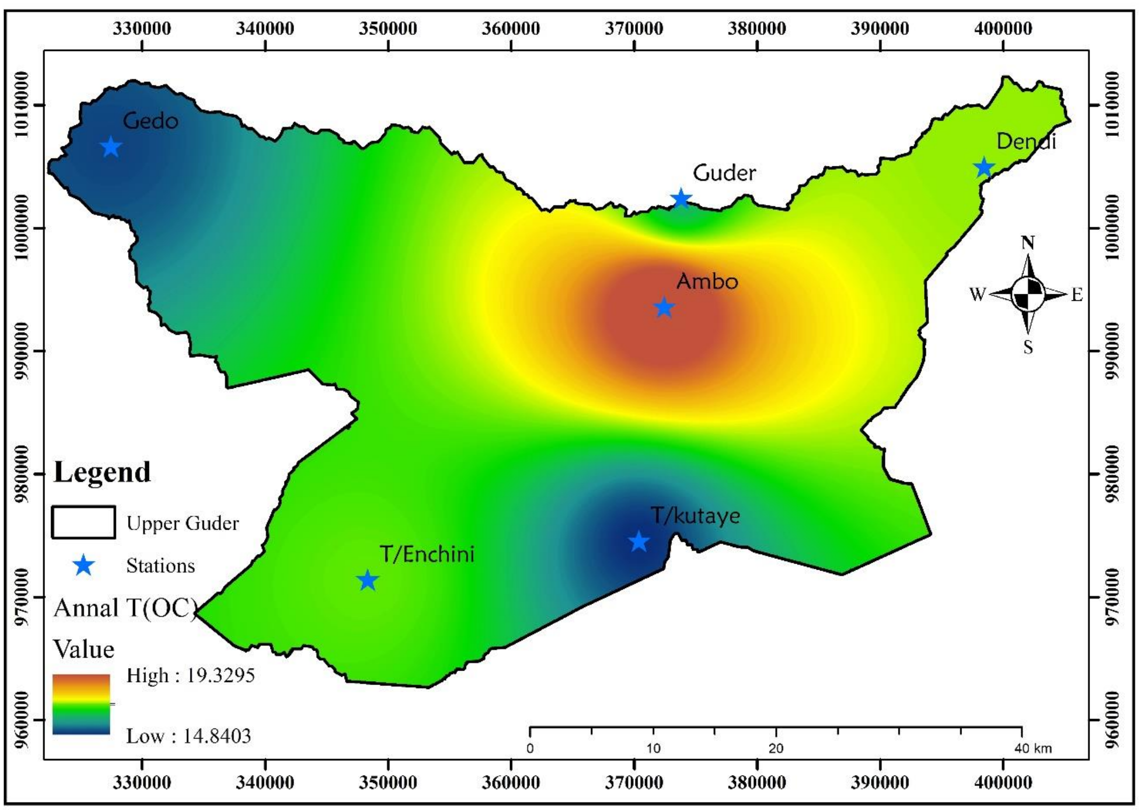

Figure 4. 4. Temperature map

4.1.4. Precipitation

(Trenberth, K. E., (2011))when water vapor in the atmosphere condenses into droplets and descends to the ground, it is known as rainfall, and it is an essential part of Earth's water cycle. It serves as the main supply of freshwater for use by humans, animals, and plants. Globally, there are differences in rainfall patterns, which have an impact on climate, agriculture, and ecosystems. For different natural processes and the continuation of life on Earth, there must be enough rainfall.

Precipitation's seasonal and spatial variations have a major impact on hydrology; in certain cases, they are critical to groundwater dynamics, river flow, and recharge. It is well known that variations in the Inter-Tropical Convergence zone's surface position have an impact on the distribution and intensity of rainfall in Ethiopia. The majority of the Upper Guder Catchment's annual rainfall occurs during this time, reaching up to 75% when rains from the Atlantic Ocean are brought in by southerly winds. When ITCZ move to the southern region of Ethiopia

The study area's rainfall data, which was used to analyze the distribution of rainfall and its temporal variability, revealed a unimodal (single peak) pattern of precipitation. It is primarily responsible for regulating a region's hydrologic cycle. Precipitation presents both opportunities and constraints for the land and water management of the upper Guder catchment, as much of its ecology, geography, and land use rely on the hydrological cycle's operation. Rainfall is the relevant type of precipitation in the catchment. Rainfall is a crucial climate variable that reveals the characteristics and weather patterns of the Catchment. Four distinct seasons are experienced in the catchment area: summer (June to August), autumn (September to November), winter (December to February), and spring (March to May). June, July, August, and September which are regarded as the summer season are the primary rainy months; the remaining months are regarded as dry months.

Monthly weather information was supplied from (1981 to 2020) by the Ethiopian Meteorological Agency (EMA), and rainfall information from eight long-term records of stations located in or near the upper Guder River catchment was utilized to calculate rainfall. In the study area, the annual rainfall varies from 362.4mm to 906.4mm. October is when the wet season ends and the dry season begins, with May serving as the transitional month between the two.

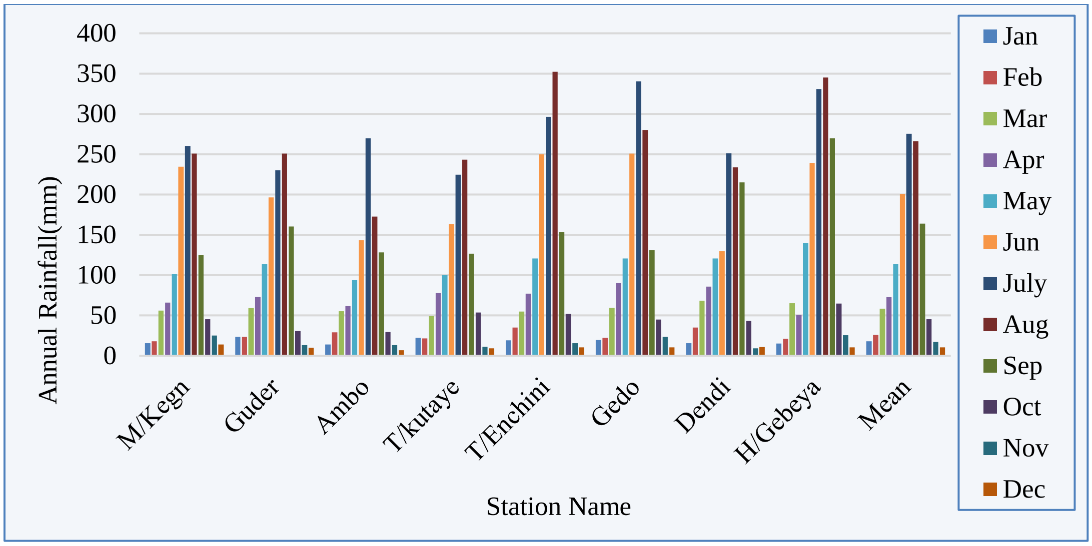

Figure 4. 5. Mean monthly precipitation of the study area.

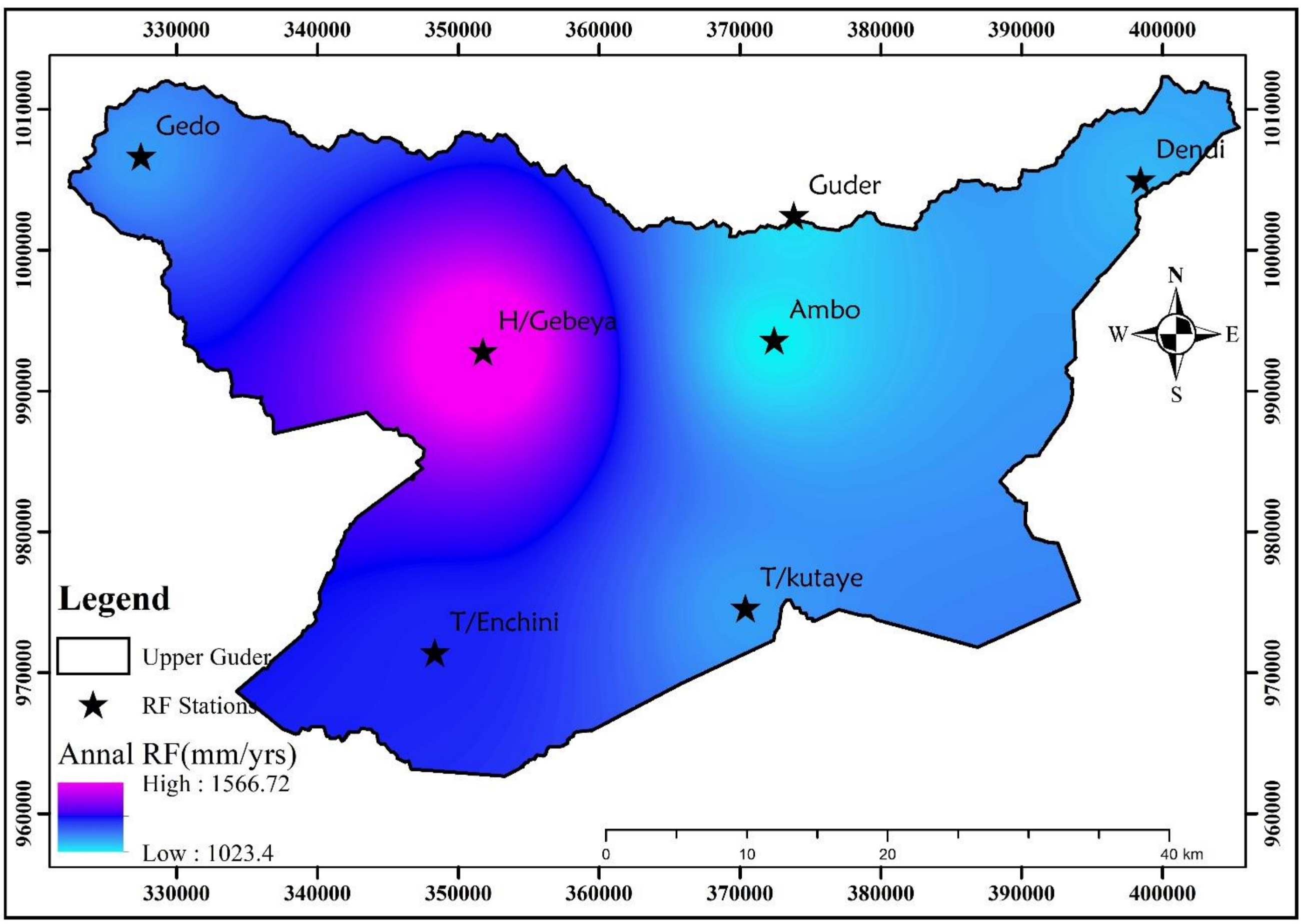

Figure 4. 6. Annual Rainfall (mm)

4.2. Determining the aerial depth of rainfall

The total amount of water that falls from the atmosphere as rain, sleet, flakes, mist, and other forms is known as precipitation. Rain gauge measurements are point observations, meaning they only provide the depth of rainfall at the specific geographic location where they are installed. They cannot represent the aerial rainfall that occurs throughout the entire Area of Interest. Therefore, a technique for determining the effective rainfall depth ought to be put into practice. The study area's aerial rainfall depth was determined using three different methods in this work.

- Arithmetic Method
- Theissen polygon method and
- Isohytal method

4.2.1. Arithmetic method

The most straightforward technique for determining the aerial depth of rainfall is the arithmetic mean, which is also more accurate in areas that are comparatively level and have evenly spaced gauging stations. The rainfall totals from all gauging stations within the study area, where the variance between each gauge record and the mean is not too great, are divided to compute it (Wilson E.M., 1983). This was taken into consideration when averaging the stations within and close to the study area to determine the annual depth of rainfall.

(Smith, A. B., et al., 2022) focused on refining these arithmetic methods by incorporating advanced spatial analysis techniques and utilizing high-resolution rainfall data from remote sensing technologies. These developments aim to improve the accuracy of areal rainfall estimation and enhance our understanding of precipitation patterns over larger areas. This was taken into consideration when averaging the stations within and close to the study area to determine the annual depth of rainfall; the result is 1267.2 mm.

$$\mathbf{P_a} = \frac{\mathbf{P1+P2+P3+\cdots+Pn}}{n}$$

where, Pa is the average depth of precipitation P1P2…Pn are rainfall recorded at each station 1, 2, etc., and ‘n’ is the number of rain gauge Stations in the area of interest.

4.2.2. Theissen polygon method

Thiessen polygons is a technique used in hydrology and meteorology to estimate areal rainfall depth by dividing a study area into polygons around each rain gauge. Each polygon represents the area closest to a specific rain gauge and assumes that the rainfall recorded at that gauge is representative of the entire polygon.

(Wang, Q., et al., 2023)have continued to explore and refine the application of the Thiessen polygon method, especially in combination with advanced spatial analysis techniques and high-resolution rainfall data. These developments aim to improve the accuracy of estimating areal rainfall depth and provide valuable insights into precipitation patterns over larger areas.

Using the relative areas of each measurement station in the Theissen polygon network, this additional graphical method determines the station weights. Using this technique, polygons are built over rain gauges to indicate each gauge's respective area of influence. To determine the areal average precipitation, the weights are multiplied by the station observation and the values are added together. 8 rain gauges located within and surrounding the catchment are used to estimate the average depth of rainfall in the area (Fig.4.7).

$$P = \frac{A1PA + A2P2 + \ldots AnPn}{A1 + A2 + \ldots An},$$

Where P is mean aerial depth of precipitation, an is Area of polygon corresponding to gauges, Pn is mean rainfall measurement at *i* th gauge, and A is total area of the catchment.

The value obtained by this method is 1243.5mm/yr.

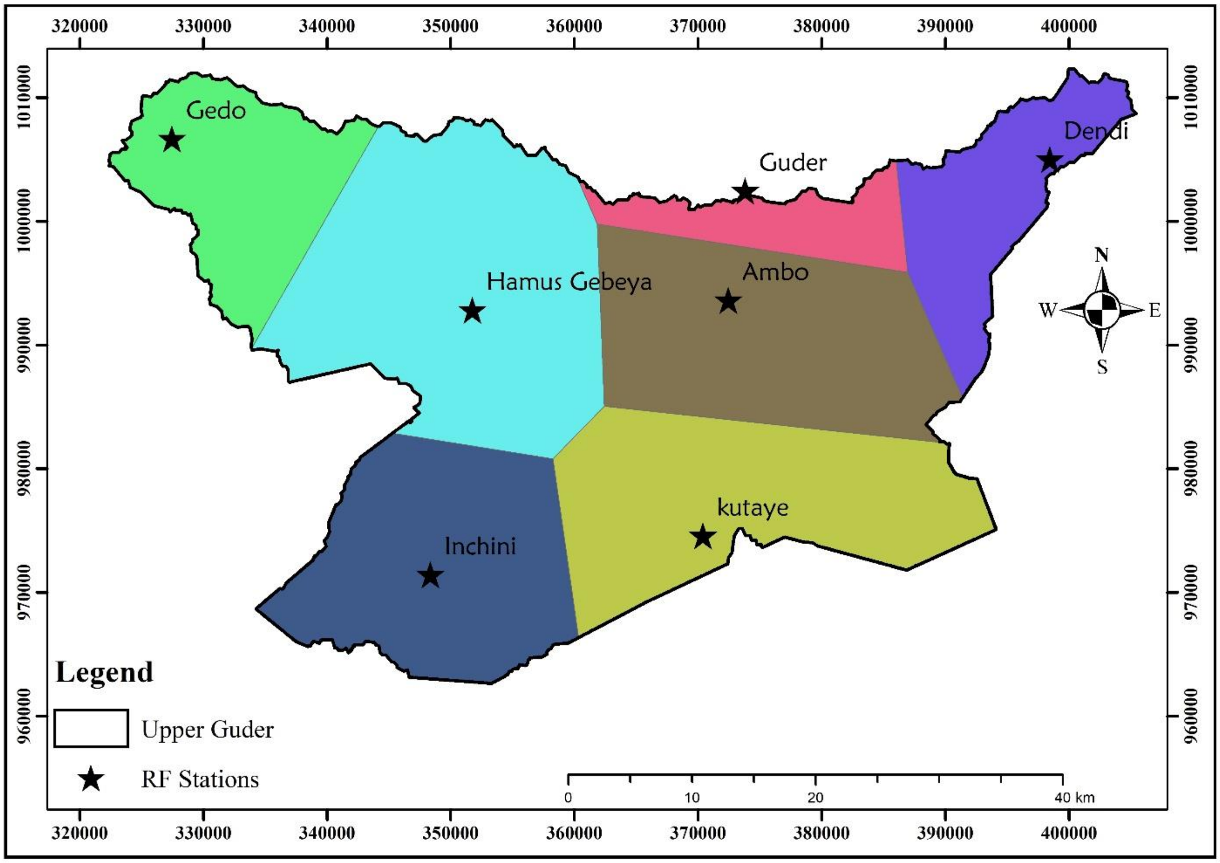

Figure 4. 7. Theissen polygon map

Table 4. 4. Mean annual depth of precipitation obtained from Thiessen polygon method.

Stations	**Annual**	**Area (km^2)**	**Area (%)**	**Weighted Rainfall**
Tikur Enchini	1213.1	355.0	0.2	195.8
Toke kutaye	1184.8	386.6	0.2	208.2
Gedo	1018.0	218.3	0.1	101.0
Guder	1104.3	109.6	0.0	55.0
Dendi	1437.6	199.3	0.1	130.2
Ambo	1393.7	379.9	0.2	240.7
Hamus Gaba	1219.1	506.4	0.2	280.6
Mida Kegn	1566.8	44.9	0.0	32.0
	1267.2	2200.0	1.0	**1243.5**

4.2.3. Isohyetal method

The Isohyetal method is a hydrological and meteorological technique that involves mapping out contour lines with equal rainfall depths to estimate the areal distribution of rainfall. Based on information from several rain gauges, these contour lines also referred to as isohyets connect locations of equal precipitation intensity throughout a research area.

Rainfall depths at various locations within the study area can be estimated using the Isohyetal method, which involves interpolating between the isohyets (Fig.4.8). Especially in places with complicated terrain or varying precipitation patterns, this technique is very helpful for illustrating and comprehending the spatial variability of rainfall throughout a region. As such, the outcome generated by this technique is thought to be more precise than the previous two. The rainfall depth calculated using this method is 1273.63 mm, as shown below.

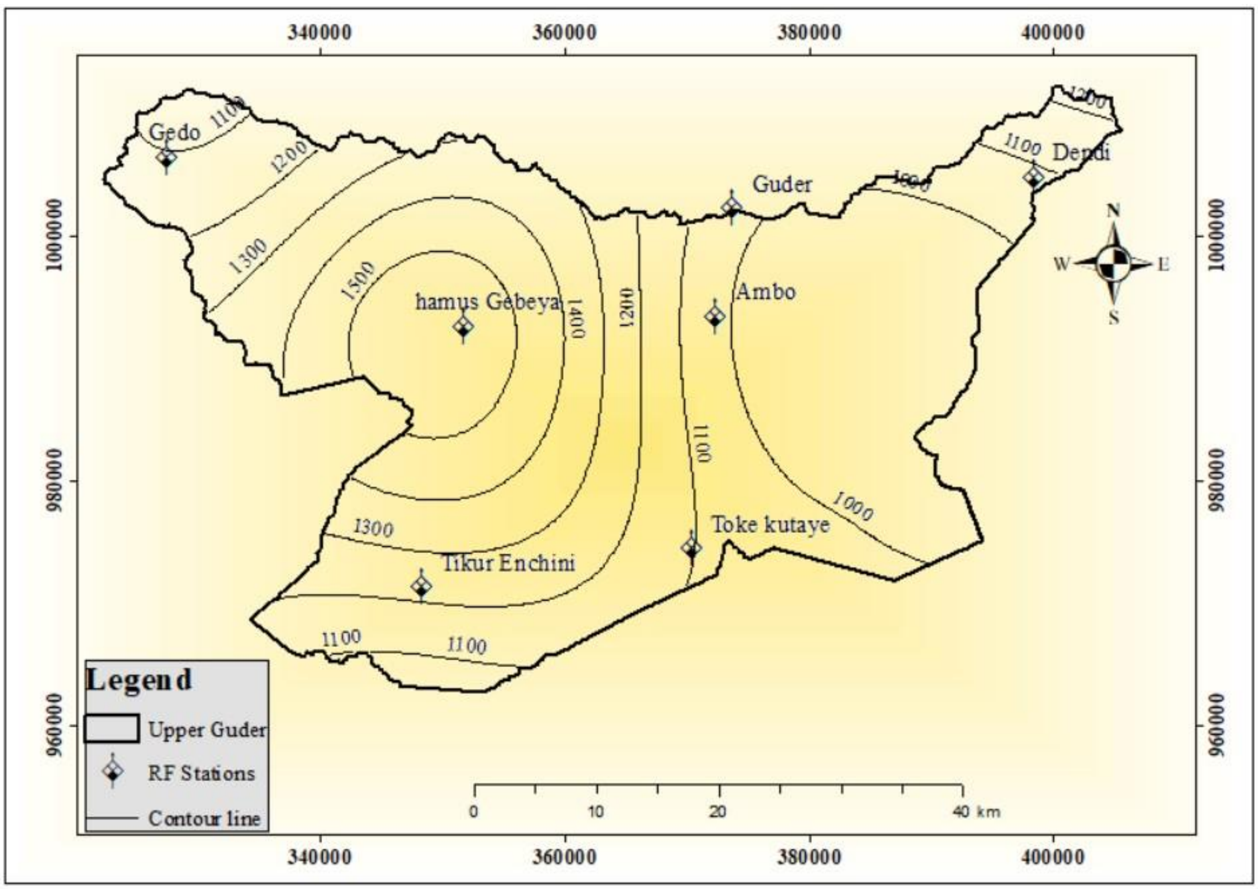

Figure 4. 8. Isohytal rainfall depth map of the study area

Table 4. 5. Mean annual depth of precipitation obtained from Isohyetal method

Isohyetal Range	**Area(km^2)**	**Area(km^2)**	**Precipitation (mm)**	**Weighted Rainfall (mm)**
>1000	243.16	0.111	950	105.452
1000-1100	313.30	0.143	1050	150.174
1100-1200	298.43	0.136	1150	156.670
1200-1300	400.15	0.183	1250	228.335
1300-1400	309.96	0.141	1350	191.022
1400-1500	155.39	0.071	1450	102.854
>1500	470.19	0.215	1580	339.132
	2200.00	1.000		**1273.639**

In general, the results obtained with the three methods mentioned above are very satisfactory and somewhat similar to the annual rainfall expected for the Upper Guder catchment based on previous studies.

The Guder sub-basin has an annual rainfall ranging between 901 mm and 1650 mm. Lower annual rainfall between 900–1000 mm in the lowlands and along the river, and higher rainfall greater than 1000 mm in other parts of the basin is observed (Yilma, Aster Denekew; Awulachew, Seleshi Bekele., 2009). In this work, the average value of the catchment's annual rainfall (i.e., 1,261.4mm/yrs) is taken into account and used for further analysis, as the differences in results obtained from the Arithmetic, Theissen, and Isohytal methods.

4.3. Temporal Variability of Rainfall

Variability of Rainfall in the area is distributed in a manner asking to that of Ethiopia's central plateau. Two main seasons the dry and the wet can usually be distinguished for the study area based on the temporal distribution of rainfall. Seasonal category with greater quantitative data based on rainfall coefficient (R. C.), defined as the ratio of the monthly mean rainfall to one-twelfth of the annual mean of the total rainfall, can be used to explain distribution (Gemechu, 1997)

$$\mathbf{R.C.=12P_m/ P_a,}$$

Were

R.C. = rainfall coefficient (unitless)

Pa, =annual total rainfall of the area, which is 1261.45mm

Pm=mean monthly rainfall

This value allows the following classification of months in a year:

The dry month when RC <0.6 and

Rainy months when RC ≥0.6

Table 4. 6. Classification of rainfall based on rainfall coefficient

Months	Jan	Feb	Mar	Apr	May	Jun	Jul	Aug	Sep	Oct	Nov	Dec	Total
pm	18.13	25.86	58.44	72.86	114.00	200.99	275.45	266.11	163.82	45.57	17.12	10.38	1261.45
RC	0.171	0.245	0.553	0.689	1.078	1.901	2.605	2.517	1.549	0.431	0.162	0.098	

- ✓ dry months (R.C. <0.6) like October, November, December, January, and February
- ✓ Wet months (R. C. ~0.6): These can be divided even further into the following categories:

Light rain (0.6–0.9) March and April

Heavy rain (>1.0):

- ✓ May, June, and September have a moderate concentration (1.0 - 1.9).
- ✓ July and August have high concentrations (2.0–2.9).
- ✓ Concentrations that are extremely high (> 3.0)

As a result, the study area's mean annual rainfall is primarily contributed by the rainy month (about 86.17%), while the dry month contributes only 13.83%.

4.4. Evapotranspiration

All but the most humid, cold climates use most of their water for evapotranspiration. Evapotranspiration could be decreased, which would increase the amount of water available and possibly lead to runoff or groundwater infiltration. According to (Law, et al. , 2002), the dew point threshold, surface and air temperatures, and soil moisture availability are its main constraints. In moist subtropical regions at the border between wet (monsoonal) and dry climate regimes, the relationship between evapotranspiration, temperature, and precipitation is especially strong. Evapotranspiration occurs in both potential and actual cases. When there is no shortage of water for the vegetation, potential evapotranspiration refers to the amount of water that will evaporate due to climate conditions, whereas actual evapotranspiration refers to the actual amount of water that returns to the atmosphere given the water availability.

Evapotranspiration is the process by which water molecules are changed from liquid to vapor by transpiration (plants) and evaporation (open water bodies and bare land) as they move from the surface of the watershed into the atmosphere (Axon, J. E., 1982). It's the sum of transpiration and evaporation values. When the water molecules have taken in enough energy to break free from the surface tension holding them in either a liquid or solid state, the process takes place.

They are treated as evapotranspiration together because it is difficult to measure them separately. Therefore, the word refers to the evaporation of liquid water from lakes and rivers, the surface of ice and snow, bare earth, and vegetative surfaces, as well as the evaporation that occurs from and within plant leaves (transpiration). Meteorological conditions, vegetation type, and water availability all affect evapotranspiration. The hydrological cycle is primarily impacted by this process.

4.4.1. Estimation of Potential Evapotranspiration (PET) and Actual Evapotranspiration

4.4.1.1. Estimation of PET

In 1948, C.W. Thornthwaite introduced a method for estimating Potential Evapotranspiration (PET) based on climatic factors. The Thornthwaite method calculates PET using temperature and day length data to estimate the potential water loss from a vegetated surface under specific climatic conditions and There are several ways to calculate potential evapotranspiration, but the following empirical formulas were used per the data that was available.

4.4.1.2. Thornthwaite method

Thornthwaite method, developed by (Thornthwaite, C. W., 1948) is a widely used technique for estimating Potential Evapotranspiration (PET) based on climatic data. This method takes into account temperature and day length information to calculate the potential water loss from a vegetated surface under specific climatic conditions. The Thornthwaite method is still helpful, though. The following parameters must be entered: latitude, month, and the mean monthly air temperature. Monthly sunshine average by latitude and month yield. 738.8mm/years is the potential evapotranspiration that can be achieved using this method.

$$PET_m = 16N_m \frac{(10Tm)^a}{I} \quad \text{(Shaw, 1988)}$$

Nm- Monthly adjustment factor related to hours of day light

Tm- monthly mean temperature C°

I = Σ im = $\Sigma(Tm/5)^{1.5}$ for m=1, 2….12, and $a = 0.49 + 0.0179I - 0.0000771I^2 + 0.000000675I^3$

Nm – is the monthly adjustment factor related to hours of daylight and obtained by dividing the possible sunshine hours.

Table 4. 7. Mean PET of study area based on Thornthwaite method

Months	Temp(°C)	Latitude Correction	1.6c	10ta/I	(10ta/I) ^a		Et(mm)	a	I
Jan	17.03	0.970	1.552	2.35	4.06	6.3	63.00	1.63	72.377
Feb	16.46	0.980	1.568	2.27	3.84	6.0	60.21		
March	17.19	1.000	1.600	2.38	4.12	6.6	66.00		
April	16.93	1.030	1.648	2.34	4.02	6.6	66.29		
May	17.40	1.050	1.680	2.40	4.20	7.1	70.64		
June	16.61	1.060	1.696	2.30	3.90	6.6	66.11		
July	14.76	1.050	1.680	2.04	3.21	5.4	53.96		
Aug	15.26	1.040	1.664	2.11	3.39	5.6	56.42		
Sept	15.73	1.020	1.632	2.17	3.57	5.8	58.18		
Octo	16.23	0.990	1.584	2.24	3.75	5.9	59.45		
Nov	16.32	0.970	1.552	2.25	3.79	5.9	58.77		
Dec	16.59	0.960	1.536	2.29	3.89	6.0	59.75		
PET							**738.77**		

PET is calculated using the Thornthwaite method, it provides an estimation of potential evapotranspiration based on temperature data and can be useful for various applications in hydrology, agriculture, and environmental studies. However, like any estimation method, it has its limitations and assumptions that need to be considered when interpreting the results. PET obtained from this method was 738.77mm/yrs.

4.4.1.6. Penman combination method

The mass transfer method and the energy budget method are combined in Penman's physical principle. The fundamental equations are rewritten to incorporate regular variable measurements at climatological stations, along with metrological constants (derived from WMO tables) (Shaw, 1988). The approach accounts for a wide range of metrological variables, including mean temperature, vapor pressure, humidity, sunshine hours, net radiation, and wind speed, which results in accurate PET estimates.

$PET = (\Delta/\gamma)\ HT + Eat) / (\Delta/\gamma) + 1)$

Where PET = Potential evapotranspiration

Δ/γ = is found from weighing factor Δ/γ versus temperature from (FAO, 1967) given in (Shaw, 1994) where Δ is the slope of saturated vapor pressure versus temperature and γ is the hypsometric constant with a value of 0.4859 mm Hg^{o}C (Rami, 1996).

Eat = is the energy for evapotranspiration in mm/day and it takes the formula

$Eat = 0.35(0.5 + u_2/100)\ (ea – ed) = f\ (u)\ (ea – ed)$

ea = the saturated vapor pressure at air temperature, Ta

ed = the saturated vapor pressure at the dew point = ea * HR/100

Td = ea – ed = the saturation deficit

u_2 = mean wind speed at 2m above the surface, miles/day

Ea = energy for evaporation based on the air humidity and air temperature

HT = RI (1-r) – R0 = 0.75RI – R0 is the net heat

The procedures followed throughout the calculation are provided below and also in (Table 4.8).

According to the land use and land cover types in the equation above, r is the area's reflective coefficient, or albedo. The study area in this work is somewhat dominated by agricultural land, primarily used for growing seasonal crops. This farmland typically becomes barren following the harvest of the ripe crops. Consequently, the area's ability to reflect light is enhanced by the mature forest, crop residue, and bare land. Based on these variables, the study area's r = 0.24 is determined.

RI = incoming radiation, R0 = outgoing radiation, r = albedo

$R0 = \sigma Ta^4\ (0.47 – 0.075\sqrt{ed})\ (0.17+0.83n/N)$

Where, σTa4 = the theoretical black body radiation at Ta

Ta = mean air temperature for a month, (^{O}C)

σ= the Stephan Boltzmann Constant, = $5.67 * 10^{-8} Wm^{-2}/K^4$

$H = 0.75Ra\ (0.18 + 0.55n/N) - 0.95\sigma Ta4\ (0.10 + 0.9\ n/N) – (0.56 – 0.092\sqrt{ed})$

RI (1-r) = 0.75Ra*fa (n/N)

fa (n/N) = 0.16 + 0.62n/N – for latitudes south of 54 and 1/20 N

But this formula takes different form depending on latitude (Shaw, 1994). In this case since study area is located at latitude south of 54 and 1/20 N.

Ra = solar radiation (fixed by latitude and season) = 100 considered for the study area, n = bright sunshine over the same period, HT = the available heat

N = mean daily duration of maximum possible sunshine hours (North Latitudes) = 100considered for the study area. (After M. Shaw, 1989

This approach provides a reasonable approximation of PET since it considers numerous metrological factors that control the rate and volume of evapotranspiration. This method yielded an annual PET of 995.83mm for the catchment, which is used for additional analysis.

Table 4. 8. Mean annual PET obtained from Penman combination method

Variable	Jan	Feb	Mar	Apr	May	Jun	Jul	Aug	Sep	Oct	Nov	Dec	Annual
T (ºC)	16.7	17.7	18.1	18.1	17.7	16.6	15.5	15.5	15.8	16.1	16.1	16.1	
N	11.6	11.8	12.0	12.3	12.6	12.7	12.6	12.4	12.1	11.8	11.6	11.0	
Ra(mm/day)	12.8	13.9	14.8	15.2	15.0	14.8	14.9	15.0	14.8	14.2	13.1	12.5	
U (mil/day)	95.0	103.6	98.0	98.0	82.0	66.0	62.8	55.3	59.0	85.9	95.0	95.0	
n/N	0.8	0.9	0.7	0.7	0.7	0.6	0.3	0.3	0.6	0.8	0.9	0.9	
H (%)	50.8	49.1	49.2	56.2	60.2	70.6	77.8	78.4	74.6	58.7	54.2	51.4	
σTa^4	14.2	14.3	14.4	14.4	14.3	14.1	13.9	13.9	14.0	14.0	14.0	14.0	
ea(mmHg)	14.3	15.1	15.5	15.6	15.1	14.2	13.2	13.2	13.4	13.7	13.7	13.7	
ed(mmHg)	7.2	7.4	7.6	8.8	9.1	10.0	10.3	10.3	10.0	8.0	7.4	7.0	
ea-ed	7.0	7.7	7.9	6.8	6.0	4.2	2.9	2.8	3.4	5.7	6.3	6.7	
E_{at}	3.6	4.1	4.1	3.1	2.8	1.7	1.2	1.0	1.3	2.7	3.2	3.4	
Δ/γ	2.4	2.6	2.7	2.7	2.6	2.5	2.3	2.3	2.4	2.4	2.4	2.4	
R1(1-r)	8.0	9.0	8.0	7.8	7.7	6.1	3.3	3.4	6.9	9.0	8.6	8.5	
Ro(mm/day)	3.3	3.4	2.9	2.6	2.6	2.1	1.3	1.3	2.2	3.1	3.3	3.5	
F(n/N)	0.7	0.7	0.6	0.6	0.6	0.5	0.3	0.3	0.5	0.7	0.7	0.7	
H_t	2.7	3.4	3.1	3.2	3.2	2.5	1.1	1.2	2.9	3.6	3.1	2.9	
PET (mm/day)	3.0	3.6	3.4	3.2	3.1	2.3	1.1	1.1	2.5	3.4	3.2	3.0	
PET (mm/mon)	90.5	109.2	101.9	96.8	93.5	69.5	34.9	34.8	74.6	102.0	95.9	92.3	**995.83**

Based on the calculated PET above using the combination of Thornthwaite and Penman, Penman's result appears to be the representative value.

Penman's approach involves utilizing multiple metrological parameters to influence evapotranspiration, while Thornthwaite's approach relies only on temperature and typically underestimates potential energy expenditure. The PET value that is utilized for additional analysis is therefore the one that Penman obtained using the Penman method, (i.e 995.83 mm/year).

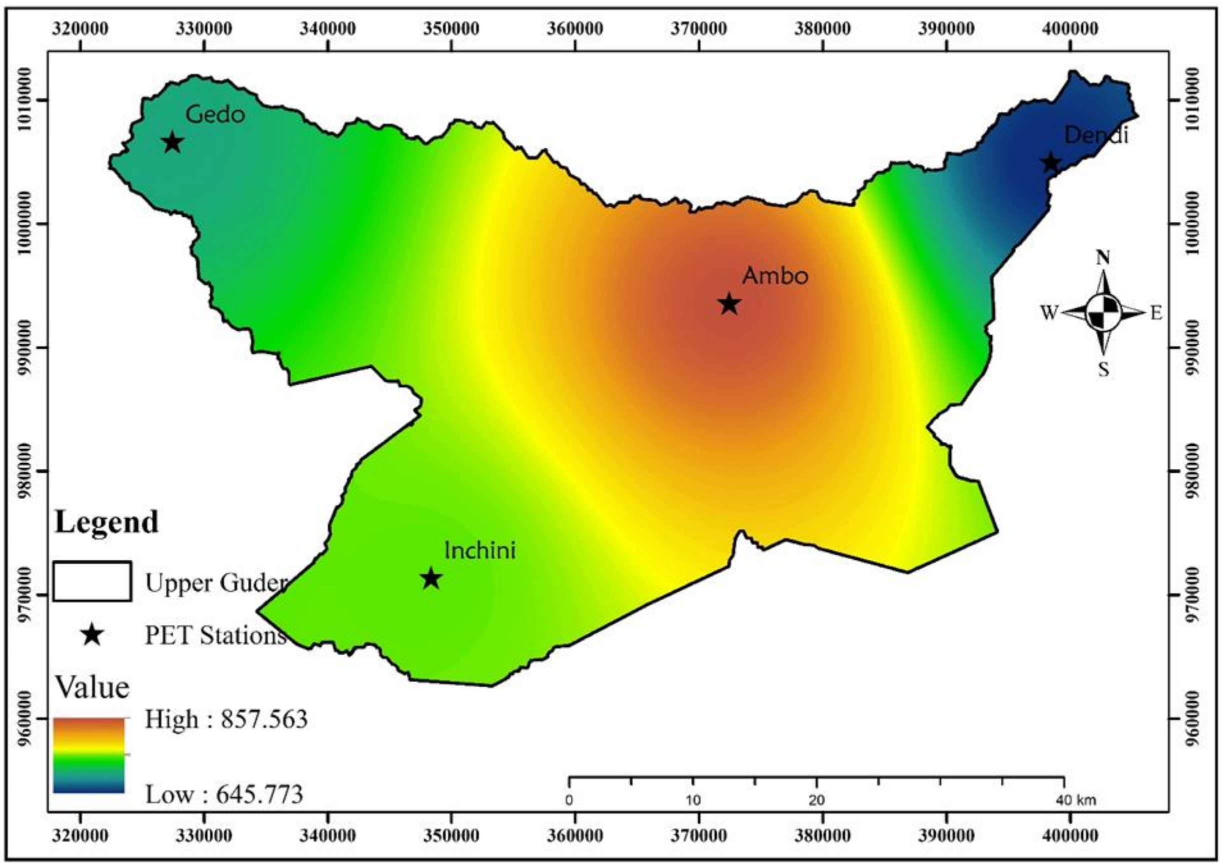

Figure 4. 9. PET map of the study area

4.4.1.3. Actual Evapotranspiration

The amount of water that is removed from the surface by evapotranspiration under the specified climatic and soil moisture conditions is known as actual evapotranspiration (Fetter,, 2001). It is either the same as or less than potential evapotranspiration.

The evaporation from vegetation cover when there is a natural or artificial supply of moisture is known as actual evapotranspiration. It describes the amount of evaporation that happens in the field and is dependent on the amount of water available to meet atmospheric demand. The potential evapotranspiration is calculated to determine the actual evapotranspiration. There are various methods for calculating actual evapotranspiration; one of these is the soil moisture balance method +developed by (Thornthwaite C.W, Mather .J. R., 1957).

4.4.1.4. Empirical Calculation of AET

Turc (1954) developed a formula that is one of the imperial methods for estimating actual evapotranspiration.

According to Shaw (1989), this formula is frequently used to estimate the annual AET for catchment areas. The catchment area's mean annual temperature and mean annual precipitation are taken into account in the formula.

$$\text{AET}= \frac{P}{\sqrt{0.9+(\frac{P}{L})^2}}$$

Where, P = mean annual precipitation (mm), which is 1261.45mm, L= 300 + 25T +0.05T^3 and T is mean annual air temperature (C^o), which is 16.7 C^0

Using this method, the estimated annual value of AET of the catchment is found to be 774mm.

4.4.1.5. Thornthwaite and Mather's (1957) water balance method

This technique estimates monthly actual evapotranspiration by using potential evapotranspiration and rainfall values as input. The main goal of calculating the soil water balance of the study area has been the temptation to determine the actual evapotranspiration. This method's fundamental premise is that provided the soil zone's moisture storage capacity is at maximum, actual evapotranspiration equals potential evapotranspiration when monthly rainfall is greater than or equal to the corresponding monthly potential evapotranspiration (Thornthwaite and Mather 1957, Shaw 1994). However, the actual evapotranspiration falls short of the potential evapotranspiration when the soil's moisture content is restricted and vegetation is unable to draw enough water from it.

According to Shaw (1994), soil type and vegetation have an impact on the values of soil moisture deficit and actual evapotranspiration. As a result, the catchment area has been texturally categorized into five major soil groups: clay, clay loam, loam, silt loam, and silt clay. Additionally, there are three different types of vegetation cover with varying root depths: deep-rooted shrubs, scrub, and grass, moderately deep-rooted intensively farmed land that includes rice, corn, and other crops, and forest.

Having precipitation and potential evapotranspiration serving as the primary inputs, the Thornthwaite and Mather standard soil water balance model is used to calculate the area's actual evapotranspiration based on the soil and vegetation cover mentioned above.

In the model, the first month of the dry season is used to start the summation of the negative values of the monthly precipitation and potential evapotranspiration differences. This yields the accumulated potential water loss, which represents the severity of the water shortage.

$$\mathrm{SM} = \mathrm{AWC}\exp\left[-\frac{(|APWL|)}{AWC}\right]$$

Were, SM: Soil moisture during the month M (mm), APWL is Accumulated potential water loss at month M (mm), AWC is Available water capacity of the root zone (mm),P is average monthly precipitation (mm) determined by arithmetic, isohyets, and the Thiessen polygon ,P – PET is The difference between potential evapotranspiration and rainfall; a negative value indicates a potential water shortage or monthly moisture demand by the vegetation that is not met by monthly rainfall, whereas a positive value indicates a potential water surplus or soil moisture additions.

Accumulated potential water loss (APWL) is When P-PET is negative, the values are added together to determine the accumulated potential water loss (APWL). The running sum is the total amount of unmet potential evapotranspiration that has been experienced by the soil. Usually, during the first month that P-PET is negative, soils yield water more readily. Soil moisture is less likely to evaporate in the following month as the APWL expands.

AET: - Monthly actual evapotranspiration is determined as follows:

If Pm > PET, then AET= PET, Otherwise, AETm is m (month) + Pm (monthly precipitation) + change in soil moisture, SMD is the difference between PETm and AETm is the monthly SMD.

The soil is saturated when there is a lot of moisture in the air and rainfall. When rainfall stops, saturated soil releases water and turns unsaturated. At this point, the soil is said to be at field capacity because it can only hold a certain amount of moisture against gravity. This means that the actual evapotranspiration rate equals the potential evapotranspiration, meaning that evaporation happens at the fastest rate that can be achieved given the meteorological conditions. The demand of vegetation gradually depletes soil moisture, resulting in a soil moisture deficit due to the amount of water needed to restore the soil to its field capacity when there isn't any rain to replenish the water supply. AET becomes progressively less than PET as the soil moisture deficit rises.

A monthly total available runoff (TARO) of 50% is thought to genuinely run off, with the remaining 50% being retained (D) in the catchment's channels, groundwater, and subsurface, and becoming available for runoff in the following month, according to Thornthwaite and Mather's (1957) assumptions. TAROm = Sm + Dm-1, where detention is represented by "D" and surplus by "S."

In the absence of this, AETm = Pm + Sm-1-Sm, where'm' denotes the month and Sm and Sm represent the soil moisture during months m-1 and m, respectively. The AET decreases relative to PET as the soil moisture deficit rises. The difference between PETm and AETm is known as the soil moisture deficit (SMD).

Based on the previous idea, the catchment's actual evapotranspiration is calculated when accounting for the catchment's various land uses, land covers, and soil types. For this study, the Upper Guder Catchment's soil is divided into four major soil textures: clay, loam, clay loam and silt clay and which is take in account 38%, 32%, 23%, and 6% of the total area, respectively. It is determined how much of each soil class is covered by vegetation about its area. After adding the results from each soil class, the actual evapotranspiration value was found to be 733.48mm/year. Below is the calculated actual evapotranspiration for the catchment.

Table 4. 9. AET for the area represented by clay, loam, clay loam and silt clay and which is take in account 38%, 32%, 23%, and 6% of the total area, respectively, with total available water capacity of 200mm.

Months	Jan	Feb	Mar	Apr	May	Jun	Jul	Aug	Sep	Oct	Nov	Dec	Annual
p	18.1	25.9	58	72.9	114	201	275	266	164	45.6	17.1	10	1267.2
PET	90.5	109	102	96.8	94	70	35	34.8	74.6	102	95.9	92	995.83
P-PET	-72	-83	-44	-24	21	132	241	231	89.2	-56	-79	-82	
Acc PWL	-290	-373	-416	-440	0	0	0	0	0	-56	-135	-217	
SM retained	47	31	25	22.1	200	200	200	200	200	151	102	68	
ΔSM	-21	-16	-6.1	-2.8						-49	-49	-34	
AET	38.6	41.9	64	75.7	94	70	35	34.8	74.6	94.8	66.2	45	733.48

P-PET is the difference by subtraction, P is precipitation, PET is potential evapotranspiration, and APWL is the accumulated potential water loss, which is obtained by adding up the negative values in row; AET is the actual evapotranspiration; SM is the soil moisture; and ΔSM is the change in soil moisture over the month.

- ✓ The Turc method yields a result that overestimates the true values. This could be because the Turc method is developed for a specific climatic region, so it might not work well for another.
- ✓ Turc empirical formulae use only temperature and precipitation, which do not account for the effect of the rest hydro-meteorological, pedological, and botanical (land cover) effects on the rate of actual evapotranspiration. As a result, the soil water balance result is believed to accurately reflect the evapotranspiration of the study area and will be used in subsequent analyses.

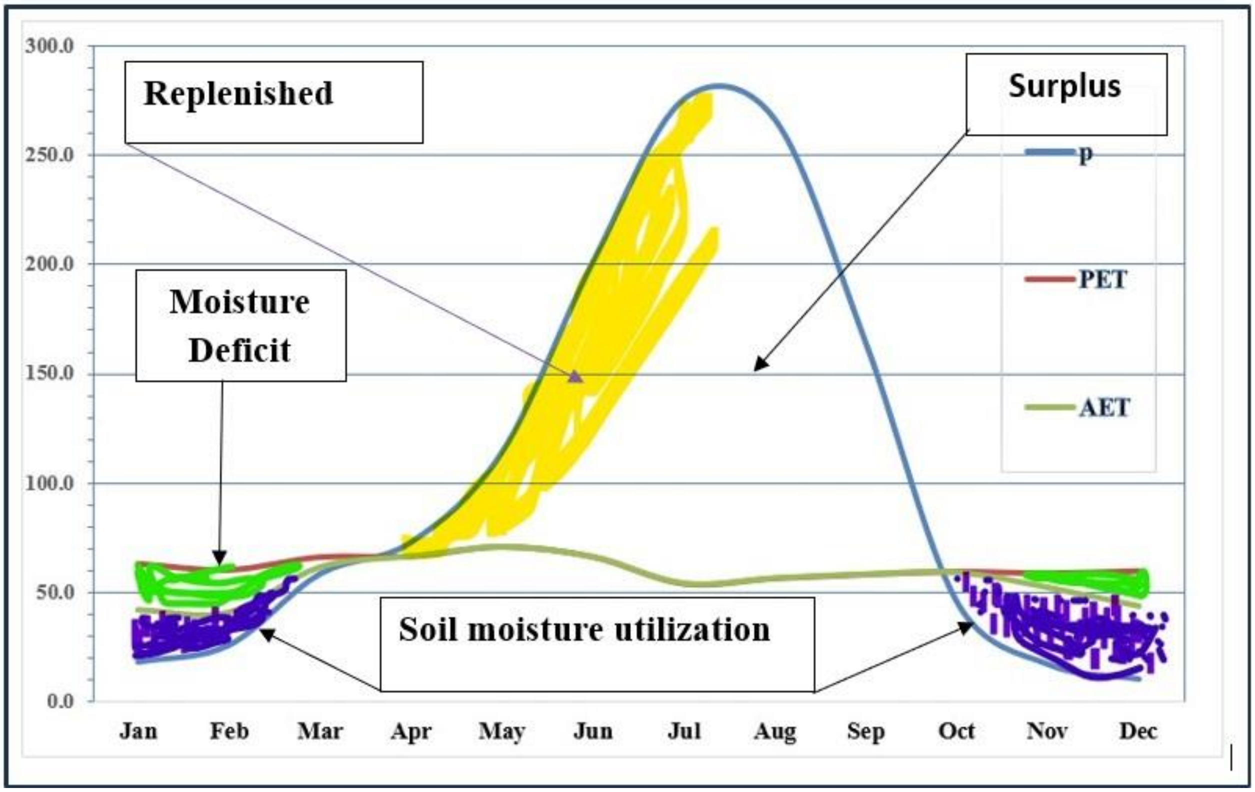

Figure 4. 10. Monthly average water balance of the study area

4.5. Runoff estimation

4.5.1. Runoff estimation using rainfall coefficient

Using this method, the runoff is estimated by multiplying the runoff coefficient by the area's rainfall depth. (Chow, 1988) The percentage of rainfall that is converted to runoff is known as the runoff coefficient. You can use the runoff coefficient method to calculate runoff by following these general steps:

Find the Runoff Coefficient: Determine the suitable runoff coefficient value for the particular land use or land cover type in the area you are analyzing, or estimate it. The usual range of runoff coefficients is 0 to 1, where 0 denotes no runoff and 1 denotes total runoff from precipitation.

Obtain Information on Precipitation: Compile information on the area of interest's total precipitation. Weather stations, satellite observations, and other sources may provide this information.

Compute Runoff: To find the amount of runoff generated, multiply the total precipitation by the runoff coefficient. By using the runoff coefficient method, the following formula can be used to calculate runoff:

It is given by: R = PK.

Where, R is runoff (mm), P is rainfall depth (mm), K is runoff coefficient (dimensionless).

But K is obtained by,

$$K = \frac{A1K1 + A2K2 + A3K3 ... + AnKn}{A1 + A2 + A3 ... + A}$$

(Barlow,, 1915) provided the values of the runoff coefficient for various land uses and land covers. The runoff coefficient for the study area was estimated using Barlow, the first Chief Engineer of the Hydro-electric Survey of India. As a result, the five main categories listed below (Table.9) correspond to the land use and land cover as described in Chapter 2.

By considering the runoff coefficients associated with different land use types and their respective proportions in a given area, you can calculate an overall runoff coefficient that reflects the combined impact of land use on runoff generation.

$$\mathbf{K} = \frac{1741.9*0.3+111.2*0.11+161.7*0.1+176.1*0.67}{2190.9} = 0.30$$

The runoff coefficient is not typically calculated for water bodies like lakes or rivers because it is a parameter commonly used for land surfaces to estimate the amount of rainfall that will run off the surface. Water bodies have different hydrological characteristics and behaviors compared to land surfaces, so other methods and parameters are used to analyze and understand their runoff and water flow dynamics. Factors such as inflow, outflow, water levels, and hydraulic processes are more relevant for water bodies than the runoff coefficient used for land surfaces (Smith, J., et al. (2022).

The runoff value of 386 mm/yrs. was obtained for the study area by multiplying the runoff coefficient value (i.e., 0.30) with the rainfall depth (1267.2 mm/year) using the above equation.

Consequently, the annual runoff of the catchment is taken to be 386 mm/yrs. for the water balance method calculation.

Table 4. 10. Runoff coefficient for different land use and landcover in the study area

No	Classification of land use land cover	Area in (Km^2)	Runoff Coefficient
1	Cultivated (state farms and perennial crops grown intensively to moderately).	1741.9	0.3
2	(Rangeland)Open and dense woodland; pasture; bushland; grassland.	111.2	0.11
3	Trees	161.7	0.1
4	Built-up area	176.1	0.67
5	Waterbody	7.8	-

4.5. 2.Recharge estimation

4.5.3. Water balance method

Quantitatively evaluating the groundwater resource is a major goal of the majority of groundwater studies. Two water balance approaches that cover essentially the same ground but present it in different ways have been used to achieve these goals. The first method, called soil water balance, was initially developed by (Thornthwaite and Mather in 1957). It assists in estimating the area's yearly actual evapotranspiration based on the potential evapotranspiration that has already been calculated using physical and empirical formulas.

The general equation for water balance forms the basis of the second approach. This equation makes certain basic assumptions, like the division of surface water and groundwater occurring at the same time, except at the river's mouth, where ground water escapes as base flow, the catchment is bounded by both surface and groundwater divides. There is no groundwater inflow or outflow across the boundary, the water balance is calculated annually, the annual storage change is assumed to be zero, and human abstraction is negligible.

The water balance equation for the catchment is as follows, based on the assumptions made:

Inflow = Outflow + Change in storage

The components that enter a system are precipitation, groundwater inflow, irrigation, and artificial water transport. The components that exit the system are groundwater outflow, abstraction, direct runoff, evapotranspiration, recharge, and water transfer to another system. The methodology of this water balance approach entails the identification and quantification of the specific components of inflow and outflow that are possible within the area under consideration. The water balance equation for the catchment is as follows, based on the assumptions made:

$$R = P - (AET - Q)$$

The variables P, AET, Q and R represent mean annual precipitation, mean actual evapotranspiration, mean annual surface runoff and mean annual groundwater recharge, respectively. Therefore, the mean annual groundwater recharge of the Upper Guder Catchment is estimated as follows using the above relation of the conventional water balance equation:

AET = 733.48mm (From Soil water balance methods), Q = 386mm and P = 1267.2mm

Therefore, R= 1267.2mm – 733.48mm - 386mm =148mm/year.

4.5.4. Chloride mass balance method

The recharge estimates from the WetSpass model were compared with those from the Chloride Mass Balance (CMB) method in order to confirm and improve their reliability. Researchers have widely used the CMB method, which was developed by (Eriksson, E., & Khunakasem, J., 1969) to estimate recharge rates in a variety of aquifers (Lorentz, S., et al., 2003).

This approach uses reasonably stable environmental tracers to estimate recharge to ground water. Chloride ions play few important biochemical roles, are not significantly adsorbed on mineral surfaces, do not form salts of low solubility, do not form significant solute complexes with other ions unless the concentration of chloride is very high, and are primarily circulated through physical processes in the hydrologic cycle. In comparison to all other tracers tested, including tritium that had actually been incorporated into the water molecules, chloride ions moved with the water through the majority of the soils tested with less retardation or loss.

Recharge estimation using the Chloride Mass Balance (CMB) method is a widely used technique in hydrogeology to assess groundwater recharge rates. The CMB method relies on the conservative behavior of chloride ions in groundwater to estimate the amount of water entering an aquifer.

Based on the mass assumption between the atmospheric chloride input and the subsurface chloride flux, the method is employed. The mass balance equation can be used to interpret the fluxes in a catchment, even when pollution is not taken into account directly (Drever, J. I., & Clow, D. W., 1995).

The fundamental basis of the CBM method is that the water mass flux crossing the plan of the water table can be calculated if: -

- ✓ The chloride in the groundwater originated only from the precipitation.
- ✓ Chloride is conservative in the system.
- ✓ Chloride application rate is constant and known
- ✓ There is no appreciable chloride runoff or run-on from the sampling sites and
- ✓ Steady-state conditions prevail.
- ✓ Chloride mass flux cannot change over time.
- ✓ There is no recycling or concentration of chloride in the aquifer. if these conditions are met and then a really average recharge flux to the aquifer.

The average chloride concentration for the three stations in this work are taken once mid-June (Ambo, chalia, and Guder) area was 0.94 mg/l. The precipitation samples were collected and tested for chloride at Ambo City Water Quality Analysis. Conversely, the average concentration of chloride ions in groundwater derived from 15 boreholes is 5.028 mg/l.

The general formula for estimating the mean annual recharge based on chloride attributes and data is $GR = P\times[Cl^{-}p]/ [Cl^{-}GW]$.

Assuming that P is the mean annual precipitation depth in mm and GR is the mean ground water recharge in mm/year.

Average chloride concentration in ground water is expressed as $[Cl^{-}GW]$, and precipitation concentration is expressed as $[Cl^{-}p]$ in mg/l.

In this case, P = 1267.2mm/yr., $Cl^{-}p$ = 0.94mg/l, [Cl-GW] = 5.028mg/l, GR = 236.89 mm/yr.

It is evident that the recharge value attained through this approach is less than /greater than the values attained through alternative approaches. Therefore, it has the following limitations:

- ✓ It depends on the detecting limits of the laboratory; a slight error in detection can cause an incorrect result;
- ✓ Only three samples of rainfall (in mid-June) were taken; it would be better if more rainfall data were collected over a year to know the variation of Cl^- with time.

Part of the precipitation that contains chloride ions runs off and leaves the catchment, but the majority is not retained in the soil. Additionally, a higher concentration of Cl^- in the precipitation that falls over the catchment is responsible for the direct input of pollution that is observed.

In addition, the WetSpass model's estimated groundwater recharge was compared to values found by other researchers in the study catchment as well as nearby catchments. Further understanding of the estimated recharge values' dependability and consistency with earlier research carried out in comparable hydrological contexts was made possible by this comparative analysis. Table 4.11 provides a summary of the comparison between the estimates of groundwater recharge from the WetSpass model and those determined by different authors within and adjacent catchments.

Table 4. 11. shows a comparison between the results obtained by earlier researchers and the estimated recharge values from the WetSpass model.

No	Researchers	year	Estimated Recharge(mm/year)	Applied Methods	Study area
1	**Tilahun Azagegn**	2014	209mm/year	CMB	Guder sub-Basin
		2014	122mm/year	CMB	Jema Sub Basin
		2014	286mm/year	WBM	Guder sub-Basin
		2014	196mm/year	WBM	Muger sub-Basin
2	**Urgessa Hirpha**	2023	106mm/year	Wetspass	Gur Sub Basin
		2023	103mm/year	CMB	Gur Sub Basin

4.6. Methods of Recharge Estimation

4.6.1. Wetspass modeling method

WetSpass modeling was developed for temperate regions, which have different land and climate conditions than the tropics, by (Batelaan, O., & DeSmedt, F, 2001). Therefore, some input parameter modifications are required when applying WetSpass modeling in tropical regions. In temperate regions, summer and winter last six months each, but in Ethiopia, summer lasts four months and winter lasts eight. In addition, there are differences in the seasons of rainfall and land use/land cover. Therefore, eight months of winter and four months of summer were entered into the meteorological grid map to apply the Wetspass for the upper Guder catchment. Additionally, updated land-use parameter tables for the summer and winter were employed.

The hydrogeological system of a basin is conceptualized in the model based on physical and empirical relationships. The main components of the system are the soil zone, root zone, atmosphere, and saturated groundwater zones, which are divided into grids or cells to account for heterogeneity (Gebremedhin Gebremeskel, K., 2015). In order to run the model, grid maps of the same cell size representing the long-term mean monthly values of temperature, precipitation, wind speed, and potential evapotranspiration were created on an ArcGIS environment. Additionally, parameter tables about the various land use types' root depth and leaf area index as well as soil parameter tables of field capacity, wilting point permeability, and runoff in the proper format were required.

4.6.2. Model concept

The water balance computation is done at the raster cell level because the model is distributed. The vegetated, bare soil, open-water, and impermeable fractions of a raster cell's independent water balances are added up to determine the individual raster water balance. Thus, the sum of the water balances in each raster cell determines the overall water balance of a given area.

Within the GIS environment, the area under consideration is discretized by defining the cell size. By adding up the independent water balances for a raster cell's vegetated, bare soil, open-water, and impermeable fractions, one can calculate the individual water balance. As a result, by adding up the water balances for every raster cell, the overall water balance for a given watershed can be determined.

4.6.3. Water balance components per raster cell

The total water balance of a raster cell is determined by combining the water balance components of vegetated, bare soil, open water, and impermeable surfaces. This formula is as follows:

$$ET\ raster = avETv+asEs+aoEo+aiEi \qquad (1)$$

S raster = avSv+asSs+aoSo+aiSi (2)

R raster = avRv+asRs+aoRo+aiRi (3)

where ET raster, S raster, and R raster are the total evapotranspiration of a raster cell [LT-1], surface runoff of a raster cell [LT-1], and groundwater recharge of a raster cell [LT-1] respectively, each having a vegetated, bare-soil, open-water and impervious area component denoted by av, as, ao, and ai, respectively.

4.6.3. Precipitation

The water balance of each of the preceding raster cell components is calculated using precipitation as the starting point, with the remaining processes (interception, runoff, evapotranspiration, and recharge) occurring in a sequential order. The seasonal time scale that will be used to quantify the processes becomes dependent upon this order. The following section addresses the water balance for each component.

4.6.4. Vegetated area

The water balance computations performed for vegetated area is mainly depends up on the seasonal precipitation(P), interception fraction (I), surface runoff (Ss), actual evapotranspiration (Tv) and groundwater recharge (Rv), where all the magnitude is expressed [LT-1] units with the relation given as:

$P = I + Sv + TV + R\mathrm{v}$ (1)

4.6.5. Interception

An interception fraction is represented by percentage of annual precipitation value which mainly depends up the type of vegetation cover. Since the vegetation cover is taken as constant throughout the simulation period. The interception by a constant vegetation cover represents a constant percentage of annual precipitation value.

4.6.6. Surface runoff

Surface runoff is calculated in relation to precipitation amount, precipitation intensity, interception and soil infiltration capacity. Initially the potential surface runoff (Sv - pot) is calculated as:

Sv – pot = Csv (P – I) (2)

Where = Csv is surface runoff coefficient for the vegetated areas, and is a function of vegetation, soil type and slope. In groundwater discharge zones saturated surface runoff is likely to be observed which in turn dramatically increase the surface runoff coefficient but due to the less dependency of soil and vegetation type in the surrounding area of a river, the runoff coefficient is assumed to be constant. In the second step, actual surface runoff is calculated from the Sv-pot by considering the differences in precipitation intensities in relation to soil infiltration capacities. That is:

$$Sv = CHor\ Sv\text{–}pot \qquad (3)$$

Where CHor is a coefficient for parameterizing that forms part of a seasonal precipitation contributing to the Hortonian overland flow. CHor for groundwater discharge areas is equal to 1.0 since all intensities of precipitation contribute to surface runoff. Only high intensity storms can generate surface runoff in infiltration areas.

4.6.7. Evapotranspiration

For the calculation of seasonal evapotranspiration, a reference value of transpiration is obtained from open-water evaporation and a vegetation coefficient. It is given by:

$$Trv = cEo \qquad (4)$$

Where Trv is the reference transpiration of vegetated surface [LT-1] Eo is potential evaporation of open water [LT-1] C is vegetation coefficient [-] The vegetation coefficient can be determined from the ratio of the reference vegetation transpiration expressed by the Penman-Monteith equation to the potential open water evaporation is calculated by the following equation:

$$C = 1+\gamma/\Delta 1+\gamma/\Delta(1+rcra) \qquad (5)$$

Where γ = psychrometric constant [ML-1T -2C -1], Δ = Slope of the first derivative of the saturated vapor pressure curve (slope of saturation vapor pressure at the prevailing air temperature) [ML-1T -2C -1], rc = Canopy resistance [TL-1], ra = aerodynamic resistance [TL-1], Again the value of the aerodynamic resistance is calculated by:

$$r_a = \frac{1}{k^2 u_a}\left(\ln\left(\frac{Z_{a-d}}{Z_0}\right)\right)^2 \ldots\ldots(6)$$

Where k is Von Karman constant (0.4) [-], Ua is the wind speed [LT-1] at measurement level

Za =2m, d is the zero-plane displacement length [L], and Zo is the roughness length for vegetation or soil [L].

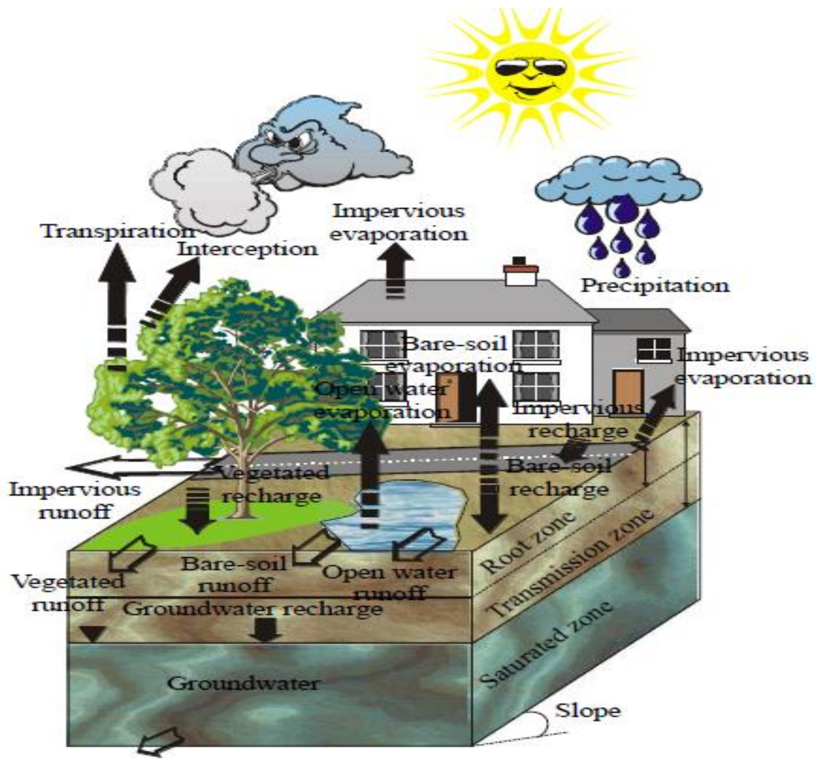

Figure 4. 11. Graphical iterative representation of water balance calculation of a hypothetical raster cell showing surface and sub-surface processes, after Batelaan and De Smedt (2001)

The Penman coefficient (γ/Δ) varies with temperature and can be obtained from the following table:

Table 4. 12. Variation of penman coefficient (γ/Δ) with temperature

T (C^o	-20	-10	0	5	10	15	20	25	30	35	40
γ/Δ	5.86	2.83	1.46	1.07	0.76	0.59	0.45	0.35	0.27	0.27	0.17

For vegetated groundwater discharge areas, the actual transpiration (Tv) is equal to the reference transpiration as there is no soil or water availability limitation:

$$Tv = Trv \text{ if } (Gd - ht) \leq Rd \quad (7)$$

where Gd, is groundwater depth [L], ht is the tension-saturated height [L] and Rd is the rooting depth [L]. For vegetated areas where the groundwater level is below the root zone the actual transpiration is given by:

$$Tv = f(\theta)Trv \text{ if } (Gd - ht) > Rd \quad (8)$$

Where f(θ) is a function of the water content and for a time-variant situation it is defined as

$$(\theta) = (1 - a1)\ w/Trv \quad (9)$$

$$w = P + (\theta fc - \theta pwp) \quad (10)$$

Where a1 is a calibrated parameter related to the sand content of a soil type [-], w is the available water for transpiration [LT-1] and θfc - θpwp is the plant available water content [T-1] per time step, stated as the difference in water content at field capacity and at permanent wilting point.

4.6.8. Recharge

The last component, the groundwater recharge, is then calculated as a residual term of the water balance, i.e.,

$$Rv = P - Sv - ETv - I$$

Where ETV is the actual evapotranspiration [LT-1], which is given as the sum of Tv and Es. Therefore, based on the vegetated type, soil type, slope, groundwater depth, climatic variables of precipitation, potential evapotranspiration, temperature, and wind speed, the spatially distributed recharge is estimated. For the computation of the water balance for bare soil, open water, and impermeable surfaces, a similar process is used as for vegetated surfaces. The absence of vegetation in this instance means that there is no need for an interception or transpiration term. That is the only difference. In this instance, ETv becomes Es as a result.

4.6.9. WetSpass Input files

4.6.9.1. Physical and hydro metrological grid maps

The model needs two different kinds of data inputs to function. The first is the watershed's physical attributes, including its soil, slope, elevation, land use/cover, and meteorological data, which includes wind speed, temperature, precipitation, and potential evapotranspiration. The second one consists of parameter tables created for the matching catchment soil maps and land use/cover.

The Arc Map's spatial Analyst extension toolbox's IDW interpolation was utilized to prepare the hydro-metrological raster map. A 200 m grid cell size was used to prepare the raster map, while a 10m resolution land use/land cover from the Sentinel-2 map of the catchment and soil map from Oromia Engineering Cooperative (ECO) was used in the preparation. The elevation was acquired from the data set of the STRM(https://www.usgs.gov/centers/eros/science/usgs-eros-archive-digital-elevation-shuttle-radar-topography-mission-srtm-1)

The 3D Spatial Analyst extension was used to extract the associated slope map from the digital elevation model. The 21 existing borehole data sets, which include a complete record of the static water level and have been used consistently throughout the month, were used to create the groundwater depth map of the catchment. Using the conversion tools box in the Arc map environment, the corresponding raster map with a 200m grid size has been converted to ASCII grid format and the watershed boundary's input ASCII format has 250 rows and 417 columns. The grid cell size for the watershed is 200 meters.

4.6.9.2. Parameter tables

The study area's soil map, land use/cover map, and parameter tables have all been created and saved in the proper TBL format. Throughout the month of the simulation, the same kind of soil parameters and land use/cover have been used. To perform the computation, the parameter tables are utilized as lookup tables that link the corresponding grid maps of land use/cover and soil.

WetSpass needs the following ArcView/ArcInfo grid files and tables (dbf files) as inputs:

Table 4. 13. Wetspass model inputs files

Arcview/Arcinfo grid files	Soil, Topography, Slope, Land use, Temperature, Wind speed, Precipitation, PET, Groundwater depth
Tables (dbf)	Soil parameter and Land use parameter

4.7. Outputs of wetSpass model

As previously mentioned, monthly time step preparations of the model inputs for temperature, precipitation, and potential evapotranspiration have been made. For every month, the same groundwater depth value has been utilized. The map algebra toolbox in the spatial analyst extension of Arc Map has transformed the output of the corresponding month into two seasons. A raster map is used to display the output results. The following explains the output results discussion:

4.7.1. Actual Evapotranspiration (AET)

WetSpass calculates the yearly evapotranspiration by adding the transpiration of the vegetated cover, the evaporation of open water bodies, the evaporation from bare soil, and the interception loss by the vegetation. The process that brings water back into the atmosphere and thus completes the hydrologic cycle is called evapotranspiration. Furthermore, it covers evaporation from ground surface, vegetation, and open water. In addition, Teklebirhan et al. (2012) describe transpiration as the process by which plant roots draw water from the soil, transport it through the plant and into the leaf, and evaporate it from the inside of the leaf into the atmosphere.

Using the WetSpass model, actual evapotranspiration is one of the water balance components used to calculate the upper Guder catchment's groundwater recharge as can be seen from output (Fig.4.13). The catchment loses 558.4 mm of water due to evapotranspiration. 44% of the annual precipitation in the catchment is accounted for this. About 51% of the yearly evapotranspiration is lost in the winter and 49% is released in the summer. The reason for this variance is that winter temperatures are higher than summer ones. The wintertime evapotranspiration is therefore greater than the summertime.

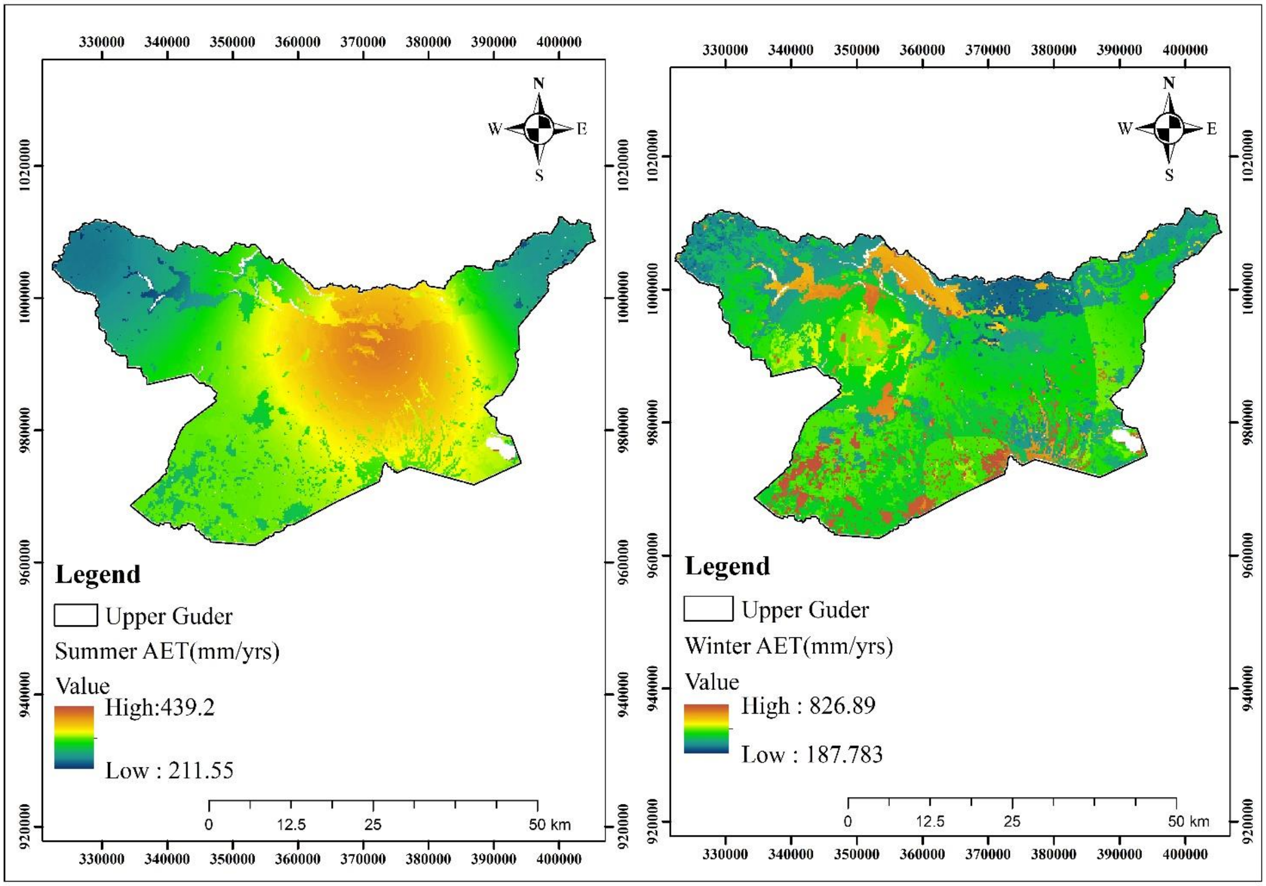

Figure 4. 12. Summer and winter actual evapotranspiration of the study area.

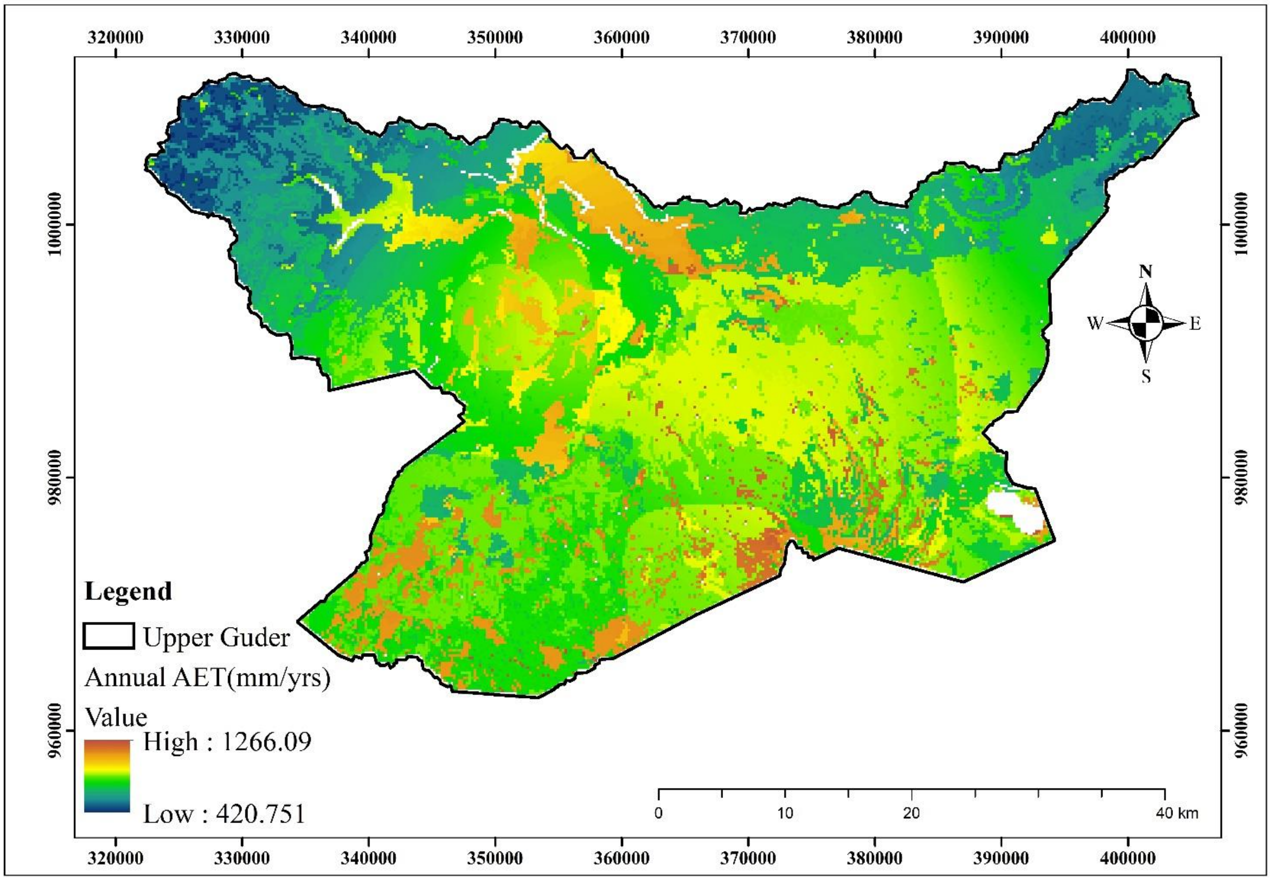

Figure 4. 13. Annual Actual Evapotranspiration (mm)

4.7.2. Runoff

The primary factors influencing surface runoff within a given watershed are the type of land cover and use, the soil texture, and the amount of rainfall. 415.9 mm is the long-term annual surface runoff, as can be seen from the output (Fig.4.15) within the catchment. 75.4 mm of surface runoff, or roughly 18% of the total yearly runoff, is measured during the dry season. As opposed to this, the rainy season produces about 82%, or 340.5 mm, of the total surface runoff. Of the yearly precipitation, surface runoff contributes roughly 32.8%. Thus, it follows that surface runoff is responsible for the majority of the precipitation lost within the catchment area.

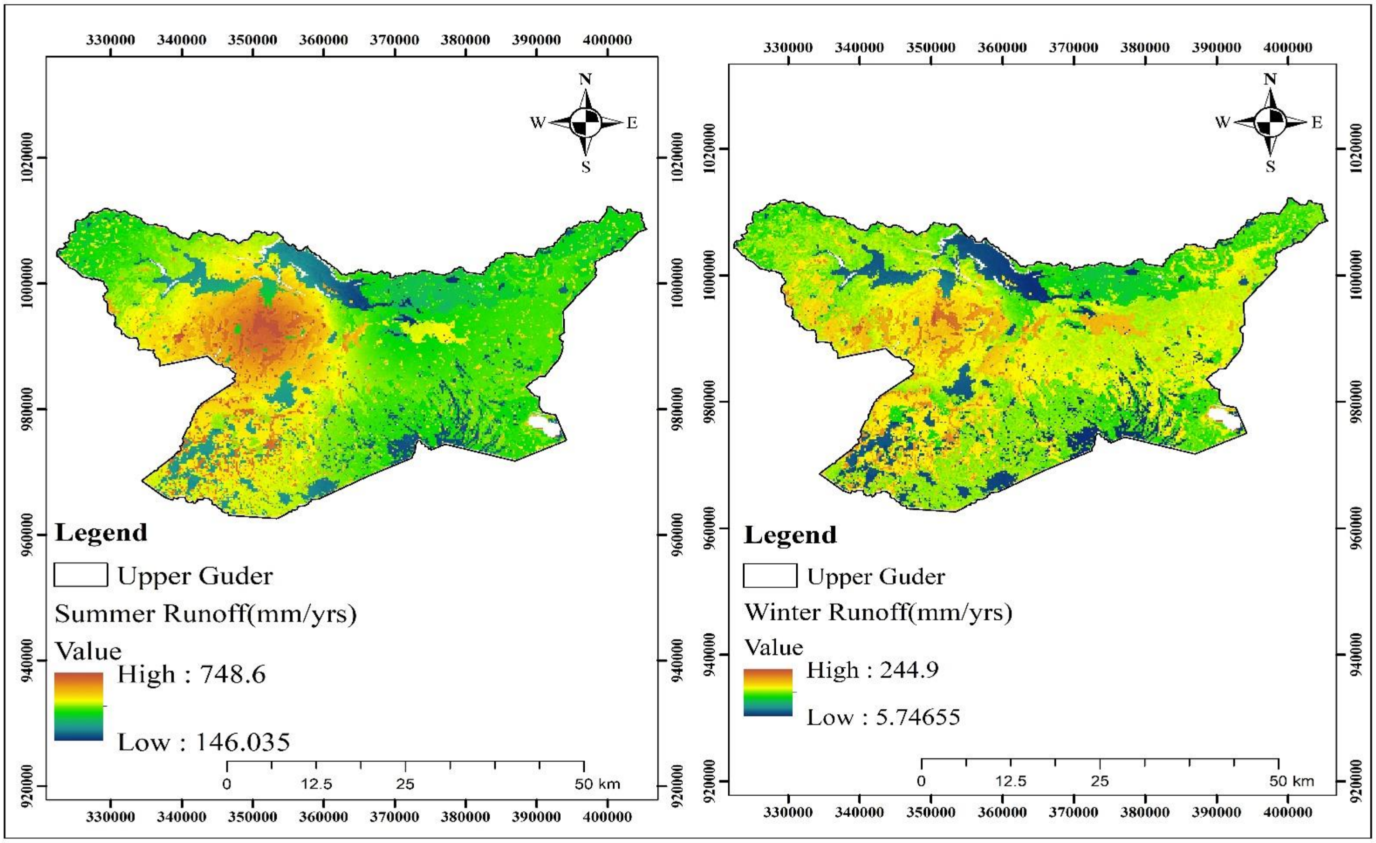

Figure 4. 14. Summer and winter runoff map of the study area.

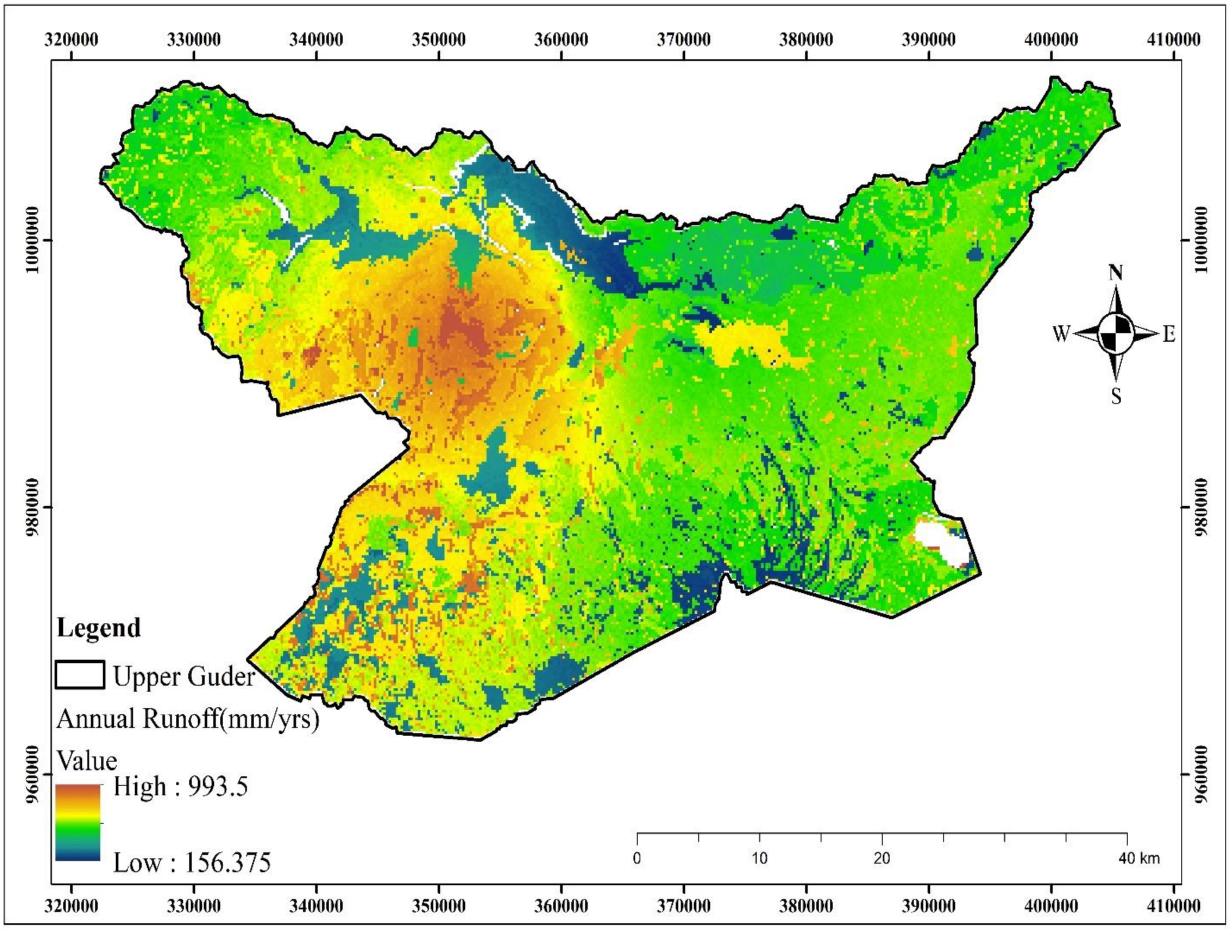

Figure 4. 15.Annual runoff map of the study area

As can be seen from the above map, the areas with settlements and clay cover have the highest runoff within the catchment. High rainfall intensity is also associated with high runoff, particularly in the Habus Gaba area. Where there is bare land, there is also a lot of surface runoff.

4.7.4. Recharge

The physical features of the watershed primarily determine how much water percolates into the subsurface. The ability of various land uses, land covers, and soil textures to transfer water through them varies. The average annual and seasonal value of surface runoff and evapotranspiration is subtracted from the annual and seasonal precipitation in the model to determine the amount of recharge that percolates to the saturated zone.

Groundwater recharge is a hydrological process that replenishes groundwater by moving infiltrated precipitation water downward into an aquifer's saturated zone (Wu, Y., et al. , 1996). The study area's estimated yearly groundwater recharge is 298 mm or 23% the total yearly average precipitation.

The highest value of the annual recharge is taken into account because of a number of inputs, including the high precipitation around Hamus Gaba, the highly vegetated area, the loam and clay loam, the elevated topography surrounding Roge Mountain, and the distribution of pervious surfaces within the watershed.

According to Tilahun (2008), major recharge occurs in the Jema, mugger, and Upper A wash basins where rainfall is Medium to high and revealed that annual recharge is 158-290 mm.

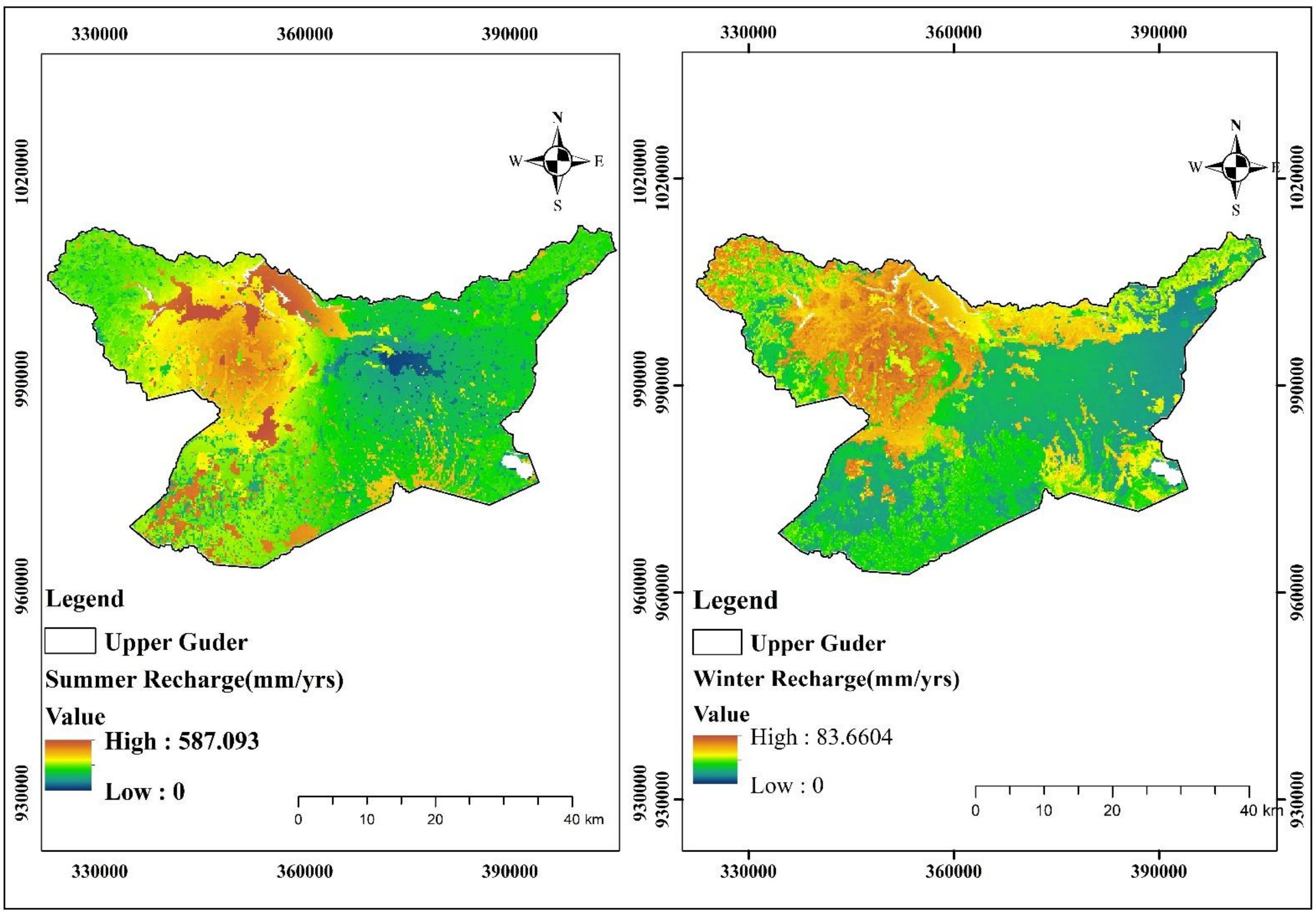

Figure 4. 16. Summer and winter recharge map of the study area.

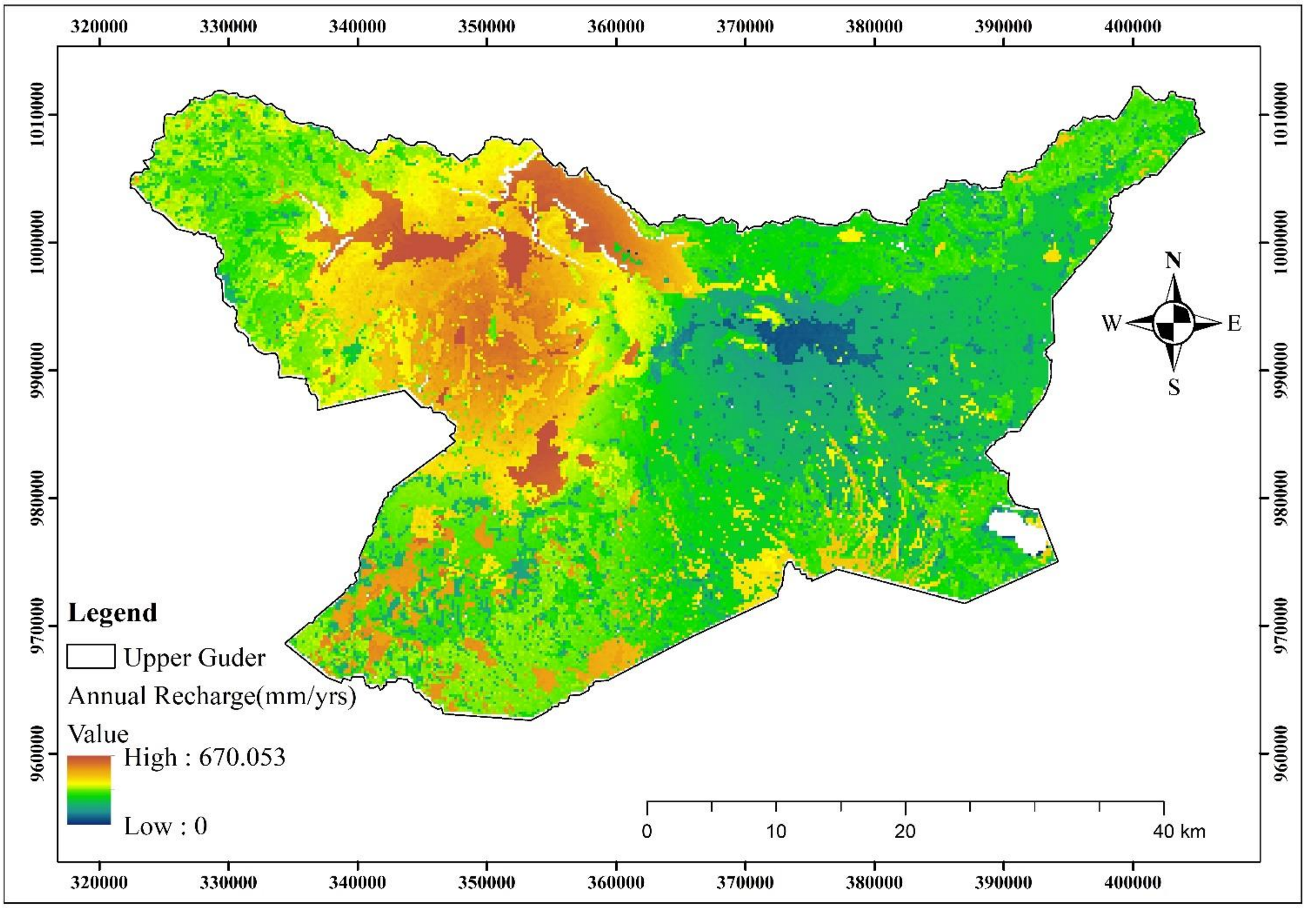

Figure 4. 17. Annual recharge (mm) map of the catchment

CHAPTER FIVE

5. Hydrogeology

Hydrogeology is distributed, and moves through the soil and rocks that make up the Earth's crust; this is known as hydrogeology (commonly in aquifers). It includes how geologic processes and materials interact with water (Fetter, 2001). The predominant hydrogeologic components within the catchment area are volcanic rocks, whose hydrogeologic characteristics are altered by weathering, fission, and/or local faulting processes.

The primary hydrogeological units that make up the upper Guder catchment are volcanic rock that has undergone varied degrees of weathering and fracturing. The catchment is located in the Ethiopian plateau. Since volcanic rocks exhibit a diverse range of chemical, mineralogical, structural, and hydraulic properties, the aquifers they contain can be extremely abundant or used for specialized purposes (Kresic, 2006).

Aquifers in volcanic rocks have a variety of hydraulic characteristics. Significant differences in porosity and permeability can be found within short time and distance intervals. These complicated temporal and spatial variations are explained by their various stratigraphic relationships, their erratic contacts with both very old and recent rocks, their mode of emplacement, their structural and textural variability, their varying degrees of weathering, and their variable topographic position, all of which sophisticated the hydrogeological behavior of the volcanic rocks (Alemayehu, T., 2006). Because of this, different volcanic rocks have different capacities for storing and transferring water, resulting in different types of aquifers.

From upstream to downstream, the hydrogeological property of the upper Guder catchment varies. The catchment's groundwater availability is determined by the presence of redeposited alluvial and some eluvial sediments along the flat land, as well as weathered and slightly fractured Tertiary rock. Groundwater movement is shifted in the direction of impassable rock formations, which act as barriers to flow. Fault zones and lineaments are examples of additional features that can function as barriers or as conduits for groundwater flow. Due to the presence of various volcanic rocks covered in thick alluvial sediments from the catchment, the hydrogeology and groundwater occurrence are complex.

The area's volcanic rocks and unconsolidated sediments have been categorized into various aquifer units according to their field hydraulic characteristics, pumping test data (transmissivity), and yields from boreholes and springs. In addition, the assessment of hydro stratigraphic unit productivity has taken into account the recharge conditions and topographic setting.

The shield volcano's fractured lava flows serve as great conduits, but their storage capacity is restricted. The degree of interconnectivity among fractures influences their capacity to serve as conduits for groundwater flow. As the likelihood of a fracture intersection increases, fracture connectivity rises with increasing fracture length and density (Cook, 2003).

In the study areas, the primary water-bearing formations are the flood basalt and the quaternary alluvial and eluvial deposits. The depth at which groundwater is found varies greatly, essentially ranging from the surface to significant depths below it.

The hydrogeological systems of this study area have been categorized using both qualitative and quantitative techniques, according to the report on the hydrogeological and hydro chemical map of Addis Ababa and Akaki Beseka map sub-sheet. The impermeable rock unit, secondary fissured permeability, and dominant primary porosity were the basis for the qualitative approaches used to classify and characterize the aquifers. Pumping test data, which was either measured in the borehole or acquired from regional offices, and field water point inventory data served as the basis for the quantitative classification (Manaye, Bereket Fentaw and Mihret, 2010).

The study area includes basement rock (ignimbrite), which is primarily exposed around the sibila and shako area. The upper part of these rocks is heavily weathered and affected by highly fractured rock. Based on all of the wells' lithologic logs, it is evident that two major secondary processes increase the permeability of this unit, allowing it to be classified as an aquifer. The surface is covered by thick clay soil. It shows the existence of intense weathering of rock near the stream where the surface is slope becomes small.

The uppermost portion of the aquifer is affected by weathering; the weathered column of this aquifer varies from 24 meters at the Sumbala Shiko area. The weathering column at Sumbala Well is thicker, most likely due to the higher temperature and lower altitude that intensify chemical reactions and increase weathering activity. This well is 110 meters deep. This site features a thick succession of fractured and weathered columns, which made drilling there is easy to do.

5.1. Groundwater point

Spring

According to (Todd, 1980), spring is a concentrated release of groundwater that manifests as a water current that flows across the ground's surface. It represents the outflow of groundwater from the saturated zone due to the hydraulic head difference between the recharge zone and discharge zone (thermal springs may result from convective upward flowing of heated ground water in the absence of gravity).

There are numerous intermittent and perennial springs throughout the catchment. In the study area, every spring is chilly. People use these chilly springs for all kinds of activities. People who live in rural areas, in particular, primarily depend on spring for domestic needs as well as for their livestock. In certain cases, they even use it for small-scale irrigation (laga huluka and guder river fall), which produces large yields.

The catchment's springs are the product of various geomorphic and geologic processes. Some of the lowland springs originate from the contact of highly weathered and less weathered lithology, and those that are situated on hillside and mountain foot emerge as topographic breaks. However, most of them are structural springs that were created by lithologies that were fractured.

Hand-Dug well

A hand-dug well is a type of water well that is manually excavated using simple tools such as shovels, picks, and buckets. It is typically dug into the ground to reach an aquifer or water table. In areas with extremely shallow groundwater, locals know about a different source of water supply: hand-dug wells. The study area contains a small number of hand-dug wells that are almost evenly spaced throughout the catchment's recharge zones, suggesting that they may not necessarily represent the regional groundwater zone but rather access shallow circulating groundwater. A perched aquifer that finally overflows the margins of the impermeable bed may contain hand-dug material, particularly in highland areas.

The majority of the wells that have been dug are located in the study area's shallow aquifers in the southwest and southeast. The lacustrine sediments and alluvial and eluvial soils supply the majority of the water used in dug wells. Additionally, the main water-bearing layers for dug wells are the heavily weathered top regolith of basalt and welded pyroclastic rock.

Borehole

Borehole is to a narrow, deep hole drilled or constructed to access underground water resources. These boreholes are essential for groundwater exploration, extraction, and monitoring, providing access to water-bearing layers for various purposes such as drinking water supply, irrigation, and industrial use.

The study area is surrounded by a number of deep boreholes. Governmental and non-governmental organizations frequently drill them in order to supply water to rural and urban areas. The primary aim of the boreholes in the study area is water provision. It is the primary hydrogeologic interest water point that allows an evaluation of the aquifer.

In the study area, lacustrine and basalt sediments are the main water-bearing units for the majority of the boreholes. Furthermore, important water-bearing layers include the trachyte and pyroclastic. Borehole depths vary from 70m (around chalia area) to over 256m (Balami(HB_2)) below the surface and static water ranges from minimum 5.4m located Ballami locality that yields 5 l/s and maximum 89.48m at Ambo town that yield 10.9 l/s

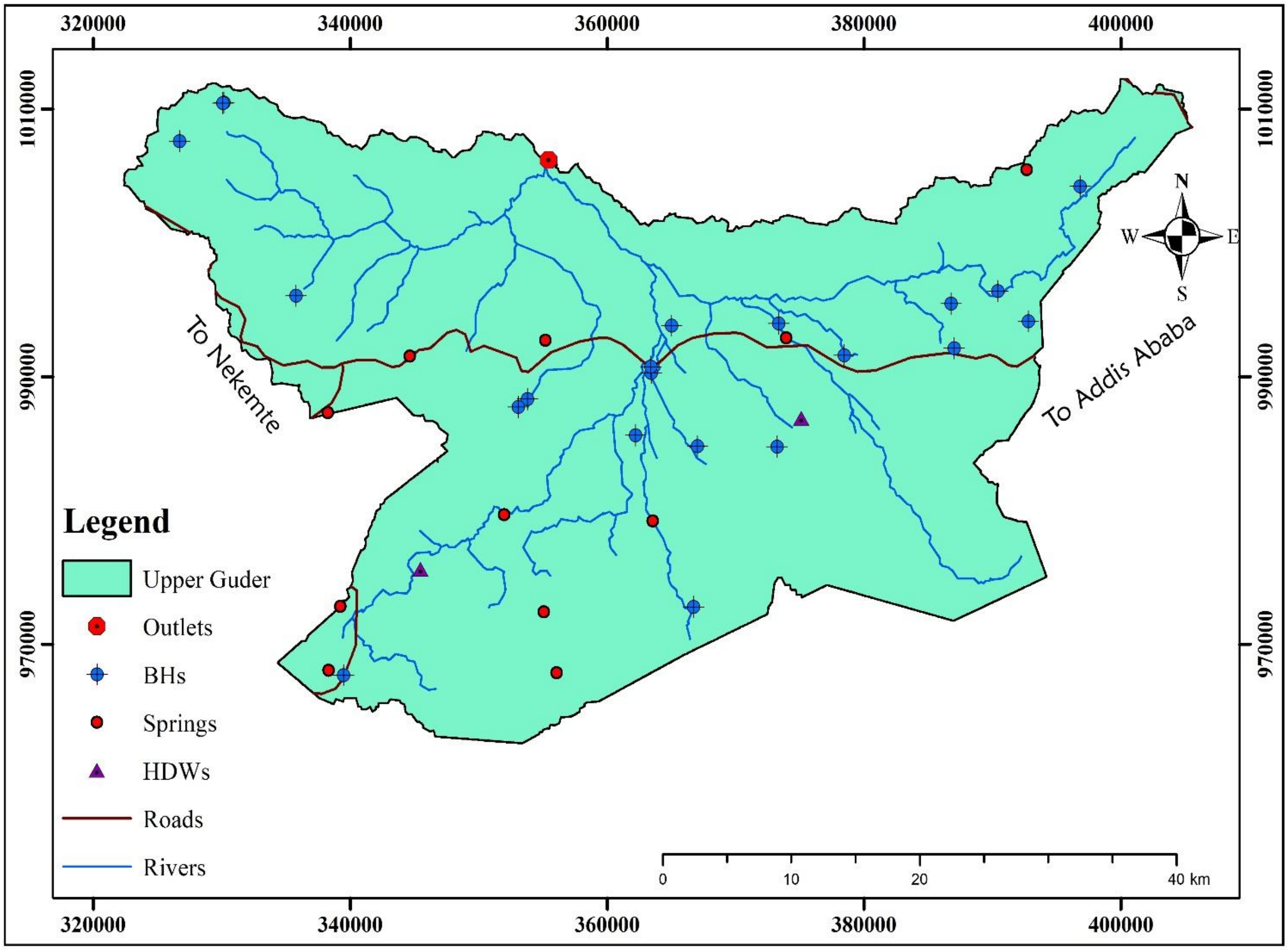

Figure 5. 1. Distribution Available water points in the catchment

5.2. Aquifer systems in the study area are categorized qualitatively.

5.2.1. Aquifers with porous permeability

Alluvial and Eluvial quaternary sediments are exposed in the study area and represent hydrogeological units with a dominant porous medium. These units' pore throat connectivity, size, sorting, and cementing material all affect the occurrence of groundwater within them. It has been observed in the upper Blue Nile sections of the study area based on the hydrogeological map. The textures of alluvium are made up of gravel, silt, and sand with varying grain sizes. The alluvium is a good source of groundwater resources for shallow aquifers due to its high transmissivity and sorting (Thomas.et.al.,, 2018).

5.2.2. Aquifers with fissured permeability

The hydrogeological units of these rocks are primarily composed of sedimentary rocks that have undergone secondary deformation and tertiary volcanic rocks. The fracture that can provide access for water transfer and storage is the primary factor governing the occurrence of groundwater in these rocks. Because the majority of the volcanic rocks in the study area have experienced significant weathering, fractures, and joint sets, they are thought to have high to medium permeability and the ability to store and transfer a sizable amount of groundwater (Thomas.et al., 2018).

5.2.3. Aquifers with mixed (porous and fissured) permeability

The majority of the hydrostat graphic units in the study area that show both primary and secondary permeability are exposed on the plateau. According to Thomas. et al. (2018), these permeability types primarily developed in porous basalts and tertiary sedimentary rocks intercalating volcanic rocks in the plateau.

The hydrogeological system elements in the area have been determined by taking into account the geomorphology, geological descriptions, and those as mentioned earlier qualitative and quantitative parameters. The aquifer and aquitard systems listed below are part of the hydrogeological system from the Akaki Beseka and Addis Ababa sheets (GES,2010).

The following classification of the various rock units with their areal extent within the area was defined based on the qualitative and very limited quantitative data (the yield of springs and boreholes) and geological description:

1. Extensive (**243.6 km^2**) and moderately productive porous aquifers (T = 1.1 - 10 m^2/d, q = 0.011 - 1 l/s.m, Q = 0.51 - 5 l/s for wells and/or springs). These aquifers are shown on the map in deep red and consist of Dendi-Wenche pyroclasts, lacustrine sediment, and alluvial soil.

2. Extensive (**1431km^2)** and highly productive fissured aquifers (T = 10.1 - 100 m^2/d, q = 1.1 - 10 l/a.m., Q = 5 - 25 l/s for wells and/or springs). These aquifers are shown on the map in dark green and include parts of the Tarmaber-Mageze formation, Addis Ababa basalt, and Guder-Babich basalt.

3. Extensive **(120.9km^2)** and highly productive fissured / karst aquifer (T = 10.1 –100 m^2/d, q = 0.11 –1 l/s.m, with spring and well yield Q = 5.1 –25 l/s). The aquifer is shown in blue sky. The aquifer consists of Mesozoic limestone.

4. Aquitards (**402.6 km^2)** with limited groundwater resources. These lithological units are represented on hydrogeological maps in brown. They consist of Chefe Donsa pyroclast, Trachytes of Ziqwala, Wechecha, Furi, and Yerer, and rhyolites of Gash Megal, Bora-Bericha, rhyolitic and trachytic domes of the Nazret group.

5. Extensive **(9.8 km^2**) and locally developed and highly productive porous aquifers (T = 1.1 –10 m^2/d, q = 0.011– 0.1 l/s.m, with yield of spring and well Q = 0.51–5 l/s). The aquifers are shown in light red. Aquifers consist of Quaternary unconsolidated, Mesozoic sediment, and adigrat reddish-brown sandstone and limestone.

5.3. Aquifer productivity

5.3.1. Extensive and Moderately Productive Porous Aquifers

This unit is exposed in the south eastern parts covering a very extensive area. This aquifer system includes alluvial, pyroclastic and lacustrine sediments.

The groundwater hosting part of this unit is the primary permeability resulted from the availability of primary effective porosity. The groundwater availability is highly dependent on the grain size, distribution as well as sorting. The grain size on this aquifer varies from sandy to gravel (medium to coarse sometimes fine) with a well sorted pattern, thereby increasing the transmissivity of the aquifer. This aquifer is recharged directly from precipitation and the adjacent plateau volcanics.

The moderate fracturing, high weathering and scoriaceous nature of Aiba-Alaje basalt, Jimma Lower and upper basalts, provide the rocks with a good permeability and hence moderate productivity. The Jimma volcanic flows are recharged from the Jibat highlands and Wonchi and Dendi volcanic cones and ridges in addition to direct precipitation and local perennial and intermittent streams. The thick soil development over the aquifer is a good media for enhancement of recharge.

Many springs emerge from this aquifer from the topographic breaks of hills and river valleys through the interstitial spaces, and they are the source of many watercourses draining to the Guder

River. In general, the Dendi-Wonchi pyroclastic deposits are mapped as moderate productive aquifers with an average dry season spring yield of 2.5 l/s (GSE, 2019).

5.3.2 Extensive and Highly Productive Fissured Aquifers

These aquifers are represented on the map as dark green areas, covering approximately 1431 km^2. The dark green aquifer comprises portions of the Tarmaber-Mageze formation, Addis Ababa basalt, and Guder-Babich basalt, accounting for 65% of the sheet area. This type of aquifer is exposed in the study area's northern, northwest, and central areas.

***Tarmaber-Megzez, Addis Ababa and Guder-Babich basalts*.** This unit is found in the northeastern and northwestern parts of the study area forming a flat plain, and undulating highland terrains with elevated ridges. The permeability in this aquifer is highly dependent on the degree and intensity of fracturing, the enhancement of jointing, and the interconnection of primary porosity. In the study area, part of the Tarmaber-Megezez basalt has good fracturing, which gives it good hydraulic properties. The scoraceous nature of this aquifer is favorable for groundwater storage and movement. In addition, the columnar joints are enhanced by secondary fractures and weathering, resulting in the occurrence of springs in the highlands. In some places, particularly on the rift escarpment, the faulting increases the permeability and results in the development of a groundwater conduit and significantly increases the water-bearing characteristics of aquifers. On the flat plain, there is thick soil development over this aquifer, which enhances groundwater recharge by infiltration and then percolation. The geological, geomorphological, and climatic conditions of the area make the Tarmaber and Babich-Guder basalt high groundwater discharge layers. The groundwater discharged from this aquifer is manifested by natural springs, boreholes, and dug wells. There are many perennial springs with variable discharge. Most of the springs emerge through fractures, weathered surfaces, and contacts with less permeable layers and from topographic breaks. During the fieldwork, it was observed that the discharge of springs from Tarmaber-Megezez and Babich-Guder basalts is highly variable and ranges from 0.01 to 37.5 l/s. The variation is assumed to be due to differences in geomorphology, amount of recharge, and degree of fracturing.

Most springs emerge through fractures on hillsides where there are topographic breaks. It is possible to see such conditions at Toke kutaye (Csp-38),Tikur Inchini (Csp- 35) and Toke (Csp-40) with a dry season average discharge of 5.5 l/s. The NE-SW and E-W trending faults manifested in this aquifer serve as a conduit for groundwater and are responsible for the appearance of some of the springs on the escarpment.

Basalt and sandstone that have been extensively weathered and fractured make up the hydrostratigraphic units of this zone. Due to its columnar joint composition, basalt is prone to fracturing, which enhances the aquifer's potential. Although the primary materials in this zone are fractured basalts and sandstone, scoria is also found in some boreholes as a water-bearing formation (Balami, Babicha, Ale ula dabi (B2H) etc.). The water-bearing qualities of scoraceous formations are a result of their high weathering and fracturing rates. Thus, a combination of high weathering and fracturing, columnar joints, paleosoil, and inters lava flow between distinct lava successions favor this zone's productivity. This basaltic unit may be exposed tertiary lower basalt that forms a steep cliff and a gentle slope on a plateau (EWWDS, 2012).

In the catchment, the Lower Basalt, Middle Basalt, and Upper Basalt volcanic units are the three main and most important sources of groundwater. However, the highest, most extreme parts of the catchment in the northwestern, and where yearly rainfall is greatest, are dominated by lower basalt (Hamus Gaba).

This basalt is easily subjected to secondary processes because of its significant primary porosity. Because of the intense plant roots and heavy rainfall, this unit has weathered and the joint has become wider. It can have a multi-layer confined aquifer nature in certain situations, which is explained by the fact that geologic processes affect it at varying depths. In fact, where a volcanic formation has a secondary structure, its significance as an aquifer increases and improves.

An extremely productive aquifer of lower basalt with an average yield can be found near Babicha (Table 5.1) based on data from boreholes. Sandstone with variegated colors is the main aquifer system. The thickness of the aquifer is approximately 200m. The aquifer system is contained and flowing during drilling, with a discharge rate of 32 l/sec and a pump position at 90 m below the surface. The well is cased up to 282m (EWWDS, 2012).

Table 5. 1. Representative lithologic description of Babicha deep well

No	Depth, m	Lithologic description
1	0-4	Black cotton soil
2	4-16	Sandy clay
4	16-32	Weathered basalt
5	32-66	Massive basalt
6	66-72	Weathered basalt
7	72-282	Variegated color Sand stone

5.3.3. Extensive and highly productive fissured / karst aquifer

In the area, the limestone is indicative of a large (120. 9 km^2) productive fissured aquifer that may be karst. 5.5% of the sheet area is made up of the aquifer, which is visible in a blue sky. Aquifer outcrops are restricted to the deepest regions of the Guder and some of its tributary rivers, so the drainage of the aquifer is only recorded by a small number of water points. These are narrowly inhabited, challenging-to-access valleys. It appears that a significant amount of the aquifer's groundwater is directly drained to rivers that are concealed (covered) by the main rivers well developed alluvial sediments. The idea is confirmed both by the chemistry of the lower reach of the Guder River tending towards sulphate types and by the relatively high river flow during the dry season reflecting maintenance of surface flow by drainage of groundwater from medium to highly productive aquifers (GSE.2010).

The springs discharge 5.1 l/s on average. It was determined that the lowest discharge was 0.05 l/s. A measurement of 25 l/s was made of the maximum discharge. Significant variations in spring discharge are caused by the aquifer's karstic nature.

Aquitards made of gypsum beneath and mudstone above enclose the limestone aquifer. The gypsum and mudstone units are both sizable, however they do not correspond to regional units like limestone and lower sandstone. Because of this, as part of the deep regional groundwater circulation, groundwater from the upper aquifers (upper sandstone and volcanic rocks) may seep into the limestone and perhaps even the lower sandstone. Where mudstone covers limestone, it acts as a confining layer for the limestone aquifer. Groundwater flowing along the boundary between the limestone and gypsum before it emerges from the spring and/or the presence of gypsum in the limestone matrix can account for the high sulfate content found in some springs (GSE,2010).

5.3.4. Extensive and Low productive fissured/porous

This aquifer has local, discontinuous fissures where flow is primarily developed in an irregular system of fissures and wechecha trachyte's, plagioclase, and feldspar phyric trachytic lava flow and dome with limited groundwater resources. In the center of the catchment area, the north of dend area, this unit is exposed around the Extension of SW to NE (GSE,2010). The drilled well located near the central periphery of the catchment (Table 5.2) provides a source of water for the rural community of Lidisa (GPS location: 349659mE, 970625mN). It is evident that secondary processes improve the permeability of this unit, making it suitable for classification as an aquifer-like lineament and this project area is located in the main aquifer of min highland catchment, the groundwater yield is expected high other than its location near the recharge zone.

Table 5. 2. Representative lithologic description of Lidisa deep well

No	Depth Range(m)		Lithologic description	Aquifer Characteristics
	From	To		
1	0	8	Black cotton soil	No water at all
2	8	18	Highly weathered volcanic	
3	18	25	Highly Weathered &fracture and volcanic basalts	
4	25	48	Fractured basalt	less water bearing layer
5	48	62	Trackyt basalt	
6	62	84	Highly weathered and fractured basalts	Good water bearing layer
7	84	98	River gravel deposit	
8	98	114	Highly weathered basalt	
9	114	120	Hardly fractured basalt	No water at all

The uppermost portion of the aquifer is impacted by weathering. This aquifer's weathered column is between 8m and 25m deep. The thicker weathering column is most likely the result of a higher temperature and lower altitude (2491 meters), which intensify chemical reactions and weathering activity.

Therefore, based on the well's pumping test results of lidisa, the aquifer's yield and transmissivity are 9 l/s and 25.6 m^2/d, respectively. Since transmissivity and yield are high, a formation may be classified as a moderately productive zone.

In conclusion, the degree of weathering, the thickness of the weathered column, and the intensity of the fractures all have a significant impact on the water bearing capacity and the ease of its release in this unit. It is evident that weathering and fractures are not distributed fairly. Thus, weathering and fracturing are localized factors related to ground water potential in this unit. The unit became both heterogeneous and anisotropic as a result of these phenomena.

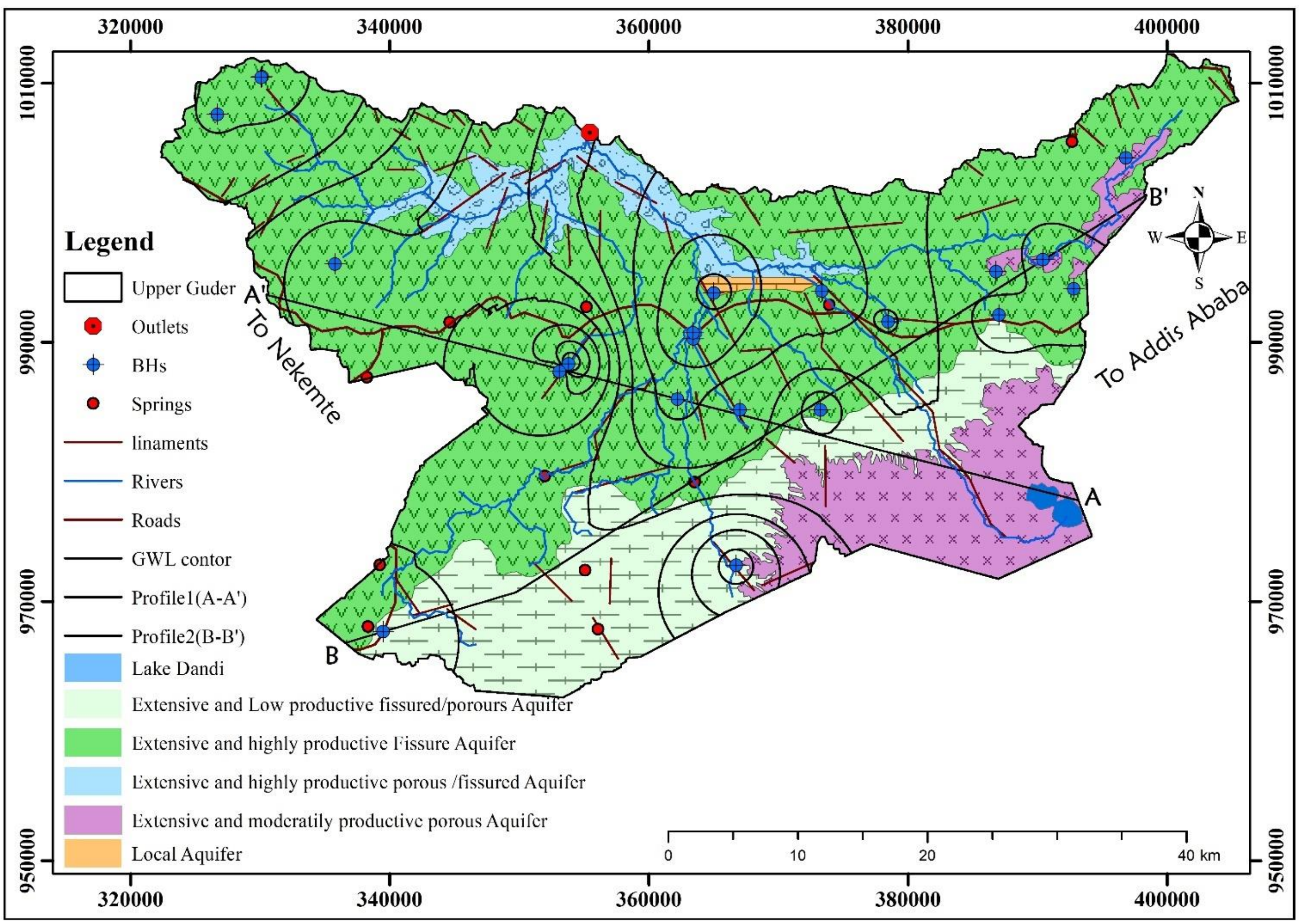

Figure 5. 2.Hydrogeological map of the study area (computed from GSE,2010)

5.4. Aquifer characterization by using pumping test data

Aquifer thickness, pumping hour with drawdown data, static water level, and other hydraulic parameters found in well log data can be used to estimate the aquifer characterization of a given area. (Figure 5.3) shows the time versus drawdown graph of the wells using the Cooper and Jacob solution method for the following wells: Babicha#Well (WAMW-02), Guder#Well (WAMW-04), Chalia#Well, Lidisa#Well, Homicho#Well, and Sumbala#Well plotted on log-log paper.

The six boreholes, namely Babicho#Well (WAMW-02), Guder#Well (WAMW-04), Chalia#Well, Lidisa#Well, Homicho#Well, and Sumbala#Well, showed remarkably similar curves (Figure 5.3). The corresponding aquifer adheres to the wells that are revealed to be confined aquifers based on the time drawdown graph and the lithological data from boreholes. There were a few wells where the static water levels did not significantly rise above the water strike depth, which suggests that confined aquifers are typically found in the catchment.

The hydraulic properties of an aquifer, particularly its transmissivity (T), hydraulic conductivity (K), and transmissivity (T), can be used to characterize the aquifer properties of an area, such as its capacity to transmit water, store a reasonable amount of water, and allow for reasonable flow rates.

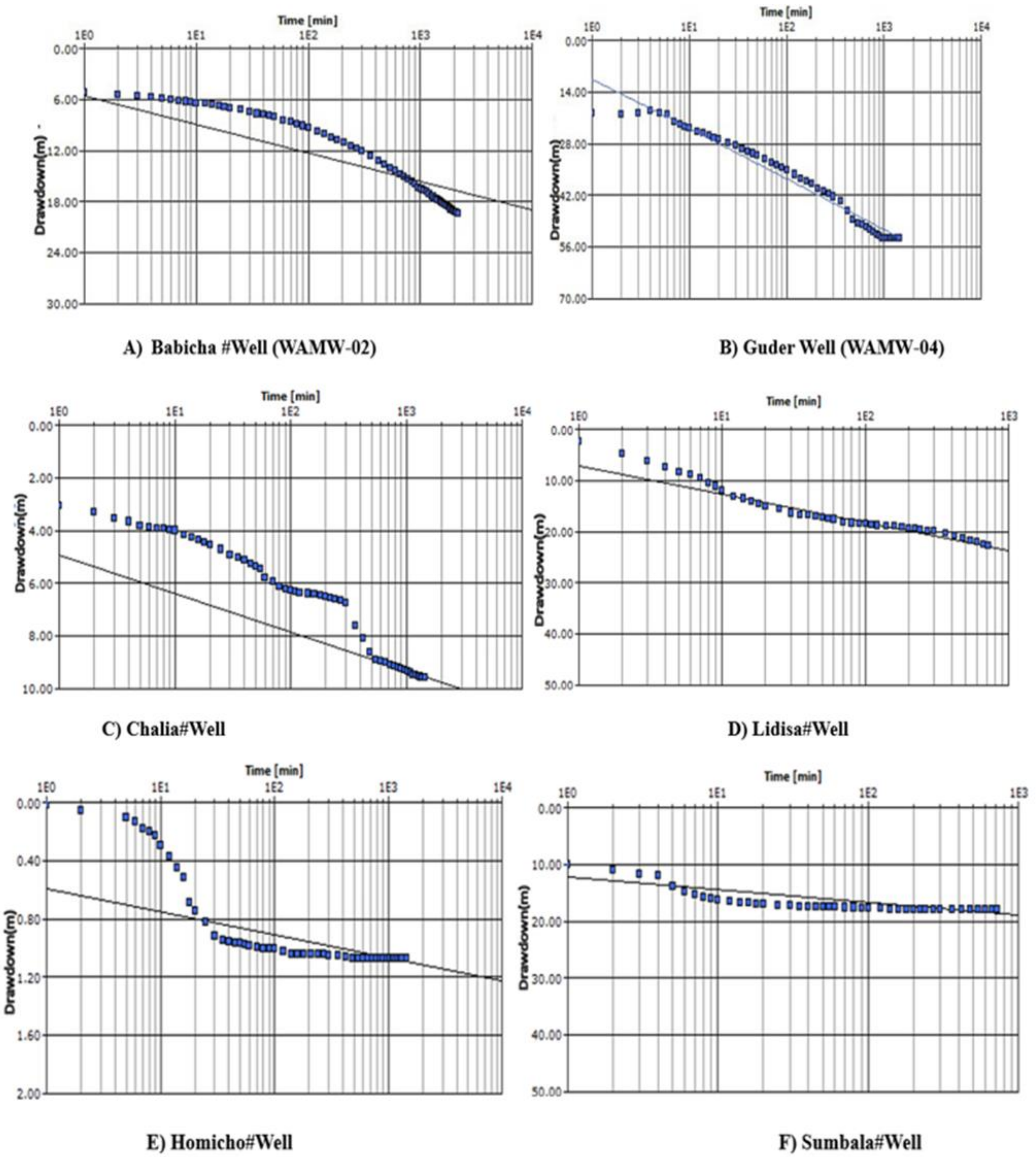

Figure 5. 3. Time verses drawdown graph of the wells with Cooper and Jacob I solution method

Transmissivity

Transmissivity is the rate of flow through a unit width of an aquifer with a given saturated thickness under a unit hydraulic gradient. This is a measurement of the volume of water that can pass through a fully saturated aquifer's unit width at a hydraulic gradient of one. The value of transmissivity serves as a foundation for groundwater development, abstraction, exploration, and protection in the future. It has to do with an aquifer's hydraulic conductivity and saturated thickness. An aquifer's transmissivity can be determined using equation. The slope of time-drawdown data plotted on semi-log paper was ultimately used to calculate all of the transmissivity. Aquifer transmissivity in relation to hydraulic conductivity is computed using Cooper and Jacob I time drawdown analysis as follows (Rushton, 2003): The values of transmissivity analyzed using Aquifer test program from pumping test data are given in (Table 5.3).

$T = \frac{2.3Q}{4\Pi\Delta S}$ Where, **T** is transmissivity in m^2/s, **Q** discharge of the well in m^3/s and **ΔS** is change in drawdown.

Table 5. 3. Spatial Distribution of Transmissivity

Location	**Thickness of Aquifer(m)**	**Type of aquifer**	**T(m^2/day)**
Babicha (WAMW-02)	99.64m	Confined Aquifer	1.51×10^2
Guder (WAMW-04)	94m	Confined Aquifer	1.38×10^1
Chalia Well	54m	Confined Aquifer	1.30×10^2
Lidisa Well	54m	Confined Aquifer	2.56×10^1
Homicho Well	70.7	Confined Aquifer	7.34×10^2
‘Sumbala Well	32m	Confined Aquifer	8.44×10^1

The transmissivity distribution obtained from the aquifer pumping test is variable through the catchment section. The estimated transmissivity of an aquifer ranged from 1.38×10^1 to 7.34×10^2 m^2/day. The analysis of the transmissivity on the Homicho, Chalia, and Babicha wells produced values of 7.34×10^2 m^2/day, 1.30×10^2 m^2/day, and 1.51×10^2 m^2/day, respectively, which are very high values compared to the other wells in the catchment for any aquifer (Table 5.3). This indicates that this location has the greatest potential for productive aquifers and high transmissivity value in an aquifer is crucial for ensuring a sustainable and reliable water supply for the community, which in turn supports various aspects of community life and development. Because of the main aquifer of this area is moderately fractured & vesiculated Basalt & moderately fractured Sand stone and specially Homicho well (converging flow) very high productive aquifer the major aquifer system is Variegated color Sand stone. And also, in the study area to classify the aquifer, depth of the out croups and aquifer thickness also play a significant role; aquifer thickness of the study area is ranged from 99.64 and 54m (Table 5.3) and depth ranged from 130m to 282m and this depth can show us the borehole is deep aquifer system and the other wells like Guder, Sumbala and Lidisa well are moderate transmissivity values it implied that smaller withdrawal of water for local water supply (private consumption) could be maintained in the well and the groundwater supply is limited consumption in the well with regarding to transmissivity (Krasny, J., 1993).

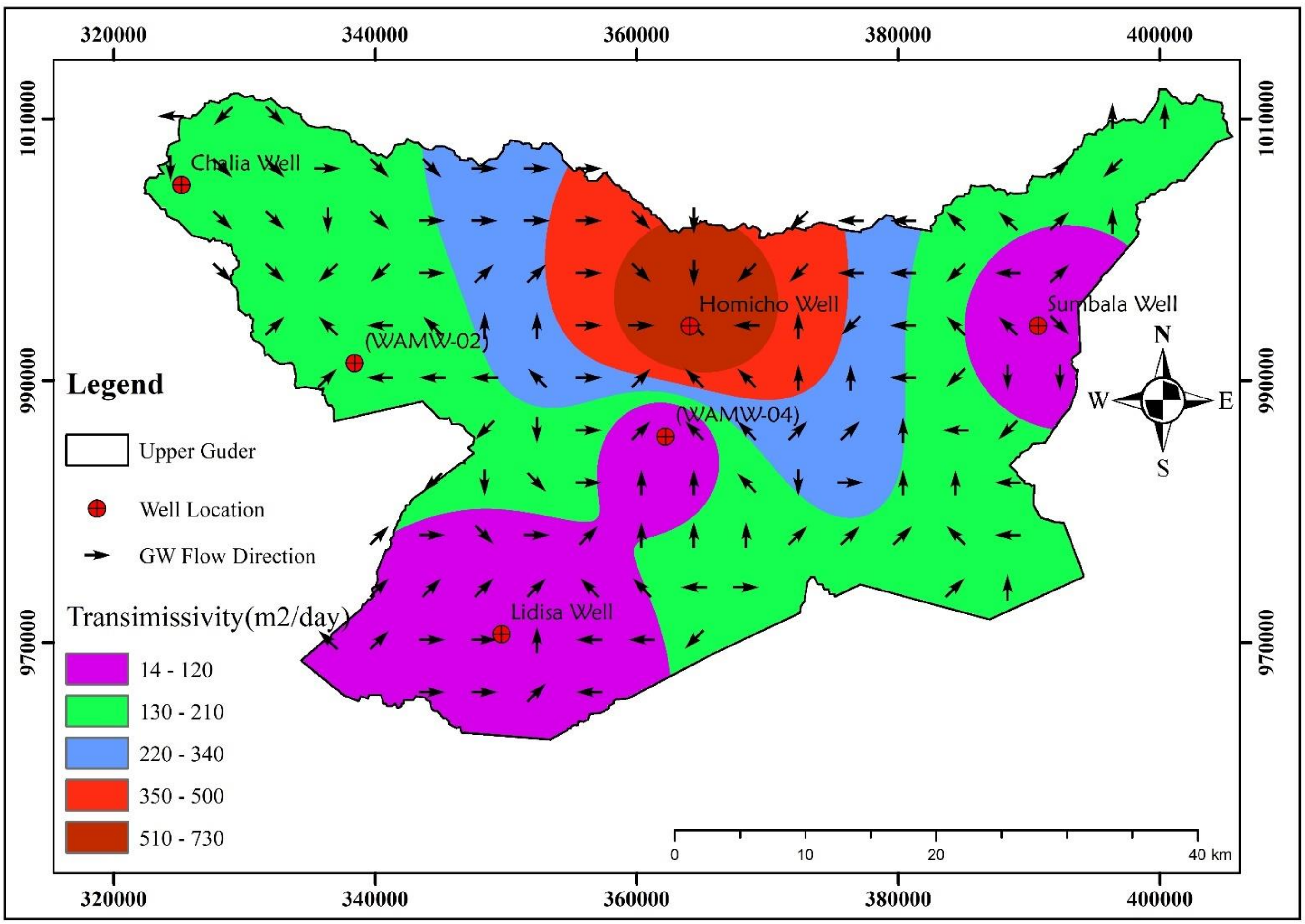

Figure 5. 4. Spatial Distribution of Transmissivity in the catchment

In general, confined condition of an aquifer is existed in all the six wells located in the catchment down dip of their outcrops. The overall average transmissivity of the well is found to be $1.89*10^2$ m^2/day.

Table 5. 4. Estimated values of hydraulic conductivity and storativity

Location	Thickness of Aquifer(m)	K(m/day)	Storativity
Babicha (WAMW-02)	99.64m	1.52×10^{0}	5.00×10^{-1}
Guder (WAMW-04)	94m	1.47×10^{-1}	4.08×10^{-1}
Chalia Well	54m	1.96×10^{0}	8.65×10^{-3}
Lidisa Well	54m	4.74×10^{-1}	9.85×10^{-2}
Homicho Well	70.7m	1.04×10^{1}	1.95×10^{-2}
Sumbala Well	32m	7.91×10^{0}	5.00×10^{-1}

Ethiopia Water Works Construction Enterprise and the West Shoa Water and Minerals Office provided the current pumping test results for six wells. Aquitest 3.5 software is used to reanalyze the raw data from the pumping test (constant and recovery test). The analysis of the wells' pumping test results is representative of the entire catchment.

The hydraulic conductivity and storativity distribution of the area ranges between 0.147-10.4m/day and 0.0086-0.5 respectively. the highest value of hydraulic conductivity (10.4 m/day) is found at north eastern and south eastern part of the study area which covers largest part in the study area (Table 5.4). Because around homicho and sumbala well the main aquifer is the river gravel, sandstone weathered and fractured basalt and scoraceous basalts…. are the main aquifer with high hydraulic conductivity and due to its highly productive aquifer low drawdown.

The amount of water released from storage per unit decrease in the aquifer's hydraulic head, measured per unit area, is known as storativity. An aquifer's storativity (S) is estimated using a semi-log distribution. (Table5.4) provides the analyzed values of storativity. The average storativity was 0.26, with a range of 8.65×10^{-3} to 5.00×10^{-1} (Table 5.4). the wells located in the north western lowland parts of the catchment closes to Chalia well are presented with lower value of storativity. An aquifer's storativity decreases from the northwest to the north of the study area.

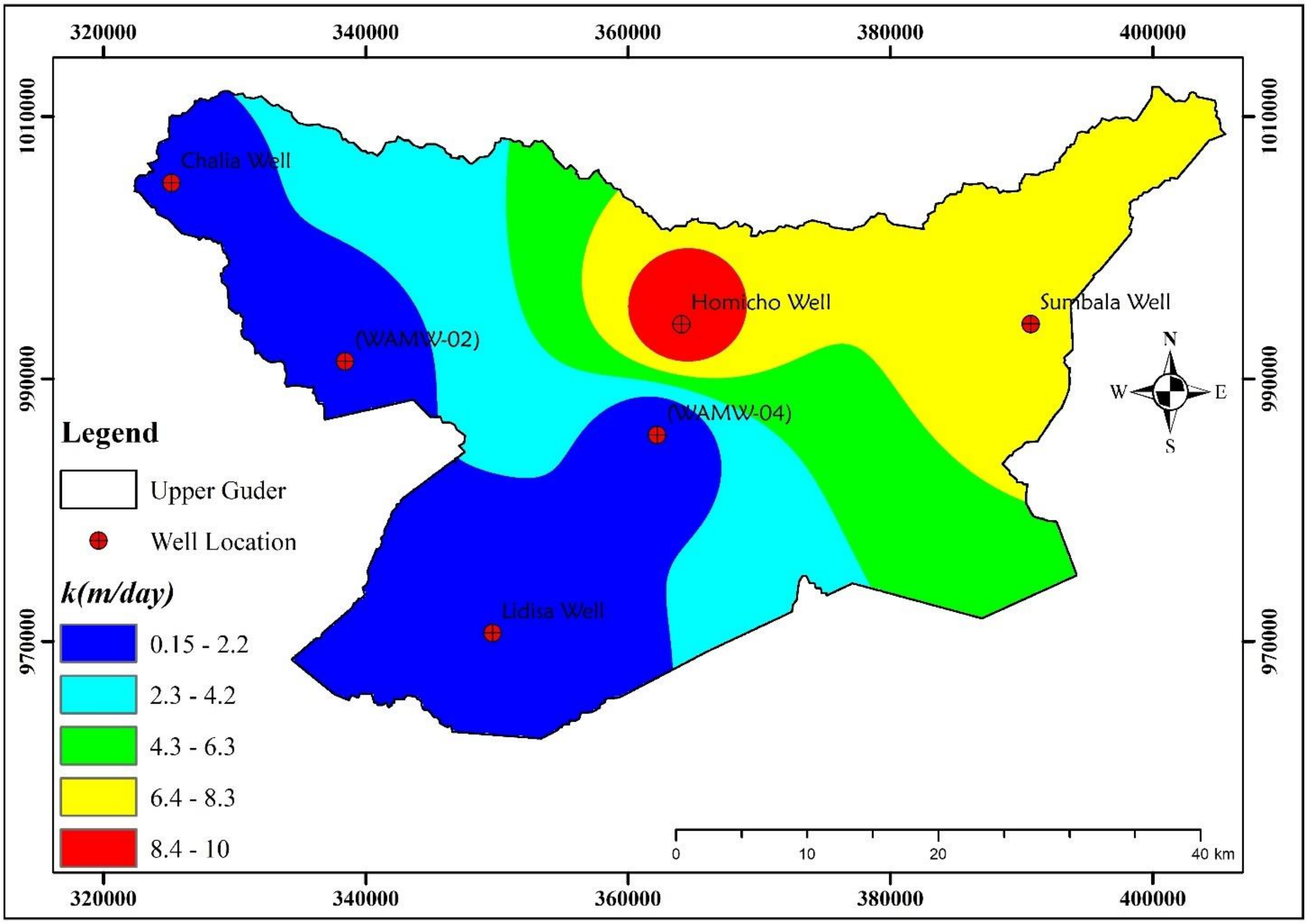

Figure 5. 5. Spatial Distribution of Hydraulic conductivity in the catchment

5.6. Groundwater flow Direction

Primary factors that influence groundwater flow direction are the topography, geology, and structural makeup of the entire area. However, depending on the characteristics of a particular catchment, the degree to which these effects affect flow direction varies. Most of the time, topography and geology have a significant impact. Nonetheless, groundwater flow is controlled by structural alignment in the region where geologic structure predominates.

The dense lineament that runs SW-NE through the southern portion of the catchment is what gives rise to numerous streams. Thus, lineaments may be both partially controlling the local flow system and serving as a conduit for groundwater.

In the catchment groundwater flow primarily follows a gentle slope, and the groundwater table runs parallel to the terrain. Because of this, the general trend of groundwater flow is southwest to northeast following a general decline in potentiometric head, from the nearby ridge and highland.

Everywhere along the catchment that traces the cross section to the Guder Babicha plain exhibits a gradual decline in elevation as it approaches the outlet. This suggests that groundwater flow mimics topography. The map below shows the gradual elevation from Dendi rigde and Roge Mountain to Guder Babicha Plain; likewise, from Chalia Highland and Chilimo Ridge to Guder Babicha Plain and the outlet. Comparably, for 21 (twenty-one) boreholes, the groundwater depth (Elevation of borehole-static water level) drops from the nearby ridge and highlands to the watershed's outlet.

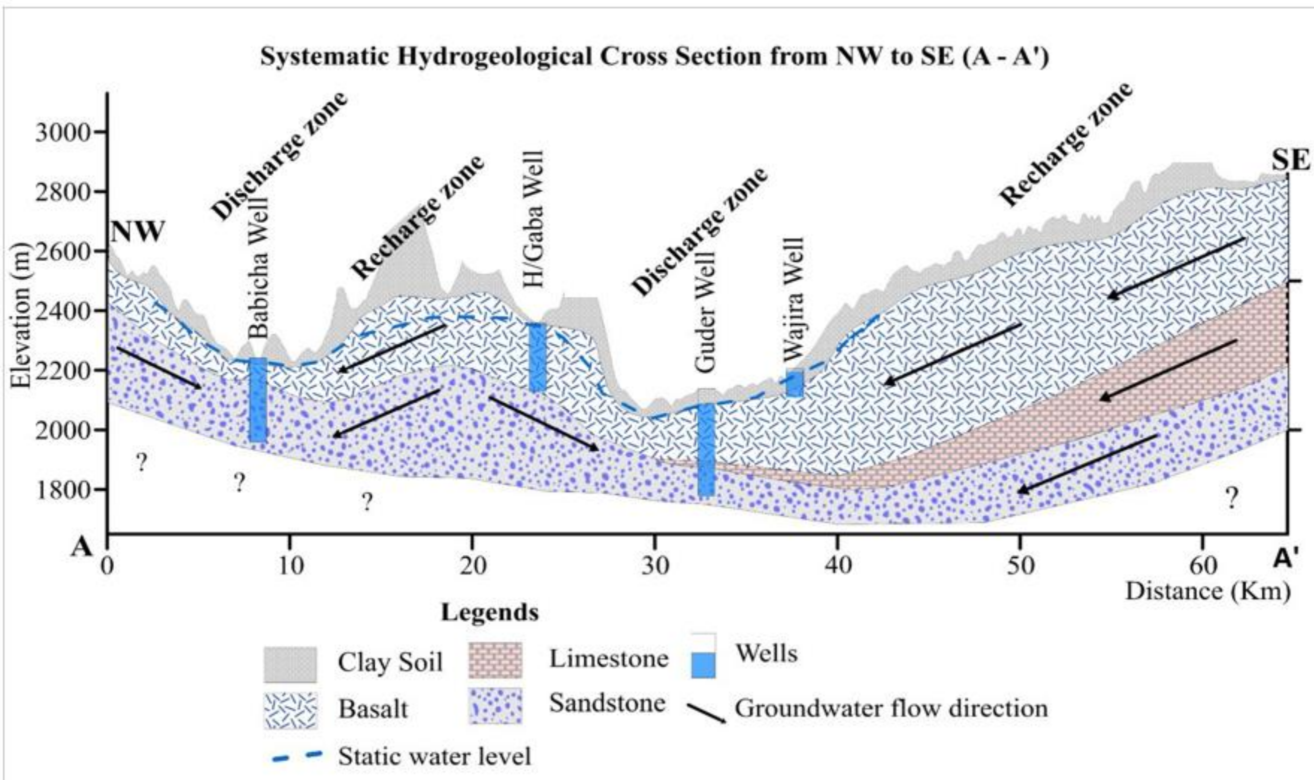

Figure 5. 6. Hydrogeological cross section from NW to SE(A-A')

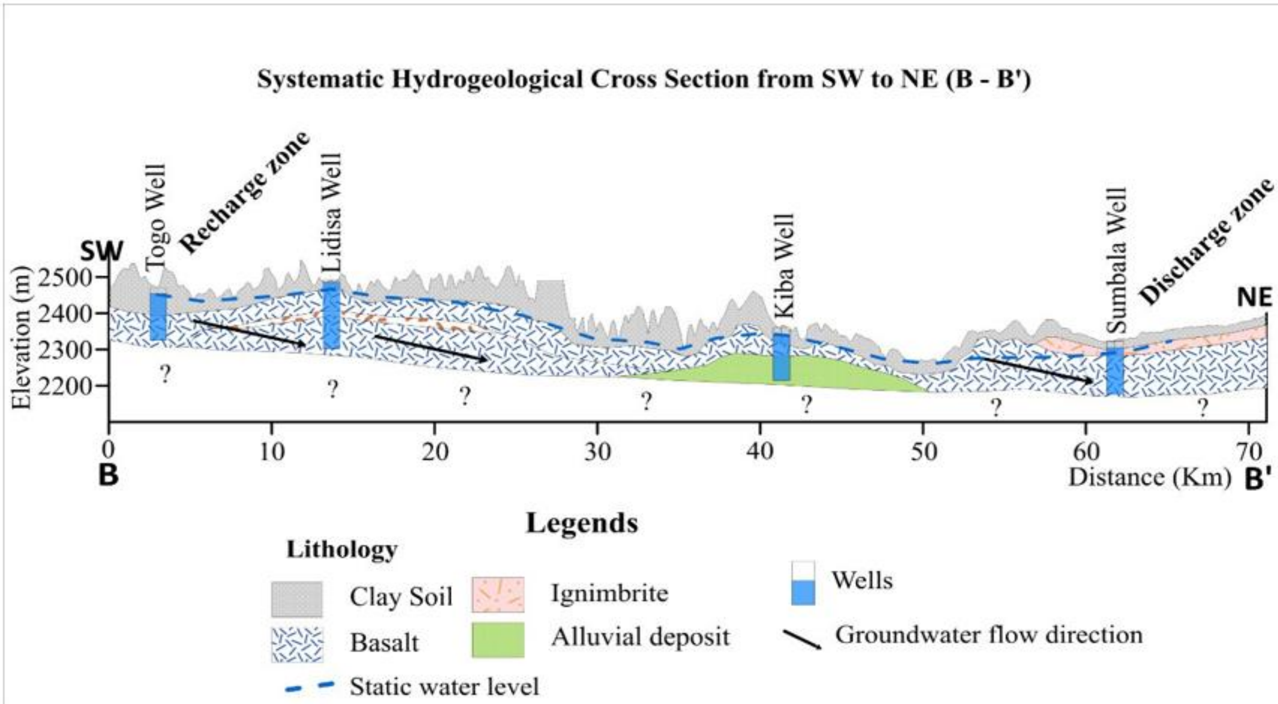

Figure 5. 7. Hydrogeological cross section from SW to NE(B-B')

5.7. Recharge and Discharge zone

According to Winter (1999), the groundwater flow system has been developed such that groundwater discharges in topographically lower areas and recharges in areas with higher topography. According to hydraulic gradients and hydraulic conductivities, water enters ground water systems in recharge areas and flows through them to discharge areas (Zelalem, 2009).

The occurrence and movement of ground water is governed by a complex interplay of hydrological, hydro-geological, and climatological factors. The accurate evaluation of groundwater recharge and discharge is challenging because there are currently no methods or data available for their direct measurement. Because of this, all of the techniques used to estimate groundwater resources are indirect. Since groundwater is a dynamic and replenishable resource, its value is typically determined by taking into account the components of yearly recharge. Sustainable groundwater structures may be used to develop groundwater (Kumar, 1997).

Groundwater recharge is the process by which water flows downward, reaching the water table and adding to the groundwater reserve (also known as an aquifer). Each catchment has three distinct types of groundwater recharges, though the amounts may vary (Tenalem, A., & Alemayehu, T., 2001).

- The first is the direct recharge of groundwater, which is caused by precipitation. We should be concerned about the ultimate recharge of groundwater.
- The second is localized groundwater recharge, which is connected to very small lateral flows of water that penetrate the ground and eventually join the groundwater table at a certain distance from the infiltration point.
- Surface water bodies provide indirect recharge, this kind of recharge can originate from man-made structures (such as dams, irrigation systems, reservoirs, canals, etc.) or natural sources (such as rivers, streams, ponds, lakes, etc.).

Ayenew and Tamiru Alemayehu (2001) state that indirect recharge is common in arid and semi-arid regions. In a drainage basin, the groundwater recharge area is the area where the water table is typically located at a certain depth and the net saturated flow of ground water is directed away from the surface (Freeze & Cherry, 1979). The primary areas of recharge in the catchment are the hills and ridges that divide the surface water. Groundwater from these mountains and high-velocity surface runoff race down the slope to the discharge area.

The catchment is fed from all directions by the majority of the highlands in the catchment area, which are located in the northeast and northwest (Chalia and Chilimo Ridge) and the southeast and southwest (Roge and Dendi Mountain) (Figure 5.4). The area between the water table and the surface of the land is frequently deeply unsaturated in recharge zones. Water is therefore rarely available at the surface unless there is contact with another person or an intermountain depression.

The water table is typically found at or very near the surface, and discharge areas, on the other hand, are defined as the movement of the net saturated flow of groundwater directed toward the ground surface (Freeze and Cherry, 1979). Topographically high regions are typically thought of as recharge zones, and topographically low areas can be thought of as discharge zones. Springs typically appear as indicators of ground water discharge areas. Many springs emerge from the eroded and cracked sections of steep ridges and deep gorge cliffs here in the catchment. The capillary rise of water from shallow groundwater tables is an additional way that groundwater is discharged.

The depth of the groundwater table and the kind of soil or rock material affect the rate of capillary rise. This is mostly seen forming saturated mud at the surface before the start of the dry month. This type of groundwater discharge is typically a localized, temporal phenomenon. As a result, while it may not accurately depict the groundwater discharge in the area, it does provide a rough idea of its condition. The water table is located near or at the land surface in the discharge area (Fetter, 2001). Saturated soil and numerous wetlands are indicative of Discharge.

In highland regions, springs release groundwater, primarily in the vicinity of Tikiru Inchini, southwest of Ambo, and Roge Mountain. Similarly, seepage is the source of discharge in low-lying areas. In addition to water flowing into rivers, wetlands, and springs, evaporation from the upper regions of capillary fringes, where groundwater is near the surface, also counts as a discharge from the natural groundwater system.

In the catchment area's lowlands, where groundwater levels are near the surface, the situation is probably ideal. The groundwater recharge and discharge areas within the study area are depicted in (Figures 5.3 and 5.4).

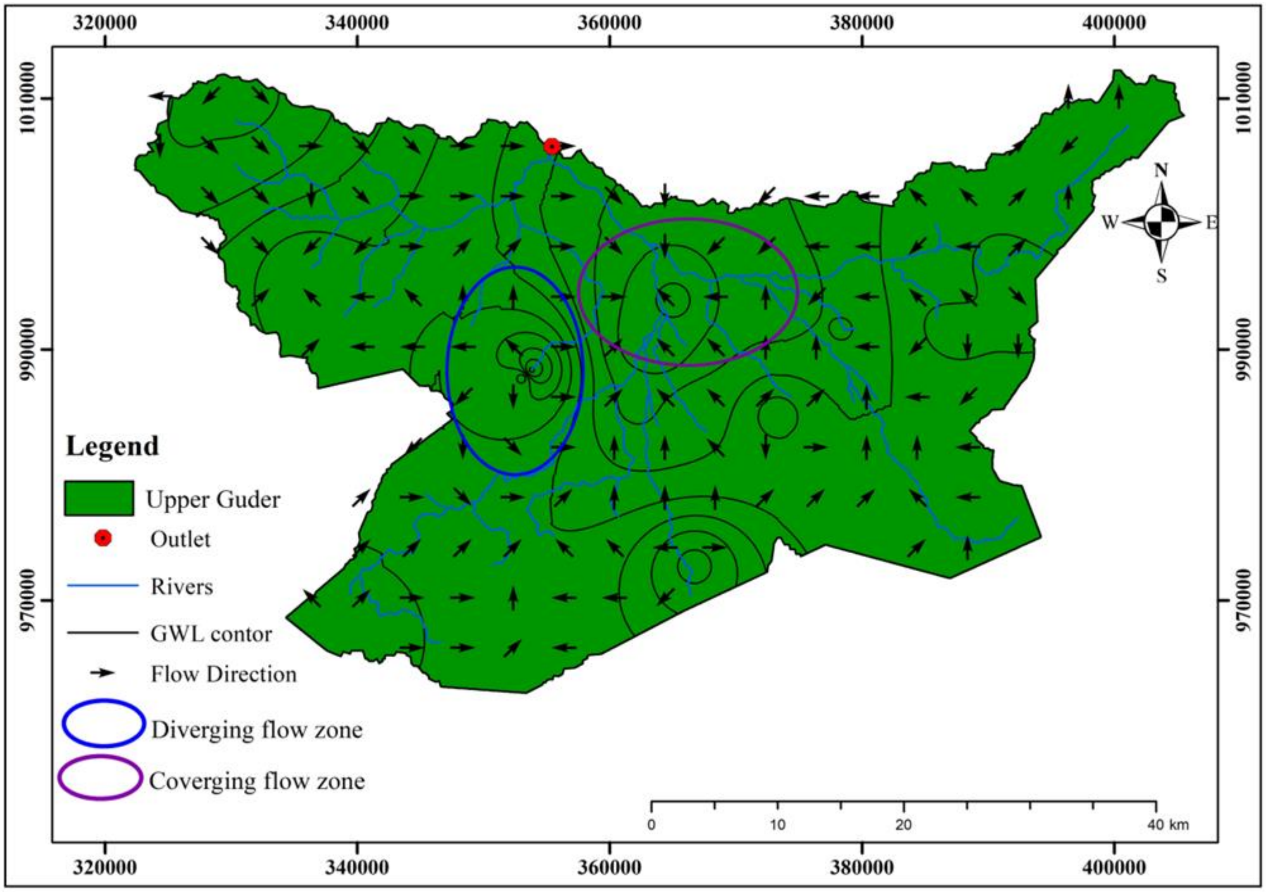

Figure 5. 8. Groundwater level contour lines, converging and diverging flow zones

(Figure 5.3). From the central portion of the study area of discharging zones to the south western highland areas, the diverging groundwater flow lines are feasible. On the other hand, the catchment area's eastern plateaus are habitat to the recharge zone. The catchment's highland areas in the west, northwest, south, and southeast, with high annual rainfall and slope, experience the majority of the recharge. Rapid infiltration happens in regions with fractured volcanic rock, and to a lesser degree in sedimentary rocks and thick permeable soils in relatively dry areas. This is because discharge areas, such as Local Guder, northeast of Babicha, and the eastern portion of Toke, are located in the northeastern and central portions of the catchment.

An understanding of the topographic setting in relation to the local relief situation provides insight into the overall direction of groundwater flow and its impact on groundwater recharge and discharge. The catchment's identified slope classes, which are divided into four classes, range from 0 to 91 percent. Slopes can be classified as gentle (0–7), moderate (8–10), steep (10–20), or extremely steep (>30%). Because the catchment area's northwest, northeast, southern and southeast have higher slope values which are primarily steep slopes there is less groundwater discharge as a result of increased runoff. However, the catchment's western and northwest regions have milder slopes that are thought to produce less runoff, which results in less groundwater recharge (Figure 5.4).

Therefore, the northwest, northeastern, and southeast regions of the catchment are regarded as having a high groundwater potential zone due to the catchment area's slopes. On the other hand, the eastern and southern regions of the lower catchment area have a high surface runoff that reduces the amount of time that precipitation can percolate, making this area a zone with poor groundwater potential. It keeps other factors constant while flowing quickly on the surface.

Communities in the catchment around Guder, Babicha, and Wajira use it in the dry season for agricultural purposes. As opposed to the recharge area, the water table is the target of the net saturated groundwater flow, and the discharge flow vector lines converge (Fig 5.4). If the discharge zone is large, however, this convergence might not happen. A transitional zone is defined as an area that exhibits characteristics of both a recharge and discharge area.

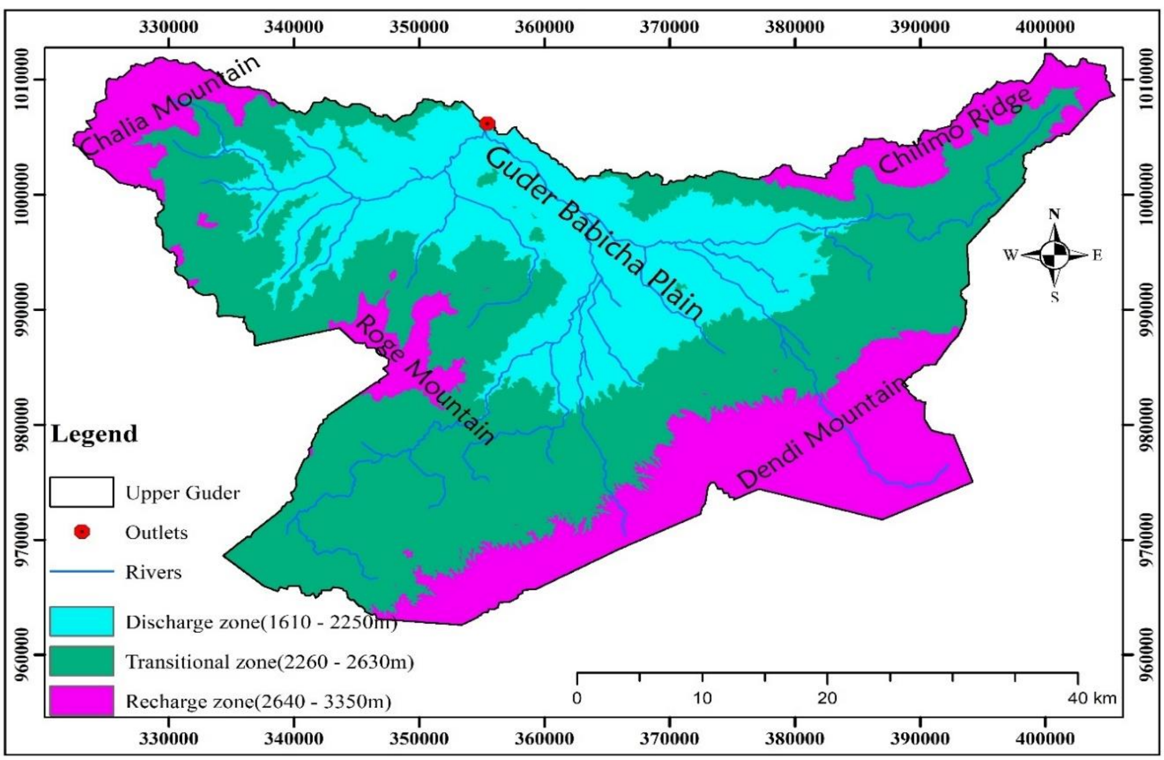

Figure 5. 9. Recharge and discharge zones in inferred from elevation map

CHAPTER SIX

6. Hydrochemistry

6.1. General

In the field of hydrogeological study, hydrochemistry is an impressive scientific method for giving data on the source, composition, and historical background of natural water in both space and time. Interpreting the general occurrence of different constituents in waters, controlling factors, and the relationship between these constituents and water use is critical.

The chemical and physical characteristics of water are greatly influenced by its reactivity with different elements. Water absorbs the properties of materials it comes into contact with, either through chemical reactions or physical contact, which changes the chemistry of the water. Water contains very little amounts of some solutes from dust and gases when it falls through the atmosphere as precipitation, but once it reaches the land surface, it picks up the majority of its solute. The interaction of the substance with a rock or soil causes displacement and replacement reactions between ions, which in turn alters the substance's chemistry.

There are several variances in the chemical properties of water depending on the mineral composition of the groundwater reservoir, the patterns of groundwater flow in the basins, and the duration of the water's interaction with various rock formations. In another way, the chemical composition of natural water comes from a variety of sources, such as atmospheric gases and aerosols, soil and rock weathering, precipitation and solution reactions that take place below the surface, and cultural impacts that are caused by human activity. There are numerous environmental factors that affect the solute that is taken up or precipitated and its amount in the solution. These include the climate, the structure and location of rock strata, and the biochemical effects that are related to the life cycle of both microscopic and macroscopic (Hem, J. D., 1992)

6.2 Field measured parameters

To prevent contaminating the sensitive parameter, some physical parameters must be measured in-situ. These consist of the following: electrical conductivity, temperature, and hydrogen ion activity.

Table 6. 1. Statistical description of field measured parameters

Parameters	Minimum	Maximum	Mean	standard deviations
Ec(µS/cm)	55.0	3050	543.4	494.9
TDS (mg/l)	32	2150	454.9	563.4
pH	6.5	7.8	7.2	0.4

6.2.1 Electrical Conductivity (EC)

The ability of water to conduct an electric current in proportion to the amount of dissolved solid in the water is known as electric conductivity. Groundwater circulates through geological media and becomes enriched by various constituents through reaction and leaching properties, resulting in a high electrical conductivity (EC). The solution is conductive because it contains charged ionic species. The solution's conductance rises as the concentration of the different ions occurs. As a result, the conductance measurement shows how many ions are present in the specified water. The study area's total EC value ranges from 55µS/cm to 3050µS/cm; of the boreholes or springs EC values, 55µS/cm is the lowest and is recorded for Spring (csp-35). Due to the shallow ground or because it is a shallow well, this may be related to shallow water circulation and because it is a recharge area which get replenished by fresh water that had short time water rock interaction.

Around Guder (BH-38 well) (2152m), a high EC (3050µS/cm) is recorded, which is associated with the high temperature surrounding the depressed area. High temperature contributes to increased mineral solubility and dissolution, as well as increased ionic charge in the form of solute, which enhances the electrolytic properties of water. As a result, high temperatures coming from depths can cause rock to dissolve, incorporating high mineral constituents into water at depths. There is no systematic trend in the distribution of the area's EC value. This is explained by the catchment's rugged terrain, which encourages numerous local recharges and discharges. As a result, groundwater is replenished and exposed in all forms of discharge without traveling far from the source area, which leads to low EC.

However, considering that the highland of the active recharge area has a low EC, there is a general increase from the area of recharge to discharge. On the other hand, the highest EC in the catchment is found in the upper northeastern portion of the catchment, which includes the Guder and Ambo areas. It is known that the areas surrounding these areas have high temperatures and little rainfall.

6.2.2 pH (Hydrogen ion activity)

The pH scale, which goes from 0 (high concentration of hydrogen ions and acidic) to 14 (high concentration of hydroxide ions and strong base), indicates how acidic or alkaline a body of water is. The concentration of hydroxide ions and hydrogen ions in pure water are in balance, resulting in a pH of precisely 7. But since pure water is so rarely found in the natural world, natural water typically has a PH value that is off from equilibrium. This also holds true for the study area, where pH values range from 6.5 to 7.8. The Ethiopian drinking water quality standard and WHO (2006) state that the pH of potable water should be between 6.5 and 8.5. Any water that has a PH of less than 6.5 is considered acidic, and any that is higher than 8.5 is considered basic. The majority of water samples fall within this range. If the above listed samples are below pH level of WHO, and are relatively shallow and most necessarily affected by near surface, biological and biochemical process that generate CO2. Otherwise, the natural water in the area has generally a good quality in terms of pH value.

6.2.3 Total Dissolved Solid (TDS)

All of the solid material in solution is included in total dissolved solids, which are calculated using the weight of the dry residue that remains after a sample of water evaporates at a temperature of 105^0C.When water moves through a geologic formation, it dissolves any rock that it comes into contact with along the way. One of the fundamental indicators of the quality of natural water is the quantity of dissolved materials present. It is preferable to observe the spring water and well water in the study area independently.

The TDS value ranges from 32 mg/l, the minimum value of relatively fresh groundwater, for HB-38 located at Guder (X-369619E, Y-994273N, and Z-1993m), to 2150 mg/l for a deep well with a depth of 2152 m, located at WAMW-04 at a south-western point of Guder (X-362201E, Y-985706N). BH-38 has the lowest TDS value (32 mg/l), which is also the expected value for the recharge area. Since dissolved solids can also be added to groundwater by human activity, even though this spring is located in an area that may have high TDS values, this high value may point to another source. However, the maximum TDS (2150 mg/l) recorded for WAMW-04 suggests that the time of water-rock interaction along the flow path has a significant influence on the TDS value of groundwater. Generally, there is less water-rock interaction on high land than on low land, TDS is generally lower on high land. This indicates that the TDS will increase as long as the water travels a considerable distance and takes a long time to pass through porous spaces from the source. The water in the study area is classified as fresh water by the USGS based on TDS levels.

Table 6. 2. Water class on TDS.

TDS (mg/l)	**Water type**
1-1000	Fresh
1000-10000	Brackish
10000-100000	Saline
>100000	Brine

There is a direct relationship between TDS and EC value. The more total dissolved solids (TDS) in water the more it will conduct electricity. As observed from (Fig. 6.1) they are correlated with best fit of regression (R^2= 0.992).

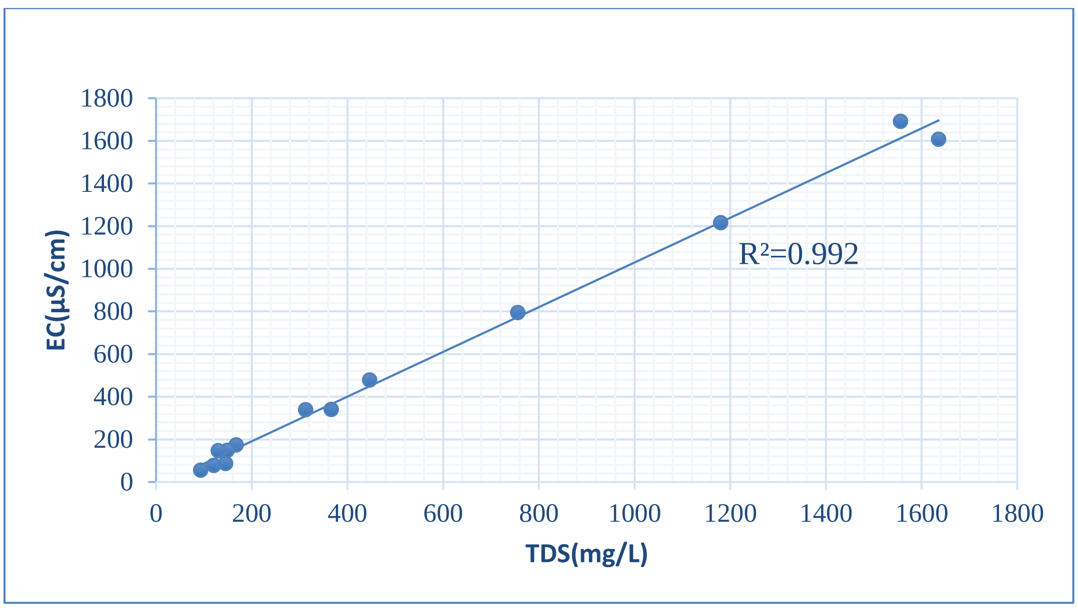

Figure 6. 1. TDS-EC relationships

6.3 Major ions

According to Fitter (1994), eights ions Ca^{2+}, Mg^{2+}, Na^{+}, K^{+}, HCO^{3-}, Cl^{-}, $SO42^{-}$, and $CO3^{-}$ make up more than 90% of the solute in water. Water chemistry is greatly influenced by this species, which is typically found in concentrations higher than 1 mg/l. Because of local geology, climate, and topography, these solutes are inherently highly variable in both surface and groundwater.

All waters contain calcium in the form of Ca^{+2}, which is easily dissolved from rocks that are high in calcium minerals. Both surface and groundwater are rich sources of this cation. Acid rainwater can accelerate the calcium evaporation of rocks and soils. According to the study area's water sample analysis results, calcium is the most prevalent cation. The concentration of this substance varies amongst groundwater sources, typically ranging from 2 mg/l to 386.4 mg/l for boreholes. The calcium concentration in surface springs is 31 mg/l. Plagioclase feldspar and pyroxene-rich basaltic rock weathering products are likely the source of this high calcium content.

In the study area, sodium is the second most prevalent cation after calcium. For deep wells, the sodium concentration in the analyzed sample ranges from 21 mg/l (BH-50) to 239 (BH-38), and for spring water, it ranges from 3 mg/l (CSP-31) to 286 mg/l (HSP-2). Deep wells contain high concentrations of Na. Deep water circulation via underground fractures with high temperatures is what insists on this.

Another important cation that is less concentrated in the study area than sodium and calcium is magnesium. Its less mobility could be the reason for this. The range of the Mg^{+2} value is 1 mg/l to 44.16 mg/l. Although it is higher than K^{+}, the concentration varies between highland and lowland areas. For borehole (WAMW-04), the maximum K^{+} concentration is 44.16 mg/l, while the minimum is 1mg/l for spring (CSP-35). Potassium is found in water in trace amounts because it is rarely liberated from silicate minerals and instead shows a strong tendency to be reincorporated into solid weathering products.

$HCO3^{-}$ is the most prevalent major anion in the study area, followed by $SO4^{-2}$ and Cl^{-}, respectively. For deep wells (BH-38) at the discharging area, the maximum value is (1100 mg/l), while the minimum value is (92 mg/l for BH-50). Similarly, for springs, the maximum value is (1074 mg/l) and the minimum value is (29 mg/l). The reaction of water with dissolved carbon dioxide produced from the underlying heat reservoir is the cause of the increased concentration of bicarbonates.

Next to Bicarbonate, another anion with a dominant concentration is sulfate. Very little sulfate is present in the majority of the examined samples. The study area has variations between 0.3 and 63 mg/l. For borehole, the maximum concentration is 63 mg/l (ATW3-14). Since most of the analyzed parameters vary in quantity from site to site, the variability of the chemical ions in solution, as expressed by variation (standard deviation), is very significant. There is little variation across samples, shown by the close approach of the standard deviation and average and Following sulfate, the low-concentration anion is chloride. In the study area, the lowest chloride concentration is 1 mg/l for boreholes and the highest is 32 mg/l for springs.

Table 6. 3. Statistical description of the major ions.

Parameter	**Maximum**	**Minimum**	**Average**	**Standard deviation**
Ca^{2+}	386.4	2.0	58.3	82.0
Mg^{2+}	44.2	1.0	14.5	12.5
Na^{+}	286.0	3.0	71.7	86.4
K^{+}	60.0	1.0	11.2	14.5
$HCO3^{-}$	1100.0	29.0	331.8	326.7
$SO4^{2-}$	63.0	0.3	9.9	15.8
Cl^{-}	32.0	1.0	9.8	9.6

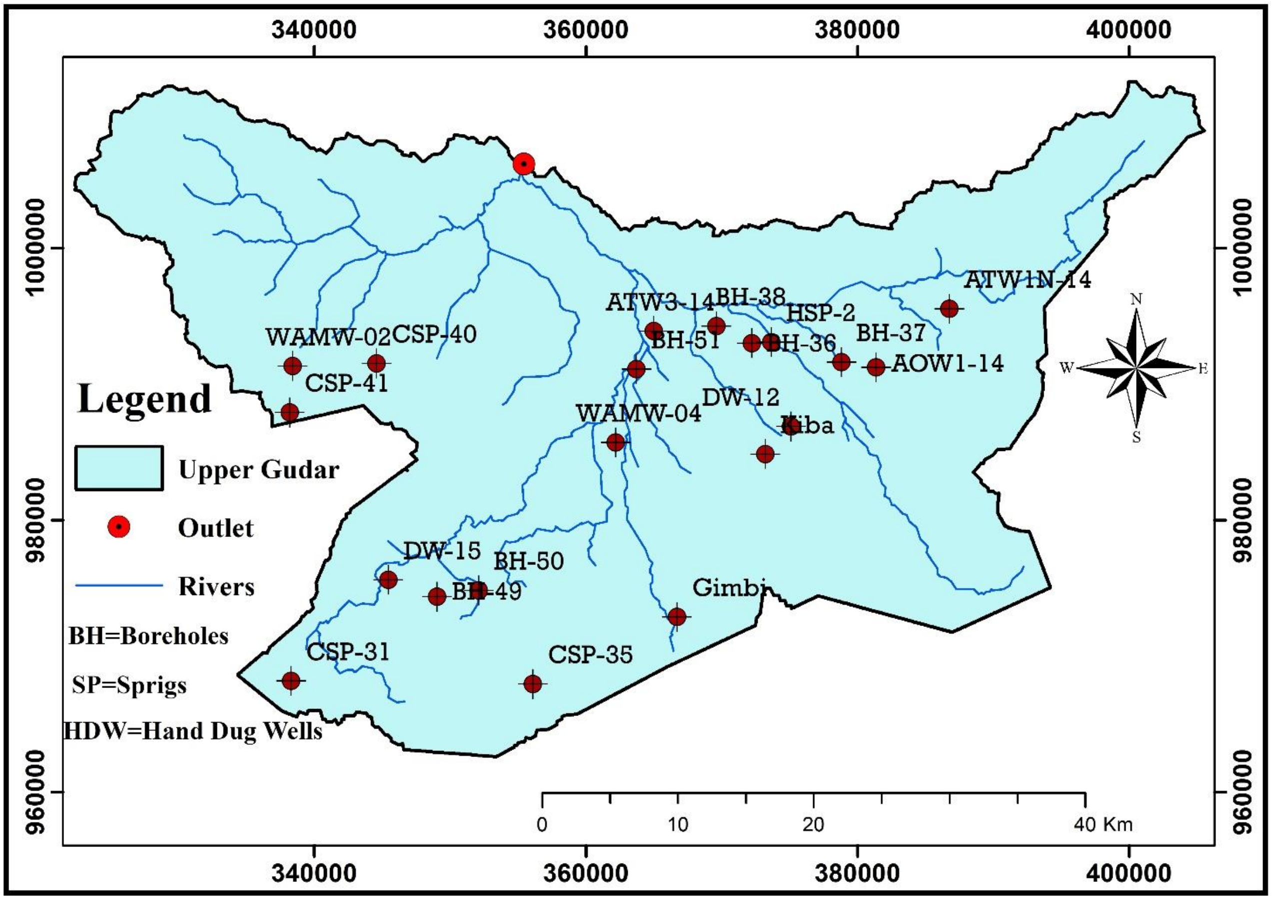

Figure 6. 2. Sampling site map of the study area

Presenting the chemical data in an interpretable way represents several of the most important tasks in hydrogeochemical study.

hydro chemical data can be presented using a variety of techniques, but the graphical approaches based on major anions ($SO4^{-2}$, $HCO3^{-}$, and Cl^{-}) and major cations (Ca^{2+}, Mg^{2+}, and Na^{+}, K^{+}) are thought to be the most effective for visual observation. To indicate the number of ions on the graph, the classification uses a percentage of mill equivalents per liter of the anions and cations. Piper plot is used for this purpose, and the analysis is presented as follows. The most popular technique for interpreting and categorizing water is the piper trilinear diagram. This is because the method can display a large number of samples at once in addition to displaying mixing effects between different types of water. Here, the plotting position of the cations and anion is used to categorize the types of water.

There are four different water types: Ca-HCO3, Na-HCO3, Ca-Na-SO4, and Ca-Mg-Cl, as shown in (Figure. 6.3). However, two water samples from the Ambo area (WAMW-04) and the Guder area (ATW3-14) exhibit a distinct water type that is Ca-Mg-Cl type. This kind of water may be related to farming practices such as using animal dung and fertilizer, or it may be the outcome of human activity and Since groundwater in many of the study area's urban areas has a SO4/Ca ratio value of less than 10, this indicates that the host aquifers are not the source of additional high SO4 levels. As previously mentioned in the major anion in the study area, the water supply near the town is WAMW-04 and Ca-Mg-Cl, which is represented by the rectangle deep green and cross green color in the piper plot.

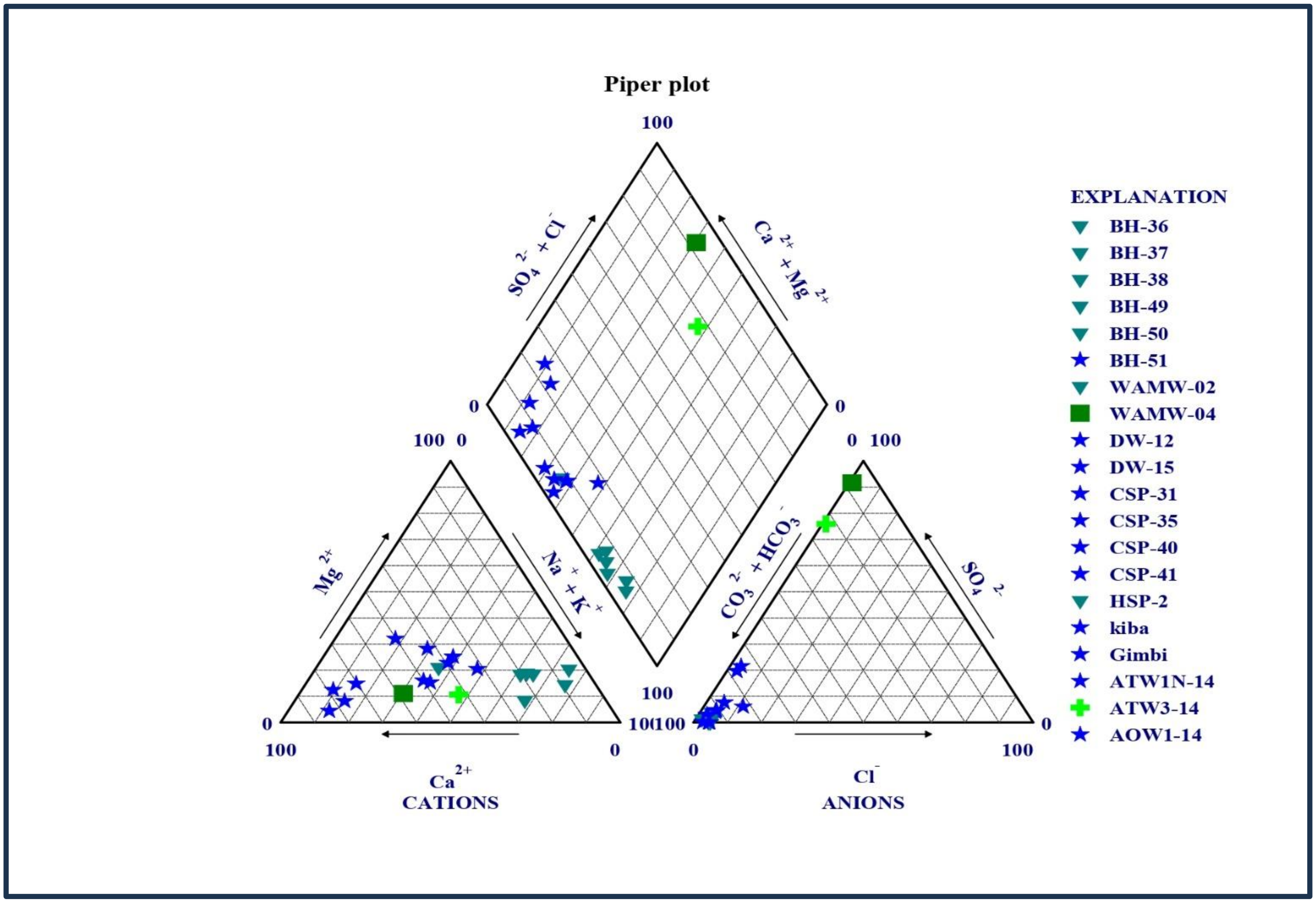

Figure 6. 3. Piper plots of the water samples

6.4. Classification of water type

As a result, there are four main categories of water that make up groundwater, which are described below. The four types of water in the area are Ca-HCO_3, Ca-Na-HCO_3, Na-HCO_3, Ca-Na-SO4, and others, as can be seen from the piper plot. The piper plot illustrates that the cations primarily cluster around the Ca^{2+}, indicating that this is the dominant cation. Certain samples are aligned towards the Na^{+} apex, indicating gradually increasing sodium enrichment. This shows that the interaction between rocks and water, rather than the mixing of different types of water (Ca-type, Ca-Mg type to Na-type), is the main controlling factor. On the other hand, the anion plot exclusively clustered around the forms of bicarbonate, sulfate, and chloride, indicating that all of the water samples were of these types.

The aim of the water type classification process is to use a graphical method to observe the major water groups, their relationship, and evolution along the flow path from water samples collected from deep bore holes, springs, and hand-dug wells. The most used graphical form is the piper diagram. The diagram projects two distinct trilinear plots that show the relative concentrations of the major cations and anions.

This presentation states that deep well water samples from areas south of Mount Dendi and next to the western highland escarpment generally exhibit the Ca-HCO_3 and Ca-Na-HCO_3 water type, making up 60% of the total water sample.

Similar to this, deep wells and hot springs near Ambo filweha in the plain's center generally reveal a water type of Na bicarbonate, which makes up 30% of all the water samples. A water type of Ca-Na-SO_4 is found in deep wells on the southwest side of Mount Roge in the Amo area. This water type makes up 5% of the total water sample and the others are 5% water sample.

Ca-HCO_3 water Type

This type of water is frequently an indicator of a recharge area. It appears that there is less water-rock interaction and that the water is fresh. Ca–HCO_3 types of waters are often considered recharge area waters in the general groundwater chemical evolution, meaning that they are still in the early stages of geochemical evolution (Bartolino, J. R., & Adkins, M. , 2003). As a result, groundwater of the Ca-HCO_3 type is dynamically circulating and evolving and can be found in the recharge areas of the northern and southern highlands. This kind of water's average TDS of 344 mg/l indicates that it is fresh and has not undergone a significant geochemical reaction. The low TDS and bicarbonate groundwater type indicate the fast hydrogeological regime of the plateau receiving a relatively high volume of precipitation where groundwater flows in relatively lithological homogeneous fissured aquifers developed in various volcanic rocks and associated (intercalated) Tertiary sediments.

Ca-Na-HCO_3 Water Type

This type of water makes up the majority of the water sample under analysis. The catchment's northern, northeastern, and southeast parts are largely observed to have this type of water. Many lithologies, including pyroclastic, rhyolite, and basalt units, as well as more recent volcanic eruptions of phonolite and trachyte origin and sandstone units, are what make this region famous. Since the feldspar-bearing rock mentioned above dissolves and releases Ca^{+2} and Na^{+} into the water, it is likely that this type of water is the result. Conversely, this area can be considered, to a lesser extent, the catchment's southeast recharge zone.

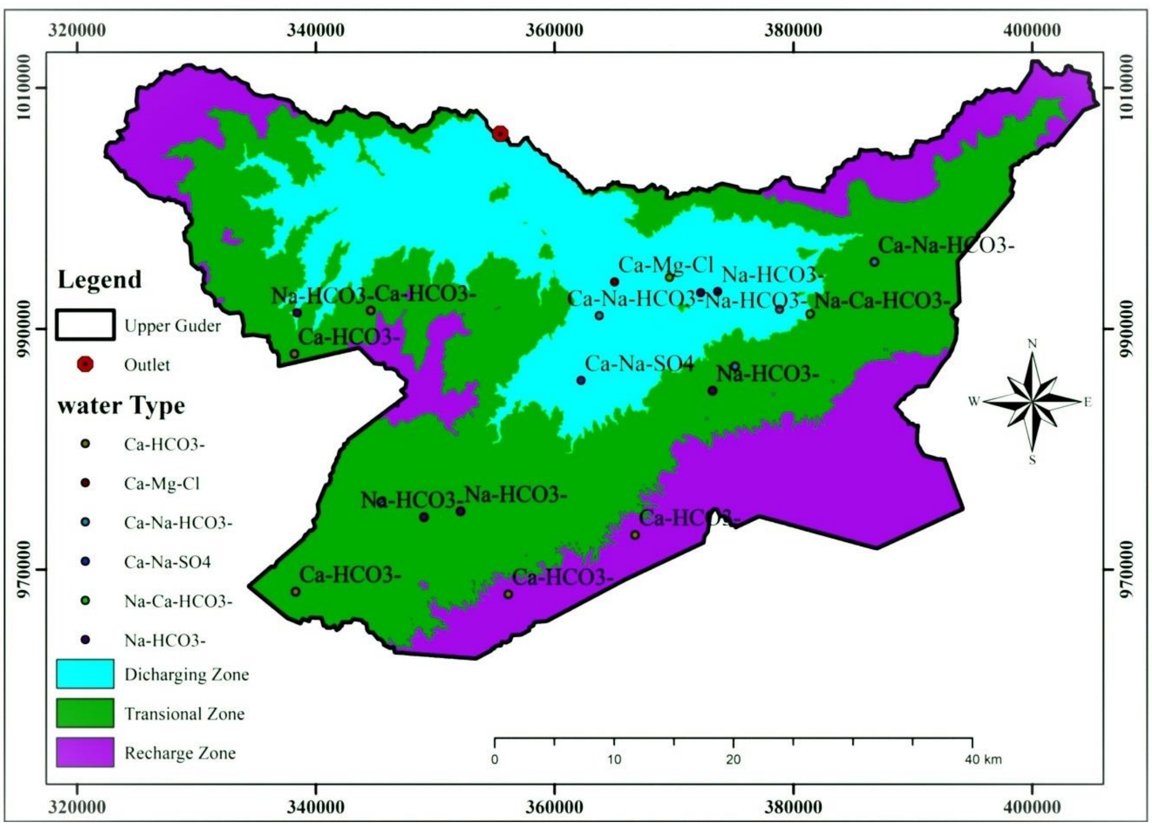

Figure 6. 4:-Spatial distribution of water Type from Piper Plot

Na-HCO$_3$ water Type

The third water type group in the area is NaHCO$_3$. The calculated low Na/HCO$_3$ in most parts of the study area indicates that the possible source of bicarbonate in the water is the reaction of carbon dioxide with alkali silicate rocks. In aquifers with clay intercalation, cation exchange is what allows low TDS waters to become NaHCO$_3$ water types, and the specific sampling locations that are part of the group are recharge areas. The limestone and sandstone aquifers in the central Guder sub-basin. This indicates a higher degree of geochemical evolution and indicates that the sampling sites are deep circulating water discharge zones. Thermal waters circulating along the YTVL zone and south of it in the Upper Awash and Central part of upper Guder sub-basins make up this group's, Deep groundwater circulation and heat flow in the central part of study area and north east lowland leads to the formation of thermal water with Na–HCO$_3$ and high TDS. The high TDS is caused by silicate dissolutions, and the specific sampling location is a discharge area for locally circulating water.

With a Na/HCO$_3$ ratio of no more than 0.5, thermal waters (HSP-2) do not support the hydrochemistry of hyper-thermal water, where HCO$_3$ should be low at high temperatures. This indicates a high concentration of HCO$_3$ relative to Na. Precipitation and shallow, cold groundwater mixing with thermal water are most likely contributing factors. Also in favor of this were the springs at Ambo, Wonchi, and Woliso, which have comparatively lower temperatures.

The Ca^{+2} ion dominance from the northern, southern, south western and south eastern part of the catchment area decreases down along the flow direction and finally replaced by Na^{+} ion evolving into this water type. There are 20 samples and the type of water for each sample is as follows.

Table 6. 4. Types of water in the catchment

Water Types	Number
Na-HCO$_3^-$	6
Ca-HCO$_3^-$	5
Ca-Na-HCO$_3^-$	5
Na-Ca-HCO$_3^-$	2
Na-Ca-HCO$_3^-$	1
Ca-Mg-SO$_4^-$	1

Ca-Na-SO_4 Type

The SO4/Ca ratio value of less than 10 Abnormal hydrochemistry at Guder coordinate UTME362201, UTMN 985706 and point elevation 2139m.a.s.l of the study area especially in urban and quarry site areas indicates the susceptibility of groundwater to pollution; hence, it is not possible to find other sources of high SO_4^{-2} from the host aquifers.

6.5. hydro chemical evolution and major process controlling the chemistry of groundwater

6.5.1 Major cation

It is well known that Ca-Mg and Na ions, respectively, predominate in the majority of the waters in the basic and acidic volcanic province. However, a variety of geochemical processes influence how much of them are present in water. Mineral silicates of feldspar, amphibole, and pyroxene, as well as carbonate rock, can provide calcium, a key component of many rocks. Though it might exist as a partial filler particle between sandstone and other detrital rocks' interstitial spaces, carbonate dissolution is unlikely to occur in the study area due to the lack of reported carbonate rock. This means that since the study area is a part of the Ethiopian plateau, the primary source of Ca^{+2}/Mg^{+2} there may be the hydrolysis of the silicate that makes up the basic volcanic. Some silicate minerals dissolve through way of cation and anions with solid clay minerals (Herczeg, A. L. , 2001).

The geochemical process that produces the cation (Ca^{+2}, Mg^{+2}) and anion (HCO_3^-) can also be represented by this silicate hydrolysis. Calcium-rich pyroxene, calcic plagioclase, and amphibole hydrolysis have all been proposed as the primary sources of calcium, magnesium, and bicarbonate ions in the study area.

Sodium is another cation that is dominant. Sodium ions are added to natural water through a variety of geochemical processes. They include cation exchange, evaporation, and the dissolution of silicate and halite. It is unlikely that this sodium is coming from the Halite dissolution. Measuring the concentration of Na^+ against Cl-should reveal a linear relationship if halite is the case, with both ions entering the solution in equal amounts during the dissolution process. The slope of the line should be approximately equal to one (1:1). But the most frequent source of Na^+ in cases where points are above or below the line is ionic exchange or silicate. But as observed from (Fig 6.4) there is 1:1 relationship between them indicating Na^+ is from halite.

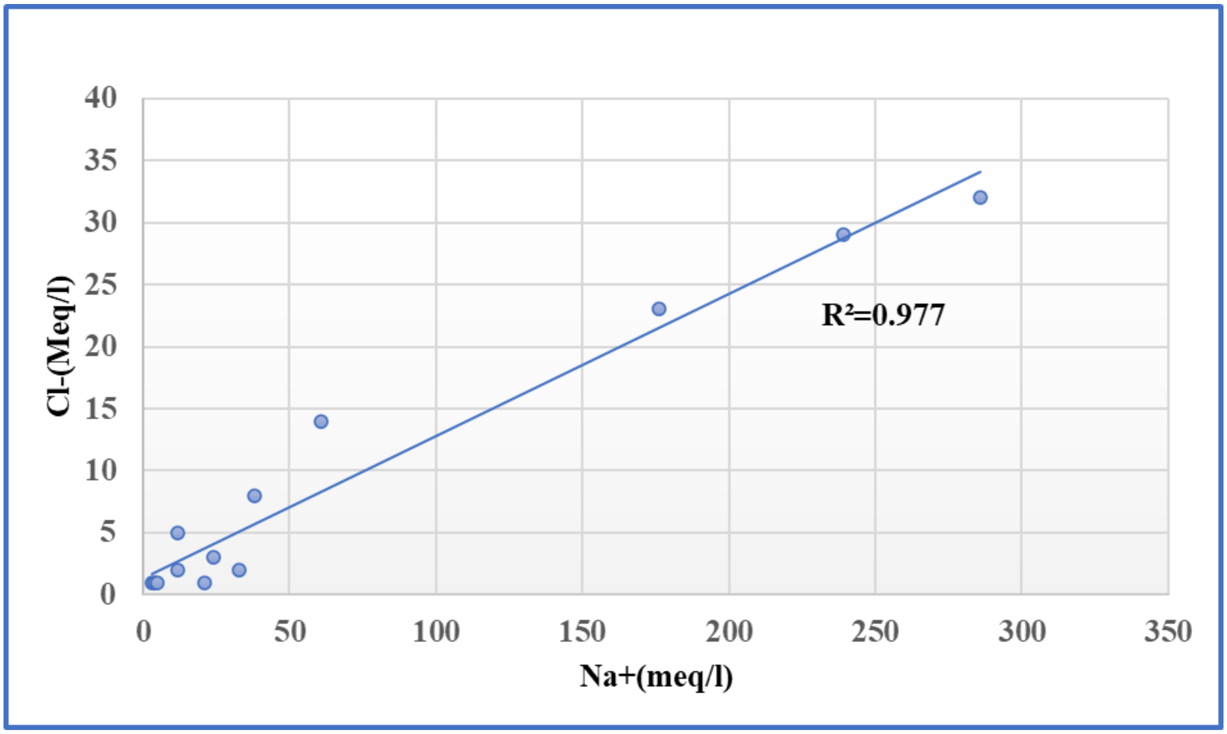

Figure 6. 5. Na^+ vs. Cl^- relationship.

The cation exchange of calcium and magnesium for sodium that is retained by adsorption on mineral surface deposits with high cation exchange capacities, like clay, could be another source of sodium. The sodium concentrations in the study area increase towards the north and center of the study area. In general, the northern parts of the study area are rich in sodium ambo area (BH-38, HSP-2).

6.5.2 Major anion

Bicarbonate, chloride, and sulfate are found in the study area. Since nearly all of the samples have high bicarbonate concentrations, bicarbonate is the dominant water type. The dissolution of carbonate rocks, like calcium carbonate, and CO_2 in the atmosphere and soil are the sources of bicarbonate ions. Due to CO_2 released by organic soil decomposition, bicarbonate is typically the main anion in groundwater (Todd, D.K. , 1988). Similarly, biological processes in the soil are thought to be the primary source of HCO_3 in the study area. In the soil zone, dissolved carbon dioxide from decomposing organic matter reacts with H_2O to form carbonic acid, which subsequently dissociates to form HCO_3^-, as shown below.

$CO_2 + H_2O = H_2CO_3$

$H2CO_3 = H^+ + HCO_3^-$

And the other source of HCO_3^- is silicate hydrolysis

$CaAl_2Si_2O_8 + 2CO_2 + 3H_2O = Al_2Si_2O_5\,(OH)_4 + Ca^{+2} + 2HCO_3^-$

In the study area, HCO_3^-concentration primarily originates from these two reactions. In terms of concentration, the other anion (Cl^-, $SO4^{-2}$) is least. Dissociation of some sedimentary rocks, evaporation, industrial and sewage effluents, and agricultural practices are some of the ways that chloride finds its way into surface waters.

According to (Hem, (1985)), chloride is more likely to be found as an impurity in minerals than as a necessary component in most minerals. As a sign of potential feces contamination, chloride is commonly linked to sewage and included in evaluations. The study area's expected sources of chloride include anthropogenic activity and evaporation. Polluted rainfall, anthropogenic sources, and leaching of minerals containing sulfur in contact with aerated water can all produce sulfurate. In addition, it was a volcanic gas that came from the subsurface heat zone.

6.6. Water quality

Analyzing water to see if it is suitable for the intended use, is the main goal. Because of this, it is necessary to determine the purpose of the quality when assessing the water quality. Therefore, the World Health Organization (WHO) and other organizations set standards for different uses of natural water, such as drinking, agriculture, and industry, when determining the quality of the water for a given purpose.

Higher concentrations of dissolved salts are typically expected in groundwater compared to surface water because groundwater frequently occurs in association with geological materials containing soluble minerals. The geological environment, as well as the source and flow of water, determine the kind and concentration of salts. Groundwater bodies are distinguished from surface water bodies by two main characteristics. Firstly, because surface water moves through the ground more quickly than groundwater, surface water typically has shorter residence times. This means that once a groundwater body is contaminated, it may stay that way for decades or longer (UNESCO guide, 1992).

Secondly, the water and the aquifer are highly interdependent in terms of physio-chemical and chemical processes. Additionally, there's a good chance that the two will interact to change the quality of the water.

6.6.1 Groundwater quality for domestic purpose

Toxic substances and microorganisms should not be present in surface or groundwater used for domestic activities like cooking or drinking. A comparison with the WHO's (2011) drinking water standards is necessary for the various water samples that were chosen and the analytical outcomes. These data indicate that there are various criteria to evaluate the water's quality and determine if it is safe to drink or not. In order to complete this work, the chemical analysis results from the water samples in the study area were assessed and contrasted with the WHO guideline values for the standard of water quality. Data on water quality show that nearly all of the sampled water is within the WHO standard range.

Table 6. 5.Comparison of water samples with WHO (2011) drinking water quality standard.

Parameter	WHO (2011) standard	% Samples exceeding WHO (2011) standard
PH	6.5-8.5	0
TDS (mg/l)	1000	15
Na (mg/l	200	15
Ca (mg/l)	200	5
Mg (mg/l)	150	0
Cl (mg/l)	250	0
SO4 (mg/l)	400	0

Sulfate and chloride are extremely rare in general. This suggests that human-caused groundwater deterioration is not a major issue in the study area, and that some water simples (WAWM-04, BH-38 and HSP-2), like sodium and TDS, originate from far away and require a long travel time and due to high temperature because they exceed WHO standards.

6.6.2 Water quality for irrigation purpose

For agricultural activities to be successful, soil type, cropping strategy, and water quality are essential. Maximum yield is possible when soil and water are managed properly, thanks to high-quality water. Nevertheless, the geological setting, the weather, and the groundwater supply all affect how suitable the water is both temporarily and spatially.

Both the quantitative and qualitative qualities of water are essential to the sustainability of irrigation-based agriculture. This indicates that a sufficient amount of water that is of a suitable quality is required. Maximum yields are possible with appropriate soil and water management when using high-quality water. To establish the irrigation utility's water quality standards, a number of factors must be evaluated. The most important ones are the local climate, the crops cultivated, the irrigation techniques, the soil and water composition, and the land's topography (Hoffman,et al., 2010). The study area's irrigation water quality has been assessed for specific, salinity hazard, and sodium hazard.

Salinity Hazard

The water salinity hazard as determined by electrical conductivity is the water quality guideline that has the greatest impact on crop productivity. The incapacity of the plant to compete with ions in the soil solution for water is the main impact of high EC water on crop productivity. Though the soil may seem wet, plants can only transpire pure water, so when the EC is higher, they have less water available to them. Accordingly, as the amount of EC increases, the amount of usable plant water in the soil solution decreases. Therefore, the water's salinity determines its suitability.

Water with a TDS value of less than 450 mg/l is considered non-salinity hazard, water in the range of 450 – 2000 mg/l is considered mild to moderate salinity hazard, and water exceeding 2000 mg/l is considered severe salinity hazard, according to FAO's (1985) irrigation water quality guidelines.

About 58% of the water samples fall into the excellent class (non-salinity hazard) based on the salinity hazard criteria mentioned above, with the remaining 42% falling into the mild to moderate salinity hazard ranges. This shows that the catchment is generally suitable and that there are no quality issues with the rise in salinity (EC).

Sodium Adsorption Ratio (SAR)

Large amounts of sodium in irrigation water are especially dangerous because of the effects they have on the soil. According to (Ayenew, T. , 2013), refer to the amount of sodium in soil and water in relation to calcium and magnesium ions as "sodicity," which is another name for sodium hazard. Sodium adsorption ratio (SAR) is typically used to calculate sodium hazard. The ratio of sodium to calcium and magnesium yields the sodium adsorption ratio (SAR).

The sodium to calcium and magnesium ratio is used to compute the sodium adsorption ratio (SAR). It is a crucial factor in determining whether irrigation water quality is appropriate. The amount of sodium adsorption ratio that can be present in soil water depends on a number of factors, including soil salinity, the type of irrigation used on farms, soil texture, and clay minerals.

Soil physical structure breaks down when high SAR water is used frequently. The irrigation water's sodium is absorbed by the soil particles and attaches itself to them, clogging their pores and interstitial spaces. When the soil gets dry, it turns hard, compacts, and becomes more and more impervious to water. To keep soils under high SARs, some correction might be necessary.

The concentrations of sodium (Na), calcium (Ca), and magnesium (Mg), both absolute and relative, control the amount of sodium in irrigation water (Hoffman et al., 2010). absorption ratio, or SAR.

According to Hem (1985) and referenced by the United States Salinity Laboratory (1954), the sodium effect could be computed by the Sodium Adsorption Ratio (SAR) using the provided relation. The ratio of the sodium ion concentration in meq/l to the under square root of the combined concentration of calcium and magnesium ions in meq/l according to their valance number is known as the sodium

$$SAR = \frac{Na}{\sqrt{(Ca+Mg)/2}}$$

Table 6. 6. Water quality for irrigation based on Sodium Adsorption Ratio (SAR).

SAR Value	Class	Remark	No. of case	%
<10 (s1)	Low	Good	11	55
10-18 (s2)	Medium	Good for coarse-grained permeable soil unsatisfactory for highly clayey soil with low leaching	6	30
18-26 (s3)	High	Suitable only with good drainage, high leaching organic addition	1	5
>26	Very high	Unsatisfactory	2	10

According to the analysis, In the catchment the SAR value for analyzed water point ranges from 0.73mg/l to 51.79 mg/l with an average value of 12.15 mg/l, the majority of the water samples have SAR values less than 10, which is good for all types of soil. Other samples, such as those from BH-38 and HSP-2 (hot spring), are unsatisfactory for highly clayey soil low leaching, and some samples are good for coarse-grained permeable soil.

Sodium percentage (Na %)

In irrigation water, the percentage of sodium among the principal cations is typically used to express the relative proportion of sodium to other cations. Shown the sodium hazard, it is ultimately also possible to classify water for irrigation using the formula below.

$$\%Na = [(Na + K) / (Ca + Mg + Na + K)] \times 100$$

Table 6. 7. Irrigation water quality based on Na% criteria.

Na%	Water class	% Sample
<20	Excellent	20
20-40	Good	15
40-60	Permissible	35
60-80	Doubtful	20
>80	Unsuitable	10

We can infer from this table that the water is suitable for irrigation because the percentage of sodium (%Na) is low in comparison to the other cations.

CHAPTER SEVEN

7.CONCLUSION AND RECOMMENDATION

7.1. Conclusion

The evaluation of the upper Guder catchment's groundwater resource was the main goal of this project. Several methods are attempted to be used in the quantitative value estimation of the water cycle components (precipitation, surface runoff, PET, AET, and ground water recharge). The value of 1267.2 mm/year, which was obtained by averaging the rainfall depth results from the three methods used to calculate the aerial depth of precipitation, was used for subsequent analysis because there were no significant differences between the results.

Potential evapotranspiration (PET) is estimated using the Thornthwaite method and the Penman combination method. These techniques produced results of 738.77 mm/year and 995.83 mm/year, respectively. Because it depends on sunshine hours and the mean monthly temperature, the Thornthwaite method underestimates the value. On the other hand, the Penman combination method requires a lot of parameter input. The technique considers several variables, including heat, vapor deficit, sunshine hours, temperature, and solar radiation. The reliable value of the resulting method is then applied for the analysis. Therefore, the PET generated using the Penman combination method was utilized in this investigation.

Actual evapotranspiration (AET) is calculated using the soil-water balance developed by Thornthwaite and Mather, 1957 and and Turc empirical formula. The estimated AET using these methods were 733.4mm/year and 774mm/year, respectively. Recharge using the water balance method is calculated using the AET derived from the soil water balance method. Still, the soil water balance method's result is not a representative value. This is because the reliability of the soil texture used is questioned when estimating the amount of water available at the rooting depth.

At the catchment outlet of the Guder River, there isn't a gauge station. It is for this reason that the water balance calculation struggles to obtain a consistent runoff value. A groundwater recharge calculation using the Chloride Mass Balance method has its own limitations. Cl^- concentration was determined using only three rainfall samples that were collected once, in mid-June. The unique value of recharge could not be found due to these and other factors that introduce errors. As a comparison to earlier research, the catchment's yearly groundwater recharge is believed to be the 298 mm/year groundwater recharge value derived from the WetSpass model.

The average value of the three methods, or 227.6 mm/year, is generally taken into account as the upper Guder catchment's annual recharge in this work because the results from the three different types of recharge methods differ significantly.

The primary aquifers within the basin are known to be composed of weathered and fractured basalt, which is a volcanic rock. The hydrogeologic characteristics of the aquifer materials in the catchment vary substantially due to the varying degrees of weathering and fracture of the volcanic rocks. Based on geological and hydrometeorological factors, transmissivity, specific capacity, and yielding capacity observed from pumping test data, the catchment is classified into five potential zones: local aquifer, extensive and moderately productive porous aquifers, extensive and highly productive fissure aquifer, extensive and highly productive porous/fissured aquifer, low productive fissured/porous aquifer, and aquitards.

In the north and northwest of the catchment area, there are numerous fracture traces that appear as lineaments in the hill shades. They have significant control over drainage density and pattern, as well as ground water flow systems. Water flows to the discharge areas from the surrounding highlands due to the low hydraulic gradient and the general northward flow of regional groundwater.

In the study area, bicarbonate water types predominate. Water types that predominate in the area are Na-HCO_3, Ca-HCO_3, and Ca-Na/Na-Ca-HCO_3. Due to the lack of a large industry that can currently contaminate ground water in the catchment, aside from a few small-scale contaminations from agricultural practices and human waste, the concentrations of chloride and sulfate are low, indicating an anthropogenic impact like quarry sites…also this hydro chemical data used understand the chemical variability of area and good indicators of discharge and recharge area throughout the catchment.

7.2. Recommendations

- ✓ The amount of evapotranspiration that is simulated for the catchment from the Wetspass result is the consequence of activities where natural vegetation has been significantly impacted by deforestation and agricultural practices in relation to surface runoff and groundwater recharge. In any case, a thorough land use and land cover study would have to be carried out for rehabilitation.

- ✓ An extensive geological and structural investigation should be conducted to identify the structures that controlled the direction of groundwater flow, as well as the circumstances and mechanisms of recharge and discharge.

- ✓ The most current borehole data are not clearly organized. It is highly recommended that water wells and springs should be put into databases by zonal water offices. Reports on well completion and pump tests, whether conducted by the government or another business, should also be recorded through the regional office.
- ✓ It is also advised to carry out a comprehensive scientific study to evaluate the catchment's potential for groundwater resources.

- ✓ To characterize the hydrogeological characteristics of the aquifer systems, it is imperative to examine the hydrodynamic relationship that exists between the groundwaters in the Basin and adjacent basins.

References

Abenezer.K. (2007). *Hydrogeological Evolution in the Ambo-Woliso Area.* M.Sc. Thesis, Addis Ababa University, Ethiopia.: Unpublished.

Alemayehu, T. (2006). "Hydrogeological Behavior of Volcanic Rocks: Structural and Textural Variability.". *Journal of African Earth Sciences*, 44(1), 1-12.

Axon, J. E. (1982). "The Role of Evapotranspiration in the Hydrological Cycle." . *Water Resources Research*, 18(4), 1035-1040. .

Ayenew, T. . (2013). Sodicity and its impact on soil and water quality. *Journal of Water Resource and Protection*, 5(2), 123-130.

Barlow,. (1915). "The Runoff Coefficient for Various Land Uses.". *Journal of the Indian Water Resources Society.*

Bartolino, J. R., & Adkins, M. . (2003). *Groundwater quality in the United States: A national perspective.* U.S: Geological Survey Circular 1224.

Batelaan, O., & DeSmedt, F. (2001). . (2001, 5 3). "WetSpass: A GIS-based model for the assessment of water and energy fluxes in the soil-plant-atmosphere system. *Hydrology and Earth System Sciences*, 395-410. doi:[DOI: 10.5194/hess-5-395-2001]

Beshawered.et.al. (2010). *GEOLOGY GEOCHEMISTRY AND GRAVITY SURVEY OF THE BAHIR-DAR AREA.* Ethiopia: Geological survey of Ethiopia.

Chow. (1988). *Applied hydrology,* . Mc Grew : Hill book Company.

Cook. (2003). *"Fracture Connectivity and its Role in Groundwater Flow.* (Vol. 115(5)). America: Geological Society of America Bulletin,. doi: [DOI: 10.1130/B25036.1]

Drever, J. I., & Clow, D. W. (1995). "The Geochemistry of Natural Waters:. *Surface and Groundwater Environments*, Prentice Hall.

Eriksson, E., & Khunakasem, J. (1969). "The Use of Chloride in the Study of Groundwater Recharge.". *Journal of Hydrology*, 7(1), 62-79.

Fetter,. (2001). *Applied Hydrogeology.* Prentice Hall.

Fetter, W. (1994). *Applied Hydrogeology Third Edition.* Newwork: MacMillan College.

Freeze & Cherry. (1979). *Groundwater.* Prentice Hall. .

Garcia, M., Martinez, J., & Lopez, A. (2022). Influence of Windspeed on Groundwater Dynamics in Coastal Aquifers. *Journal of Hydrology*, 75(2), 301-315.

Gebremedhin Gebremeskel, K. (2015). (2015). "Modeling the Hydrogeological System of a Basin: A Conceptual Approach.". *Journal of Hydrology*, 525, 1-15. doi: [DOI: 10.1016/j.jhydrol.2015.03.035]

Gemechu, D. (1997). Aspect of climate and water balance in Ethiopia. *Addis Ababa University press,Addis Ababa*, 79pp.

Hem. ((1985)). *Study and Interpretation of the Chemical Characteristics of Natural Water.* U.S. : Geological Survey Water-Supply Paper 2254.

Hem, J. D. (1992). *Study and interpretation of the chemical characteristics of natural water.* U.S: Geological Survey Water-Supply Paper 2254.

Herczeg, A. L. . (2001). Chemical weathering and the role of clay minerals in groundwater . In *Groundwater Geochemistry* (pp. pp. 1-15). America: systems.Geological Society of America.

Hoffman,et al. (2010). Irrigation and Drainage: A Global Perspective. In Water Resources and Irrigation Management. *Springer*, pp. 123-145.

Ilfious.W. (2008). *Geology of kewo,Dedu,hormat, Hamus Gebeya and Chercher of Addis Ababa Map Sheet(NC37-10).* Addis Ababa: Unpubilished Repeort.

J. Kattimani, A. Murthy, and S. R. Kumar. (2018). “Identification of ground water potential zone using remote sensing and Gis techniques,”. *International Journal of Advanced Research*, vol. 6, no. 5, pp. 948–953.

Kasahun.B. (2005). *Groundwater resource evaluation of Walga river basin central Ethiopia, south west shewa. Unpublished MSC thesis Addis Ababa, Ethiopia.* . MSC thesis Addis Ababa, Ethiopia: unpublished.

Krasny, J. (1993, 4 31). "Transmissivity of Aquifers: A Review of Concepts and Methods.". *Groundwater*,, pp. 610-617. doi: [DOI: 10.1111/j.1745-6584.1993.tb00883.x

Kresic. (2006). *Groundwater Resources Sustainability: A Global Perspective.* Boca Raton: CRC Press.

Law, et al. . (2002). "Environmental controls over photosynthesis and transpiration in a forest ecosystem." . *Global Change Biology*, 8(11), 1139-1151.

Lemessa.M. (2001). *Hydrogeology controls in sandstone of Ambo area.* Addis Ababa,Ethiopia: Unpublished Msc thesis.

Li, X., et al. (2021). Advances in groundwater temperature monitoring techniques: a review. . *Hydrogeology Journal*, 29(2), 549-563.

Lorentz, S., et al. (2003, 7 5). "Chloride Mass Balance Method for Estimating Groundwater Recharge:. *Hydrology and Earth System Sciences*, 511-520. doi:[DOI: 10.5194/hess-7-511-2003]

Manaye, Bereket Fentaw and Mihret. (2010). *The hydrogeological map of Akaki Beseka (NC 37 – 14) Sheet The detailed hydrogeologic description is forwarded by this work.* Addis Ababa: GSE.

Mengesha, T.et.al. ((1996). *The geological map of Ethiopia, 1: 2,000,000 scale.* Addis Ababa: Ethiopia: EIGS.

Meten et al. (2015). Application of GIS-based fuzzy logic and rock engineering system (RES) approaches for landslide susceptibility mapping in Selelkula area of the Lower Jema River Gorge, Central Ethiopia. *Enviromental Earth sciences*, Volume 74, pages 3395–3416, (2015).

Seifu Kebede. (2023). Groundwater in Ethiopia Features, Numbers and opportunities ,spring Berlin.

Shaw.E.M. (1994). *Hydrology in practice.* British Library: Third edition, Chapman & Hall.

Smerdon, J. E., et al. (2020). Groundwater temperature response to climate change: implications for groundwater sustainability. *Water Resources Research*, 56(4).

Smith, A. B., et al. (2022). "Advancements in arithmetic methods for estimating areal depth of rainfall using remote sensing data." . *Journal of Hydrology*, 450(3), 112-125.

Smith, A., Johnson, B., & Lee, C. (2023). The Influence of Sunshine on Groundwater Recharge in Arid Regions. *Water Resources Research*, 48(3), 567-581.

Subash.et.al. (2017). Changes on physio-chemical properties of soil in agricultural land in Ambo-Guder Watershed, Ambo, Ethiopia–A case study. *International Journal of Civil Engineering & Technology*, 8(5), 667-675.

Tasisa,et.al. ((2015)). Poor sleep quality and associated factors among pregnant women on antenatal care follow up at Nekemte Referral Hospital and Wollega University Hospital, Nekemte, Ethiopia, 2019: a cross-sectional study. *Sleep Science and Practice*, 6(1), 1-9.

Tenalem, A., & Alemayehu, T. (2001, 9 4). "Groundwater Recharge in Catchments: Types and Variability.". *Hydrogeology Journal*, 290-301. doi: [DOI: 10.1007/s10040-001-0157-3]

Thomas.et.al.,. (2018). "Hydrogeological Characteristics of Alluvial Aquifers: Implications for Groundwater Resources.". *Journal of Hydrology, 558*, 100-110. doi:[DOI: 10.1016/j.jhydrol.2018.01.012

Thornthwaite C.W, Mather .J. R. (1957). Instructions and tables for computing potential evapotranspiration and the water balance. *Publications in Climatology, Drexel Institute of Technology, Laboratory of Climatology*, (pp. 10: 185-195). New Jersey.

Thornthwaite, C. W. (1948). "An Approach Toward a Rational Classification of Climate." . *Geographical Review*, 38(1), 55-94.

Tiketa Adula, G. A. (2022). Assessment of Groundwater Potential Zones of Upper Blue Nile River Basin Using Multi-Influencing Factors under GIS and RS Environmen. *Geofluids*, 1-26.

Tilahun.A. (2008). Hydrogeochemical Characterization of Aquifer Systems in upper Awash and Adjacent Abay Plateau using Geochemical Modeling and Isotope Hydrology. *Journal of African Earth Sciences*.

Timketa.et.al. ((2020)). Morphometric analysis for prioritizing sub-watersheds and management planning and practices in Gidabo Basin, Southern Rift Valley of Ethiopia. *Applied Water Science*, 10(7), 1-15.

Todd. (1980). *Groundwater Hydrology.* . New York: John Wiley & Sons.

Todd, D.K. . (1988). *Ground water hydrology. John Wiley & Sons,*. New York: 535pp.

Trenberth, K. E. ((2011)). Changes in precipitation with climate change. *Climate Research*, 47(1-2), 123-138.

Tsegaye Abebe. (1993). *The Yerer -Tullu Wellel- Volcano - Tectonic- Lineament (YTWVTL), central Ethiopia, Magmatological, Tectonics and chronological constraints.* Addis Ababa: Ph. D. thesis (Draft copy).

Tsegaye Abebe, et al. (1998). The Yerer-Tullu Wellel volcanotectonic lineament: a transtensional structure in central Ethiopia and the associated magmatic activity. *African Earth Sciences*, Pages 135-150.

Urgessa Hirpha. (2023). *Groundwater Resource Assessment Using Numerical Modeling in Gur Catchment.* Addis Ababa Ethiopa: unpublishde Msc thesis.

Wang, Q., et al. (2023). "Enhanced spatial interpolation of rainfall using Thiessen polygons and machine learning techniques." . *Water Resources Research*, 69(4), 256-271.

Wilson E.M. (1983). *Engineering hydrology.* Third edition, Mecmillan publisher's ltd. : Hong Kong.

Wu, Y., et al. . (1996). "Groundwater Recharge Estimation: A Review of Methods.". *Journal of Hydrology*, 178(1-4), 1-20.

Yilma, Aster Denekew; Awulachew, Seleshi Bekele. (2009). Characterization and atlas of the Blue Nile Basin and its sub basins. *International Water Management Institute (IWMI)* (p. 236p). Ethiopia,Sudan: open Acces.

ANNEXES

Annex1 Estimation of available water in the rooting depth for the catchment area

7	**Area (%)**	**AWC in the soil in 1m column (mm/m)**	**LULC**		**Rootin g depth (m)**	**AW at rooting depth (mm)**	**AW w.r.t. land use (mm)**	**AW in the root zone for the soil (mm)**	**AW for the soil w.r.t. areal proportion**	**Total available water at rooting depth for the catchment (mm)**
			Type	**%**						
1	2	3	4	5	6	7 = 3*6	8 = 5*7	9 = ∑8	10 = 9*2	11 = ∑10
Clay	38	200	Deep-rooted crops (Woodland d plants, pasture, grass, shrubs,)	60	0.67	134	80.4	170.6	64.8	200
			MDR (corn, cereals, tobacco, sugar cane)	10	1	200	20			
			Forest	30	1.17	234	70.2			
Loam	32	200	Moderately DR (Sorghum, corn, cereals, cotton, barley, coffee, Teff, Wheat, etc.)	65	1	200	130	247.5	79.2	
			Deep-rooted crops (pasture bush, grass, Shrubs)	15	1.25	250	37.5			
			Forest	20	2	400	80			
Silt loam	6	200	Moderately deep-rooted crops (corn, cereals, cotton, tobacco)	30	0.62	124	37.2	197.2	11.8	
			Shallow-rooted crops (spinach, peas, beets, carrots, etc	60	1	200	120			
			Forest	10	2.00	400	40			
Clay loam	23	200	Moderately deep-rooted crops (corn, cereals, cotton, tobacco)	25	0.40	80	20	188	43.24	
			Shallow-rooted crops (spinach, peas, beets, carrots, etc	45	0.80	160	72			
			Forest	30	1.60	320	96			

Annex 2 Mean monthly Sun shine hour for available stations in the study area.

Months	Jan	Feb	Mar	Apr	May	Jun	Jul	Aug	Sep	Oct	Nov	Dec	Annual
Ambo	9.3	9.3	8.1	7.5	7.5	6.1	3.8	3.5	6	8.7	9	8.9	7.3
Gedo	10	10.7	9.1	9.2	9.6	8.3	4.4	4.4	9.1	11.1	10.9	10.5	8.9
TikurInchini	9.7	10.6	8.7	8.5	8.6	6.5	3	3.1	7.5	10.1	10.7	10.5	8.1
Mean	9.7	10.2	8.6	8.4	8.6	7	3.7	3.7	7.5	10	10.2	10	8.1

Annex 3 Mean monthly Wind speed for available stations in the study area.

Stations	Jan	Feb	Mar	Apr	May	Jun	Jul	Aug	Sep	Oct	Nov	Dec	Annual
Ambo	1.9	2.1	1.9	1.7	1.3	1	0.9	0.8	0.9	1.4	1.8	1.9	1.47
Gedo	1.6	1.7	1.7	1.9	1.7	1.3	1.2	1.1	1.1	1.6	1.6	1.6	1.51
T/Inchini	1.8	2	1.9	1.9	1.6	1.4	1.4	1.2	1.3	1.8	1.9	1.8	1.67
Mean	1.77	1.93	1.83	1.83	1.53	1.23	1.17	1.03	1.10	1.60	1.77	1.77	1.55

Annex 6 Mean monthly rainfalls for available stations in the study area.

Stations	Jan	Feb	Mar	Apr	May	Jun	July	Aug	Sep	Oct	Nov	Dec	A
M/Kegn	15.5	18.2	56.0	66.2	101.9	234.6	260.2	250.7	125.1	45.3	25.0	14.3	1213.1
Guder	23.5	23.8	59.3	73.1	113.5	196.3	230.0	250.8	160.4	30.8	13.5	10.0	1184.8
Ambo	14.2	29.3	55.2	61.5	94.0	143.2	270.0	172.8	128.2	29.5	13.2	7.0	1018.0
T/kutaye	22.5	21.6	49.3	78.0	100.4	163.6	224.8	243.3	126.8	53.6	11.2	9.1	1104.3
T/Enchini	19.2	35.2	54.8	77.0	120.8	250.0	296.3	352.3	153.5	52.1	15.8	10.6	1437.6
Gedo	19.5	22.3	59.6	90.2	120.8	250.8	340.5	280.0	131.2	44.8	23.5	10.4	1393.7
Dendi	15.5	35.2	68.2	85.8	120.6	130.0	251.0	233.8	215.3	43.5	9.2	10.9	1219.1
H/Gebeya	15.1	21.3	65.1	51.0	140.0	239.4	330.8	345.3	270.0	65.0	25.5	10.7	1566.8
Mean	18.1	25.9	58.4	72.9	114.0	201.0	275.4	266.1	163.8	45.6	17.1	10.4	1267.2

Annex 5 Mean monthly temperatures for available stations in the study area

Stations		JAN	FEB	MAR	APR	MAY	JUN	JUL	AUG	SEP	OCT	NOV	DEC
M/Kegn	Tmax	24.6	25.3	25.5	25.4	24.7	22.4	20.6	20.5	21.5	23.1	23.6	24.1
	Tmin	9.6	10.3	10.7	11.0	11.1	10.7	10.2	10.2	10.2	9.9	9.8	9.4
	Taverega	17.1	17.8	18.1	18.2	17.9	16.5	15.4	15.3	15.8	16.5	16.7	16.7
Guder	Tmax	22.8	23.8	23.8	23.6	23.1	21.5	19.4	19.3	20.3	21.5	21.8	22.1
	Tmin	8.9	9.9	10.7	11.0	10.9	10.7	10.4	10.2	9.9	9.1	8.9	8.3
T/kutaye	Taverega	15.9	16.8	17.2	17.3	17.0	16.1	14.9	14.8	15.1	15.3	15.4	15.2
	Tmax	22.8	23.8	23.8	23.6	23.1	21.5	19.4	19.3	20.3	21.5	21.8	22.1
	Tmin	6.6	7.7	8.4	8.8	8.8	8.6	8.3	8.3	7.9	7.0	6.6	6.1
	Taverega	14.7	15.7	16.1	16.2	16.0	15.0	13.9	13.8	14.1	14.2	14.2	14.1
T/Enchini	Tmax	25.2	25.9	25.8	25.6	24.8	22.5	20.8	21.0	22.0	23.5	24.2	24.7
	Tmin	8.3	9.3	9.9	10.3	10.4	10.2	9.8	9.8	9.6	9.0	8.5	8.1
	Taverega	16.7	17.6	17.8	17.9	17.6	16.3	15.3	15.4	15.8	16.2	16.4	16.4
Gedo	Tmax	23.1	23.7	23.6	23.5	22.5	20.2	18.3	18.4	19.5	21.1	21.7	22.3
	Tmin	7.9	8.6	8.9	9.2	9.3	8.9	8.3	8.2	8.3	8.3	8.3	7.8
	Taverega	15.5	16.2	16.2	16.4	15.9	14.5	13.3	13.3	13.9	14.7	15.0	15.0
Ginde Beret	Tmax	24.2	25.5	25.8	25.5	24.9	22.9	20.7	20.6	21.4	22.6	23.0	23.5
	Tmin	12.0	12.8	13.4	13.8	13.6	12.7	12.4	12.2	12.1	11.4	11.5	11.7
	Taverega	18.1	19.1	19.6	19.7	19.3	17.8	16.6	16.4	16.8	17.0	17.2	17.6
A/Gindebret	Tmax	24.3	25.7	26.0	25.6	25.3	23.2	20.8	20.5	21.4	22.7	23.1	23.4
	Tmin	12.3	13.2	13.8	14.2	14.0	13.0	12.7	12.5	12.3	11.7	11.9	11.9
	Taverega	18.3	19.4	19.9	19.9	19.6	18.1	16.7	16.5	16.8	17.2	17.5	17.7
Jeldu	Tmax	20.7	21.6	21.5	21.1	20.7	19.4	17.7	17.4	18.2	19.3	20.0	20.3
	Tmin	7.6	8.6	9.2	9.3	9.0	8.5	8.5	8.3	8.1	7.4	7.3	7.2
	Taverega	14.2	15.1	15.4	15.2	14.9	13.9	13.1	12.9	13.2	13.3	13.6	13.7
Dendi	Tmax	24.3	25.4	25.5	25.1	25.0	23.8	21.7	21.4	22.4	23.5	23.9	23.9
	Tmin	8.2	9.4	10.5	10.9	10.8	10.8	10.8	10.6	10.0	8.7	8.0	7.7
	Taverega	16.3	17.4	18.0	18.0	17.9	17.3	16.3	16.0	16.2	16.1	15.9	15.8
Ilfata	Tmax	24.0	25.1	25.1	24.8	24.4	23.0	21.0	20.7	21.7	22.9	23.4	23.7

Annex 6 SAR and %Na value

Site	X	Y	Na(mg/l)	K(mg/l)	Ca(mg/l)	Mg(mg/l)	SAR	Na%
BH-36	372218	992999	176	18	41	28	29.96	73.76
BH-37	378823	991624	61	12	71	21	8.99	44.24
BH-38	369619	994273	239	33	74	41	31.52	70.28
BH-49	349045	974361	33	3	2	5	17.64	83.72
BH-50	352108	974831	21	3	7	1.5	10.19	73.85
BH-51	363731	991093	38	5	37	13	7.6	46.24
WAMW-02	338419	991326	53.5	6.9	14.44	9.12	15.59	71.94
WAMW-04	362201	985706	220	21	386.4	44.16	14.99	35.89
DW-12	375112	986885	24	7	36	7	5.18	41.89
DW-15	345473	975598	12	4	12	5	4.12	48.48
CSP-31	338302	968161	3	2	31	3	0.73	12.82
CSP-35	356104	967949	4	2	31	1	1	15.79
CSP-40	344595	991523	12	1	31	12	2.59	23.21
CSP-41	338198	987919	5	3	31	2	1.23	19.51
HSP-2	373652	993094	286	25	31	30	51.79	83.6
Kiba	373227	984856	27	5	38.4	15.36	5.21	37.31
Gimbi	366722	972880	22	2.7	97.6	12.48	2.97	18.33
ATW1N-14	386772	995546	46.5	5.4	57.6	11.04	7.94	43.06
ATW3-14	365004	993896	98	60	104	15.84	12.66	56.87
AOW1-14	381377	991238	52.5	4.1	32	12.48	11.13	56

BH=Bore Holes, DW=Dug Well, HSP=Hot Spring, SP=springs, and the others' location codes of bore holes

Annex 7 In situ measurements of physical parameters

Site	X	Y	E(m)	Ec(µS/cm)	T(^{O}C)	pH
Ambo (BH-36)	372218	992999	2111	1216	20	7.73
Awaro(BH-37)	378823	991624	2204	795	20	7.78
Ambo mineras factory (BH-38)	369619	994273	1993	1691	30	7.35
Wayu Lixa (BH-49)	349045	974361	2436	174	18	7.03
Inchini(BH-50)	352108	974831	2447	148	20	7.13
Guder02(BH-51)	363731	991093	2011	478	19	7.71
Guder (WAMW-02)	338419	991326	2240	354	_	7.23
Babicha (WAMW-04)	362201	985706	2152	_	_	7.04
Gosukora(DW-12)	375112	986885	2339	340	21	7.16
Inchini (DW-15)	345473	975598	2416	147	18	7.23
Jibate (CSP-31)	338302	968161	2481	78	17	7.61
Roge (CSP-35)	356104	967949	2708	55	16	6.56
Iresa (CSP-40)	344595	991523	2441	339	_	7.39
Gebakemise(CSP-41)	338198	987919	2445	87	18	6.45
Ambo01(HSP-2)	373652	993094	2045	1607	51	7.51
Kiba	373227	984856	2372	386	_	6.94
Gimbi	366722	972880	2681	650	_	7.35
Meti (ATW1N-14)	386772	995546	2380	464	23	7.3
Guder (ATW3-14)	365004	993896	1928	922	25.6	6.81
Ambo (AOW1-14)	381377	991238	2242	394	26.1	6.68

Annex 8 Laboratory measured water chemistry parameters

SN	X	Y	E(m)	Ec(µS/cm)	HCO3(mg/l)	Cl(mg/l)	SO4(mg/l)	F(mg/l)	NO3(mg/l)	Na(mg/l)	K(mg/l)	Ca(mg/l)	Mg(mg/l)	pH	TDS (mg/l)
BH-36	372218	992999	2111	1216	786	23	1	1.3	2.2	176	18	41	28	7.7	1179.8
BH-37	378823	991624	2204	795	492	14	4	1.6	8.4	61	12	71	21	7.8	756.3
BH-38	369619	994273	1993	1691	1100	29	1	1.4	5.3	239	33	74	41	7.4	32
BH-49	349045	974361	2436	174	93	2	3	1.6	0.4	33	3	2	5	7	167.3
BH-50	352108	974831	2447	148	92	1	1	0.5	2.2	21	3	7	2	7.1	148.5
BH-51	363731	991093	2011	478	287	8	10	0.7	3.5	38	5	37	13	7.7	446.5
WAMW-02	338419	991326	2240	354	204	5.5	4.7	2.2	0.5	54	6.9	14	9	7.2	206
WAMW-04	362201	985706	2152	-	144	10	38	1.2	16	220	21	386	44	7	2150
DW-12	375112	986885	2339	340	200	3	5	1.2	3.5	24	7	36	7	7.2	366
DW-15	345473	975598	2416	147	73	2	3	0.6	4	12	4	12	5	7.2	129.9
CSP-31	338302	968161	2481	78	40	1	9	0.2	4.9	3	2	31	3	7.6	120.37
CSP-35	356104	967949	2708	55	29	1	2	0.2	1.8	4	2	31	1	6.6	93.25
CSP-40	344595	991523	2441	339	177	5	7	0.2	20	12	1	31	12	7.4	312.52
CSP-41	338198	987919	2445	87	45	1	9	0.2	4.9	5	3	31	2	6.5	145.38
HSP-2	373652	993094	2045	1607	1074	32	3	1.9	0.4	286	25	31	30	7.5	1635.55
Kiba	373227	984856	2372	386	203	5.8	-	0.7	8.9	27	5	38	15	6.9	232
Gimbi	366722	972880	2681	650	396	11	-	0.5	5.9	22	2.7	98	12	7.4	329
ATW1N-14	386772	995546	2380	464	337	5.4	0.3	0.6	1.3	47	5.4	58	11	7.3	190
ATW3-14	365004	993896	1928	922	630	17	63	0.6	1.7	98	60	104	16	6.8	326
AOW1-14	381377	991238	2242	394	234	19	14	0.9	0.3	53	4.1	32	12	6.7	132

Annex9 Lithological Log of the Wells

Annex 9a: -Lithological log of the well site Babicha

No	Depth, m	Lithologic description
1	0-4	Black cotton soil
2	4-16	Sandy clay
4	16-32	Weathered basalt
5	32-66	Massive basalt
6	66-72	Weathered basalt
7	72-282	Varigated color Sand stone

Annex 9b: -Lithological log of the well site Guder

No	Depth, m	Lithologic description
1	0-48	Alluvial deposit of Sandy clay
2	48-102	Slightly fractured basalt
3	102-106	Scoracious basalt
4	106-110	highly fractured and weathered scoracious basalt
5	110-120	Highly weathered basalt
6	120-128	Slightly weathered basalt
7	128-190	Slightly fractured basalt
8	190-210	moderately weathered basalt
9	210-244	Highly weathered basalt
10	244-256	Limestone of white color and friable
11	256-264	Reddish and black color limestone with shale and mudstone
12	264-360	Sandstone, reddish in color and minor quartz grains

Annex 9c: -Lithological log of the well site Sumbala shiko

No	Depth, m	Lithologic description
1	0-16	Redish clay
2	16-24	Highly weathered Ignimbrite
3	24-32	Highly weathered &fractured Ignimbrite with clay
4	32-56	River gravel with some clay
5	56-72	Highly fractured tuff deposit
6	72-88	Highly weathered &fractured basalt
7	88-96	River gravel deposit

Annex 9d -Lithological log of the well site Lidisa

No	Depth, m	Lithologic description
1	0-8	Black cotton soil
2	8-18	Highly weathered volcanic
3	18-25	Highly weathered fractured volcanic rocks
4	25-48	Fractured basalt
5	48-62	Trachyte basalt
6	62-84	Highly weathered and fractured basalt
7	88-96	River Gravel deposit

Annex 9e -Lithological log of the well site Homicho

No	Depth, m	Lithologic description
1	0-4.55	Brown color of clay soil
2	4.55-11.375	Highly weathered and fractured basalt
3	11.375-13.65	Brown color clay soil
4	13.65-40.475	Slightly fractured and weathered basalt
5	40.475-22.75	Moderately fractured basalt
6	22.75-29.85	Moderately fractured scoracious basalt
7	29.85-32.125	Slightly fractured basalt
8	32.125-38.95	Moderately fractured basalt
9	38.95-52.6	Moderated and weathered sandstone
10	52.6-57.15	Brown unwelded tuff
11	57.15-61.7	Gray colored unwelded tuff
12	61.7-109.475	Slightly to moderately fractured sandstone
13	109.475-116.3	Moderately fractured scoracious basalt
14	116.3-132.225	Slightly to moderately fractured sandstone
15	132.225-170.9	Slightly fractured sandstone
16	170.9-177.725	Moderately fractured scoracious basalt
17	177.725-180	Massive sandstone
18	180-191	Slightly fractured sandstone with vesiculated and fractured basalt
19	191-193.85	Moderately fractured sand stone

Annex 9f-Lithological log of the well site chalia

No	Depth, m	Lithologic description
1	0-9.2	Reddish Colored clay soil deposit
2	9.2-16.1	River Gravel
3	16.1-20.7	Fractured basalt
4	20.7-27.6	slightly weathered and fractured basalt
5	27.6-32.2	Highly fractured basalt
6	32.2.41.4	slightly weathered and fractured basalt
7	41.1-52.9	Fractured basalt
8	52.9-57.5	Slightly weathered basalt
9	57.5-64.4	Weathered and fractured basalt (highly saturated)
10	64.4-70	Slightly weathered basalt (Dry)

Annex 10 Hydraulic characteristics of boreholes obtained from different well completion

Well site	X	Y	Z (m)	D(m)	SWL(m)	T(m2/d)	K(m/d)	SC(l/s/m)	DD(m)
Chalia	324354	1002800	2231	70	-	130	1.96	1	-
Lidisa	349659	970625	2491	54	5.9	2.56	0.474	9	-
Homicho	364059	994138	1934	193.85	56	734	10.4	7.3	6
Sumbala	390691	994172	2210	110	5.92	84.4	0.5	12	-
Guder	362201	985706	2139	94	51.9	13.8	0.147		53.6
Babicha	330419	991526	2240	282	1	151	1.52	32	26.15
Kiba	373227	984856	2372	115	30.7	1.52	-	1.8	31.2
Gimbi	366722	972880	2681	118	53.83	109.59	-	4	0.77
ATW1N-14	386772	995546	2380	442	91.6	131	-	17.7	9.64
ATW3-14	365004	993896	1928	339	70.63	570	-	53	12.25
AOW1-14	381377	991238	2242	480	9.62	21.3	-	5	18.32
Ambo Town	991683	378444	2183	193	89.48	-	-	10.9	31
Ambo BH-1	460529	1084126	3041	-	89.48	4440	92.2	10.9	89.79
Ambo BH-2	378444	991683	2183	-	30.65	0.00344	8.6E-05	2.5	39.6
Bakekelate-1 BH	427820	1101526	2514		40.93	79.402	2.20448	16	53.56
Fincha-Debisa	292848	1061504	2362	98.6	27.24	285.01	2.89011	8.5	43.75
Guder Dawe Dolle-2 BH	238689	869434	1591	-	19.1	70.05	2.06	11.57	34.62
Birikas – BH	425984	1012243	2757	-	2	1.095	0.04455	2	42.95
Guder Dawe Dolle-1 BH	241227	869331	1559	-	15.85	15.5	0.3495	8.5	53.96
Garbabash BH-1	287604	1053587	2729	146.25	1.19	5.2581	0.03621	8.5	96.2
Garbabash BH-2	288412	1.1E+07	2740	-	6.5	0.8085	0.01551	2.8	180.2